13. Bennett CN, Longo KA, Wright WS, et al. Regulation of osteoblastogenesis and bone mass by Wnt10b. *Proc Natl Acad Sci USA* 2005;102:3324–9.
14. Bain G, Muller T, Papkoff J, et al. Activated beta-catenin induces osteoblast differentiation of C3H10T1/2 cells and participates in BMP2 mediated signal transduction. *Biochem Biophys Res Commun* 2003;301:84–91.
15. Zhou S, Eid K, Glowacki J. Cooperation between TFG-beta and Wnt pathways during chondrocyte and adipocyte differentiation of human marrow stromal cells. *J Bone Miner Res* 2004;19:463–70.
16. Tamai K, Semenov M, Kato Y, et al. LDL-receptor-related proteins in Wnt signal transduction. *Nature* 2000;407:530–5.
17. Mao J, Wang J, Liu B, et al. Low-density lipoprotein receptor-related protein-5 binds to Axin and regulates the canonical Wnt signaling pathway. *Mol Cell* 2001;7:801–9.
18. Gong Y, Slee RB, Fukai N, et al. LDL receptor-related protein 5 (LRP5) affects bone accrual and eye development. *Cell* 2001;107:513–23.
19. Kato M, Patel MS, Levasseur R, et al. Cbfa1-independent decrease in osteoblast proliferation, osteopenia, and persistent embryonic eye vascularization in mice deficient in Lrp5, a Wnt coreceptor. *J Cell Biol* 2002;157:303–14.
20. Boyden LM, Mao J, Belsky J, et al. High bone density due to a mutation in LDL-receptor-related protein 5. *N Engl J Med* 2002;346:1513–21.
21. Little RD, Carulli JP, Del Mastro RG, et al. A mutation in the LDL receptor-related protein 5 gene results in the autosomal dominant high-bone-mass trait. *Am J Hum Genet* 2002;70:11–9.
22. Sen M, Lauterbach K, Carson DA, et al. Expression and function of wingless and frizzled homologs in rheumatoid arthritis. *Proc Natl Acad Sci USA* 2000;97:2791–6.
23. James IE, Kumar S, Lark MW, et al. FrzB-2: a human secreted frizzled-related protein with a potential role in chondrocyte apoptosis. *Osteoarthritis Cartilage* 2000;8:452–63.
24. Ryu JH, Kim SJ, Chun JS, et al. Regulation of the chondrocyte phenotype by beta-catenin. *Development* 2002;129:5541–50.
25. Yu W, Gluer CC, Fuerst T, et al. Influence of degenerative joint disease on spinal bone mineral measurements in postmenopausal women. *Calcif Tissue Int* 1995;57:169–74.
26. Asai T, Ohkubo T, Katsuya T, et al. Endothelin-1 gene variant associates with blood pressure in obese Japanese subjects: the Ohasama Study. *Hypertension* 2001;38:1321–4.
27. Urano T, Shiraki M, Inoue S, et al. Association of a single-nucleotide polymorphism in low-density lipoprotein receptor-related protein 5 gene with bone mineral density. *J Bone Miner Metab* 2004;22:341–5.
28. Chapman K, Mustafa Z, Loughlin J, et al. Osteoarthritis-susceptibility locus on chromosome 11q, detected by linkage. *Am J Hum Genet* 1999;65:167–74.
29. Chapman K, Mustafa Z, Loughlin J, et al. Finer linkage mapping of primary hip osteoarthritis susceptibility on chromosome 11q in a cohort of affected female sibling pairs. *Arthritis Rheum* 2002;46:1780–3.
30. Smith AJ, Gidley J, Mansell JP, et al. Haplotypes of the low-density lipoprotein receptor-related protein 5 (LRP5) gene: are they a risk factor in osteoarthritis? *Osteoarthritis Cartilage* 2005;13:608–13.
31. Loughlin J, Dowling B, Corr M, et al. Functional variants within the secreted frizzled-related protein 3 gene are associated with hip osteoarthritis in females. *Proc Natl Acad Sci USA* 2004;101:9757–62.
32. Koay MA, Brown MA. Genetic disorders of the LRP5-Wnt signalling pathway affecting the skeleton. *Trends Mol Med* 2005;11:129–37.
33. Koh JM, Jung MH, Kim GS, et al. Association between bone mineral density and LDL receptor-related protein 5 gene polymorphisms in young Korean men. *J Korean Med Sci* 2004;19:407–12.
34. Lau HH, Ng MY, Kung AW, et al. Genetic and environmental determinants of bone mineral density in Chinese women. *Bone* 2005;36:700–9.
35. Ferrari SL, Deutsch S, Antonarakis SE, et al. Polymorphisms in the low-density lipoprotein receptor-related protein 5 (LRP5) gene are associated with variation in vertebral bone mass, vertebral bone size, and stature in whites. *Am J Hum Genet* 2004;74:866–75.
36. Mizuguchi T, Furuta I, Yoshiura K, et al. LRP5, low-density-lipoprotein-receptor-related protein 5, is a determinant for bone mineral density. *J Hum Genet* 2004;49:80–6.
37. Yamada Y, Okuizumi H, Harada A, et al. Association of transforming growth factor beta1 genotype with spinal osteophytosis in Japanese women. *Arthritis Rheum* 2000;43:452–60.
38. Hamerman D. Aging and osteoarthritis: basic mechanisms. *J Am Geriatr Soc* 1993;41:760–70.
39. Sandell LJ, Aigner T. Articular cartilage and changes in arthritis: an introduction: cell biology of osteoarthritis. *Arthritis Res* 2001;3:107–13.
40. Hwang SG, Ryu JH, Chun JS, et al. Wnt-7a causes loss of differentiated phenotype and inhibits apoptosis of articular chondrocytes via different mechanisms. *J Biol Chem* 2004;279:26597–604.
41. Akiyama H, Lyons JP, de Crombrugghe B, et al. Interactions between Sox9 and beta-catenin control chondrocyte differentiation. *Genes Dev* 2004;18:1072–87.

J Bone Miner Metab (2007) 25:253–258
DOI 10.1007/s00774-007-0757-9

ORIGINAL ARTICLE

**Tomohiko Urano · Ken'ichiro Narusawa
Masataka Shiraki · Takahiko Usui · Noriko Sasaki
Takayuki Hosoi · Yasuyoshi Ouchi · Toshitaka Nakamura
Satoshi Inoue**

Association of a single nucleotide polymorphism in the WISP1 gene with spinal osteoarthritis in postmenopausal Japanese women

Received: December 19, 2006 / Accepted: January 31, 2007

Abstract The Wnt-β-catenin signaling pathway that regulates bone density is also involved in cartilage development and homeostasis in vivo. Here, we assumed that genetic variation in Wnt-β-catenin signaling genes can affect the pathogenesis of cartilage related diseases, such as osteoarthritis. Wnt-1-induced secreted protein 1 (WISP1) is a target of the Wnt pathway and directly regulated by β-catenin. In the present study, we analyzed the association of a single nucleotide polymorphism (SNP) in the WISP1 3′-UTR region with the development of radiographically observable osteoarthritis of the spine. For this purpose, we evaluated the presence of osteophytes, endplate sclerosis, and narrowing of disc spaces in 304 postmenopausal Japanese women. We compared those who carried the G allele (GG or GA, $n = 184$) with those who did not (AA, $n = 120$). We found that the subjects without the G allele (AA) were significantly over-represented in the subjects having higher endplate sclerosis score ($P = 0.0069$; odds ratio, 2.91; 95% confidence interval, 1.34–6.30 by logistic regression analysis). On the other hand, the occurrence of disc narrowing and osteophyte formation did not significantly differ between those with and without at least one G allele. Thus, we suggest that a genetic variation in the WISP1 gene locus is associated with spinal osteoarthritis, in line with the involvement of the Wnt-β-catenin-regulated gene in bone and cartilage metabolism.

Key words single nucleotide polymorphism (SNP) · Wnt-β-catenin signaling · WISP1 · osteoarthritis · endplate sclerosis

T. Urano · T. Usui · N. Sasaki · Y. Ouchi · S. Inoue (✉)
Department of Geriatric Medicine, Graduate School of Medicine, The University of Tokyo, 7-3-1 Hongo, Bunkyo-ku, Tokyo, 113-8655 Japan
e-mail: INOUE-GER@h.u-tokyo.ac.jp
Tel. +81-3-5800-8652; Fax +81-3-5800-6530

T. Urano · S. Inoue
Department of Coca-Cola Anti-Aging Medicine, Graduate School of Medicine, The University of Tokyo, Tokyo, Japan

K. Narusawa · T. Nakamura
Department of Orthopedic Surgery, University of Occupational and Environmental Health, School of Medicine, Kitakyushu, Japan

M. Shiraki
Research Institute and Practice for Involutional Diseases, Nagano, Japan

T. Hosoi
Department of Advanced Medicine, National Center for Geriatrics and Gerontology, Aichi, Japan

S. Inoue
Research Center for Genomic Medicine, Saitama Medical School, Saitama, Japan

Introduction

Spinal osteoarthritis is a highly prevalent musculoskeletal disorder and a major cause of back symptoms [1]. Vertebral osteophytes, endplate sclerosis, and intervertebral disc narrowing are recognized as characteristic features of spinal degeneration. Recent studies indicate that the appearance of these radiographic features is influenced by physical loading and other environmental factors [2,3]. Moreover, spinal osteoarthritis has been shown to have a familial component and in some studies to be influenced by specific genetic risk factors, mainly by investigating genes encoding structural proteins of the extracellular matrix of cartilage (e.g., collagen type II α1, cartilage matrix protein, and aminoguanidine) or genes playing a role in the regulation of bone density and mass (e.g., vitamin D receptor, insulin-like growth factor-I, and estrogen receptor-α) [4,5].

The Wnt (wingless-type MMTV integration site family) represents a large group of secreted signaling proteins that are involved in cell proliferation, differentiation, and morphogenesis [6]. The name 'Wnt' is derived from *wingless* gene in *Drosophila melanogaster* [7] and murine *int-1* oncogene identified in tumors induced by mouse mammary tumor virus [8]. It is also known that Wnt and bone morphogenetic protein (BMP) signals control apical ectodermal ridge (AER) formation and dorsoventral patterning during limb development [9,10]. Wnt proteins activate signal transduction through Frizzled, which act as receptors for

Wnt proteins [11] and induce stabilization of cytoplasmic β-catenin protein, which also regulates target gene expression as a transcriptional coactivator. The physiological role of the Wnt in the regulation of osteoblastogenesis has been studied in experimental models. Mice expressing Wnt10b transgene in bone marrow have shown high bone mass by simulating osteoblastogenesis [12]. It is also shown that activated β-catenin stimulates osteoblast differentiation [13]. Further, low-density lipoprotein (LDL)-receptor-related protein 5 and 6 (LRP5/6) were also found to be required for Wnt coreceptors [14,15]. Recent reports demonstrated that the Wnt/β-catenin signaling pathway regulates bone mineral density (BMD) through LRP5 [16–19]. Moreover, we and several groups reported that single nucleotide polymorphisms (SNPs) in the LRP5 gene predicted bone mass [20–23]. These findings indicate that the Wnt-β-catenin signaling pathway plays important roles in skeletal biology.

In addition to the regulation of limb development and bone metabolism, Wnt/β-catenin signaling may be involved in the maintenance and pathophysiology of cartilage. This possibility is indirectly supported by the observation that several Wnt proteins and Frizzled receptors are expressed in the synovial tissue of arthritic cartilage [24]. In addition, a secreted Frizzled-related protein (FrzB-2) that act as an antagonist for Frizzled receptor is strongly expressed in osteoarthritic cartilage and may regulate chondrocyte apoptosis [25]. It is also shown that chondrocytes express β-catenin at a low level and that an accumulation of β-catenin is sufficient to cause dedifferentiation of chondrocytes, suggesting that Wnt signaling is involved in cartilage metabolism [26].

Wnt-1-induced secreted protein 1 (WISP1) is a member of the CCN family growth factors, which includes connective tissue growth factor (CTGF), cysteine-rich 61 (Cyr61), nephroblastoma overexpressed (NOV), WISP2, and WISP3 [27–30]. WISP1 is a target of the Wnt/β-catenin pathway, and its expression is regulated by β-catenin [30,31]. WISP1 activity and availability are modulated by its interaction with decorin and biglycan, two extracellular matrix-associated proteoglycans found abundantly in bone and cartilage [32]. In mouse chondrocytic cell lines, WISP1 increased proliferation and saturation density but repressed chondrocytic representation [33]. These data suggest that WISP1 could play an important regulatory role in bone and cartilage homeostasis. In the present study, we examined an association between a polymorphism in the WISP1 gene and radiographic features of spinal osteoarthritis including osteophyte formation, endplate sclerosis, and disc space narrowing to investigate a possible contribution of WISP1 to human bone and cartilage metabolism.

Materials and methods

Subjects

Genotypes were analyzed in DNA samples obtained from 304 healthy postmenopausal Japanese women (mean age ± SD, 66.3 ± 9.0) living in the central area of Japan. Exclusion criteria included endocrine disorders such as hyperthyroidism, hyperparathyroidism, diabetes mellitus, liver disease, renal disease, use of medications known to affect the bone metabolism (e.g., corticosteroids, anticonvulsants, heparin sodium), or unusual gynecological history. Patients with severe hip and knee arthritis were excluded from the present study. The eligibility of subjects was determined by taking the history and physical examination. All were nonrelated volunteers and provided informed consent before this study. Ethical approval for the study was obtained from appropriate ethics committees.

Radiographic grading of spinal osteoarthritis

Conventional thoracic and lumbar spinal plain roentgenograms in lateral and anteroposterior projection were obtained from all participants. The severities of spinal degeneration including osteophyte formation, endplate sclerosis, and disc space narrowing were assessed semiquantitatively from T4–T5 to L4–L5 disc level or from T4 to L5 vertebrae by using the grading scale of Genant [34]. Briefly, osteophyte formation at a given disc was graded 0–3 degrees, endplate sclerosis at given vertebra was graded 0–2 degrees, and disc space narrowing was graded 0–1 degrees. Then, we defined the sum of each degree from T4–T5 to L4–L5 disc level for osteophyte formation on anteroposterior radiographs as a score of osteophyte formation. We also defined the sum of each degree from T4 to L4 vertebra for endplate sclerosis and that from T4–T5 to L4–L5 disc level for disc space narrowing on lateral radiographs as a score of endplate sclerosis and disc narrowing, respectively. These semiquantitaive gradings on radiographics were performed by two expert medical doctors.

Determination of a SNP in the WISP1 gene

We extracted a polymorphic variation in the WISP1 gene exon 5 3′-untrans lated region (UTR) from the Assays-on-Demand SNP Genotyping Products database (Applied Biosystems, Foster City, CA, USA) and, according to its localization on the gene, denoted it 2364A/G. We determined the 2364A/G polymorphism of the WISP1 gene using the TaqMan (Applied Biosystems) polymerase chain reaction (PCR) method [35]. To determine the WISP1 SNP, we used Assays-on-Demand SNP, Genotyping Products C_9086661_10 (Applied BioSystems) (rs2929970), which contains sequence-specific forward and reverse primers and two TaqMan MGB probes for detecting alleles. During the PCR cycle, two TaqMan probes competitively hybridize to a specific sequence of the target DNA and the reporter dye is separated from the quencher dye, resulting in an increase in fluorescence of the reporter dye. The fluorescence levels of the PCR products were measured with the ABI PRISM 7000, resulting in clear identification of three genotypes of the SNP.

Statistical analysis

Age, height, body weight, body mass index (BMI), and osteoarthritis parameters (number of osteophytes, endoplate sclerosis, and disc narrowing) in the groups of subjects classified by the WISP1 SNP genotypes were compared by analysis of variance (ANOVA) and Kruskal–Wallis test. Stepwise regression analysis was carried out to assess the independent effect of four variables (age, height, body weight, WISP 1 SNP genotypes) on endplate sclerosis score. We also divided subjects into those having one or two allele(s) of the minor G allele (AG + GG) and those with only the major A allele (AA) encoded at the same locus. Multivariate logistic regression was used to estimate odds ratios and 95% confidence intervals (95% CIs) for these two groups and the risk of endplate sclerosis. Analyses for the association of WISP1 2364A/G genotypes and radiographic spinal endplate sclerosis were performed with adjustment for age. P values less than 0.05 were considered significant. Analysis was performed using StatView-J 4.5 software (SAS Institute, Cary, NC, USA).

Results

We analyzed the genotypes for the SNP of WISP1 gene at the 3′-UTR region (2364 A > G) in 304 subjects, using the TaqMan method. Among these postmenopausal Japanese women, 120 were AA homozygotes, 149 were AG heterozygotes, and 35 were GG homozygotes (Table 1). The allelic frequencies of this SNP in the present study were in Hardy–Weinberg equilibrium.

The background data (age, height, body weight, BMI) were not statistically different among these groups (Table 1). On ANOVA analysis, we found significant associations between WISP1 2364A/G genotype and endplate sclerosis score (Table 1; $P = 0.0062$). On Kruskal–Wallis analysis, we also found significant associations between WISP1 2364A/G genotype and endplate sclerosis score (Table 1; $P = 0.024$). Women with the AA allele had a significantly higher endplate sclerosis score than did subjects bearing at least one G allele (AG + GG). On the other hand, the occurrence of disc narrowing and osteophytes did not significantly differ among those SNP genotypes (see Table 1).

Recent studies have shown that the physical and constitutional factors contribute to spinal osteoarthritis. Therefore, we carried out stepwise regression analysis to assess the independent effect of age, height, body weight, and WISP1 SNP genotypes on endplate sclerosis score. Among these factors, only age and WISP1 SNP genotypes correlated significantly with spinal endplate sclerosis score (Table 2). The standard regression coefficients were 0.261 for age and −0.166 for WISP1 SNP genotypes.

Last, we analyzed the association between the alleic frequency of WISP1 SNP genotypes and endplate sclerosis score after stratification by age. In these analyses, we divided subjects into two groups, those who carried the G allele (GG or GA, $n = 184$) and with those who did not (AA, $n = 120$). We found that the subjects without the G allele (AA) were significantly overrepresented in the subjects having a one or more endplate sclerosis score compared in the subjects having no endplate sclerosis after being age-adjusted (Table 3; $P = 0.044$; odds ratio 1.78; 95% confidence interval 1.01–3.13 by logistic regression analysis). We also found that the subjects with the genotype AA were significantly

Table 1. Comparison of background and clinical characteristics among subjects with single nucleotide polymorphism (SNP) genotypes (AA genotype, AG genotype and GG genotype) in the WISP1 gene 3′-UTR region (2364A/G)

Items	Genotype (mean ± SD)			P value (ANOVA)	P value (Kruskal–Wallis)
	AA	AG	GG		
Number of subjects	120	149	35		
Age (years)	66.1 ± 9.2	66.3 ± 8.5	67.1 ± 10.6	NS	NS
Height (cm)	150.7 ± 5.6	150.2 ± 6.8	150.0 ± 5.0	NS	NS
Body weight (kg)	50.3 ± 7.6	50.2 ± 8.3	48.0 ± 5.4	NS	NS
BMI	22.1 ± 2.9	22.2 ± 2.9	21.3 ± 3.3	NS	NS
Endplate sclerosis	0.58 ± 1.09	0.34 ± 0.74	0.09 ± 0.28	0.0062	0.024
Osteophyte	5.89 ± 3.93	5.72 ± 3.40	5.57 ± 4.08	NS	NS
Disk narrowing	2.21 ± 1.79	2.09 ± 2.00	2.03 ± 1.86	NS	NS

BMI, body mass index; NS, not significant

Table 2. Results of stepwise regression analysis of four factors for endplate sclerosis score

Factors	F value			r.c.	s.r.c.
	Step 0	Step 1	Step 2	Step 2	($R^2 = 0.094$)
Intercept	63.7	12.8	9.4	−1.106	−1.106
WISP1 SNP genotypes (AA = 0, AG, GG = 1)			9.1	−0.297	−0.166
Age (years)		21.5	22.7	0.025	0.261
Weight (kg)			Not selected		
Height (cm)			Not selected		

r.c., regression coefficient; s.r.c., standard regression coefficient

Table 3. Association of WISP1 SNP genotype (2364A/G) in subjects with spinal endplate sclerosis after stratifying age

Group compared	AA vs. AG + GG		
	OR	*P* value	95% CI
Endplate sclerosis (≧1) (n = 235) versus no endplate sclerosis (=0) (n = 69)	1.78	0.044	1.01–3.13
Higher endplate sclerosis (≧2) (n = 271) versus lower endplate sclerosis (≦0) (n = 33)	2.91	0.0069	1.34–6.30

OR, odds ratio; 95% CI, 95% confidence interval

over-represented in the subjects having a higher (two or more) endplate sclerosis score compared in the subjects having lower (one or no) endplate sclerosis score after being age-adjusted (Table 3; P = 0.0069; odds ratio 2.91; 95% confidence interval 1.34–6.30 by logistic regression analysis). Thus, we suggest that a genetic variation at the WISP1 gene locus is associated with spinal osteoarthritis, especially with endplate sclerosis, independently with background parameters.

Discussion

The present study is the first report that shows the influence of a SNP of the WISP1 gene on spinal osteoarthritis. The WISP1 is an osteogenic potentiating factor promoting mesenchymal cell proliferation and osteoblastic differentiation while repressing chondrocytic differentiation [33]. We demonstrated that Japanese postmenopausal women who had the AA genotype at the WISP1 2364A/G SNP showed a significantly higher endplate sclerosis score of the spine. Our findings might also be supported by genetic linkage scan for early-onset osteoarthritis and chondrocalcinosis susceptibility loci that showed a linkage to chromosome 8q [36], which includes the WISP1 gene locus on 8q24.

It has been recently shown that haplotype analysis in LRP5 gene revealed that there was a common haplotype that provided a 1.6-fold-increased risk of knee osteoarthritis [37]. We have revealed that a SNP (Q89R) in the LRP5 gene is associated with spinal osteoarthritis [38]. It is also reported that there was a significant association of a functional genetic variant of secreted frizzled-related protein 3 (sFRP3), which antagonizes Wnt signaling, with hip osteoarthritis in women [39]. Taken together, our results and the recent evidence suggest that the Wnt-β-catenin signaling pathway including WISP1 is important in the pathogenesis of skeletal abnormality including osteoarthritis.

WISP1 is a member of the CCN family of connective tissue growth factors, which also includes WISP2 and WISP3. Members of the CCN family have been implicated in developmental processes such as chondrogenesis, osteogenesis, and angiogenesis [27–29]. Specifically, mutations of WISP3 cause the rare skeletal syndrome, progressive pseudorheumatoid dysplasia (PPD) [40]. In affected individuals, symptoms develop between the age of 3 years and 8 years and consist of stiffness and swelling of multiple joints, motor weakness, and joint contractures. It has been also reported that WISP3 polymorphisms were associated with susceptibility to juvenile idiopathic arthritis [41]. Moreover, the WISP3 was shown to be expressed in chondrocytes derived from human cartilage and be able to regulate type II collagen and aggrecan expression [42]. On the other hand, the expression of the WISP2 was preferentially detected in rheumatoid arthritis synovium [43]. These data suggest that CCN family members play a critical role in cartilage homeostasis. In the present study, we investigated a possible contribution of WISP1 polymorphism to spinal osteoarthritis in Japanese women. Taken together, the CCN family gene polymorphisms may affect the pathogenesis of cartilage disease.

In the present study, we excluded subjects with severe hip or knee arthritis, because these joint diseases themselves may induce spinal deformity or malalignment. Therefore, we could not assess such joint arthritis here. Recent studies have shown that some SNPs in the sFRP3 and LRP5 genes, involved in Wnt signaling, were associated with hip and knee osteoarthritis, respectively [37,39]. Moreover, WISP3 polymorphisms are associated with juvenile idiopathic arthritis that affects multiple joints [41]. In this regard, it may be important to examine the association of the SNPs in the WISP1 gene with hip and knee arthritis in the future. Meanwhile, it would be better if we had also evaluated the facet joint, because spinal osteoarthritis is represented not only by the anterior elements such as disc narrowing, osteophytosis, or endplate sclerosis but also by the posterior elements, especially a facet joint lesion. However, we here evaluated only the anterior elements of thoracolumbar vertebral bodies, because a reproducible semiquantitative assessment for facet joint using anteroposterior (A-P) and lateral X-ray radiographs has not been well established.

In conclusion, we have shown an association of the polymorphism in the WISP1 gene with a radiographic feauture of spinal endplate sclerosis in postmenopausal Japanese women. The women with AA genotypes had significantly higher endplate sclerosis scores. WISP1 genotyping may be benefical in the prevention and management of spinal osteoarthritis. Thus, the WISP1 would be a useful molecular target for the development of new diagnostic markers as well as therapeutic options in osteoarthritis.

Acknowledgments This work was partly supported by grants from the Japanese Ministry of Health, Labor, Welfare, Japan Society for the Promotion of Science, and the Ministry of Culture, Education, Sports, Science and Technology of Japan.

References

1. Creamer P, Hochberg MC (1997) Osteoarthritis. Lancet 350:503–508
2. Lane NE, Nevitt MC, Genant HK, Hochberg MC (1993) Reliability of new indices of radiographic osteoarthritis of the hand and hip and lumbar disc degeneration. J Rheumatol 20:1911–1918
3. O'Neill TW, McCloskey EV, Kanis JA, Bhalla AK, Reeve J, Reid DM, Todd C, Woolf AD, Silman AJ (1999) The distribution, determinants, and clinical correlates of vertebral osteophytosis: a population based survey. J Rheumatol 26:842–848
4. Spector TD, MacGregor AJ (2004) Risk factors for osteoarthritis: genetics. Osteoarthritis Cartilage 12:S39–S44
5. Loughlin J (2003) Genetics of osteoarthritis and potential for drug development. Curr Opin Pharmacol 3:295–299
6. Nusse R, Varmus HE (1992) Wnt genes. Cell 69:1073–1087
7. Rijsewijk F, Schuermann M, Wagenaar E, Parren P, Weigel D, Nusse R (1987) The *Drosophila* homolog of the mouse mammary oncogene int-1 is identical to the segment polarity gene wingless. Cell 50:649–657
8. Nusse R, Varmus HE (1982) Many tumors induced by the mouse mammary tumor virus contain a provirus integrated in the same region of the host genome. Cell 31:99–109
9. Barrow JR, Thomas KR, Boussadia-Zahui O, Moore R, Kemler R, Capecchi MR, McMahon AP (2003) Ectodermal Wnt3/beta-catenin signaling is required for the establishment and maintenance of the apical ectodermal ridge. Genes Dev 17:394–409
10. Soshnikova N, Zechner D, Huelsken J, Mishina Y, Behringer RR, Taketo MM, Crenshaw EB III, Birchmeier W (2003) Genetic interaction between Wnt/beta-catenin and BMP receptor signaling during formation of the AER and the dorsal-ventral axis in the limb. Genes Dev 17:1963–1968
11. Cadigan KM, Nusse R (1999) Wnt signaling: a common theme in animal development. Genes Dev 11:3286–3305
12. Bennett CN, Longo KA, Wright WS, Suva LJ, Lane TF, Hankenson KD, MacDougald OA (2005) Regulation of osteoblastogenesis and bone mass by Wnt10b. Proc Natl Acad Sci U S A 102:3324–3329
13. Bain G, Muller T, Wang X, Papkoff J (2003) Activated beta-catenin induces osteoblast differentiation of C3H10T1/2 cells and participates in BMP2 mediated signal transduction. Biochem Biophys Res Commun 301:84–91
14. Tamai K, Semenov M, Kato Y, Spokony R, Liu C, Katsuyama Y, Hess F, Saint-Jeannet JP, He X (2000) LDL-receptor-related proteins in Wnt signal transduction. Nature (Lond) 407:530–553
15. Mao J, Wang J, Liu B, Pan W, Farr GH III, Flynn C, Yuan H, Takada S, Kimelman D, Li L, Wu D (2001) Low-density lipoprotein receptor-related protein-5 binds to Axin and regulates the canonical Wnt signaling pathway. Mol Cell 7:801–809
16. Gong Y, Slee RB, Fukai N, Rawadi G, Roman-Roman S, et al. (2001) LDL receptor-related protein 5 (LRP5) affects bone accrual and eye development. Cell 107:513–523
17. Kato M, Patel MS, Levasseur R, Lobov I, Chang BH, Glass DA II, Hartmann C, Li L, Hwang TH, Brayton CF, Lang RA, Karsenty G, Chan L (2002) Cbfa1-independent decrease in osteoblast proliferation, osteopenia, and persistent embryonic eye vascularization in mice deficient in Lrp5, a Wnt coreceptor. J Cell Biol 157:303–314
18. Boyden LM, Mao J, Belsky J, Mitzner L, Farhi A, Mitnick MA, Wu D, Insogna K, Lifton RP (2002) High bone density due to a mutation in LDL-receptor-related protein 5. N Engl J Med 346:1513–1521
19. Little RD, Carulli JP, Del Mastro RG, Dupuis J, Osborne M, et al (2002) A mutation in the LDL receptor-related protein 5 gene results in the autosomal dominant high-bone-mass trait. Am J Hum Genet 70:11–19
20. Urano T, Shiraki M, Ezura Y, Fujita M, Sekine E, Hoshino S, Hosoi T, Orimo H, Emi M, Ouchi Y, Inoue S (2004) Association of a single-nucleotide polymorphism in low-density lipoprotein receptor-related protein 5 gene with bone mineral density. J Bone Miner Metab 22:341–345
21. Mizuguchi T, Furuta I, Watanabe Y, Tsukamoto K, Tomita H, Tsujihata M, Ohta T, Kishino T, Matsumoto N, Minakami H, Niikawa N, Yoshiura K (2004) LRP5, low-density-lipoprotein-receptor-related protein 5, is a determinant for bone mineral density. J Hum Genet 49:80–86
22. Ferrari SL, Deutsch S, Choudhury U, Chevalley T, Bonjour JP, Dermitzakis ET, Rizzoli R, Antonarakis SE (2004) Polymorphisms in the low-density lipoprotein receptor-related protein 5 (LRP5) gene are associated with variation in vertebral bone mass, vertebral bone size, and stature in whites. Am J Hum Genet 74:866–875
23. Lau HH, Ng MY, Ho AY, Luk KD, Kung AW (2005) Genetic and environmental determinants of bone mineral density in Chinese women. Bone (NY) 36:700–709
24. Sen M, Lauterbach K, El-Gabalawy H, Firestein GS, Corr M, Carson DA (2000) Expression and function of wingless and frizzled homologs in rheumatoid arthritis. Proc Natl Acad Sci USA 97:2791–2796
25. James IE, Kumar S, Barnes MR, Gress CJ, Hund AT, Dodds RA, Connor JR, Bradley BR, Campbell DA, Grabill SE, Williams K, Blake SM, Gowen M, Lark MW (2000) FrzB-2: a human secreted frizzled-related protein with a potential role in chondrocyte apoptosis. Osteoarthritis Cartilage 8:452–463
26. Ryu JH, Kim SJ, Kim SH, Oh CD, Hwang SG, Chun CH, Oh SH, Seong JK, Huh TL, Chun JS (2002) Regulation of the chondrocyte phenotype by beta-catenin. Development (Camb) 129:5541–5550
27. Bork P (1993) The modular architecture of a new family of growth regulators related to connective tissue growth factor. FEBS lett 327:125–130
28. Brigstock DR (1999) The connective tissue growth factor/cysteine-rich 61/nephroblastoma overexpressed (CCN) family. Ender Rev 20:189–206
29. Perbal B (2001) NOV (nephroblastoma overexpressed) and the CCN family of genes: structural and functional issues. Mol Pathol 54:57–79
30. Pennica D, Swanson TA, Welsh JW, Roy MA, Lawrence DA, et al. (1998) WISP genes are members of the connective tissue growth factor family that are up-regulated in wnt-1-transformed cells and aberrantly expressed in human colon tumors. Proc Natl Acad Sci USA 95:14717–14722
31. Xu L, Corcoran RB, Welsh JW, Pennica D, Levine AJ (2000) WISP-1 is a Wnt-1- and beta-catenin-responsive oncogene. Genes Dev 14:585–595
32. Desnoyers L, Arnott D, Pennica D (2001) WISP-1 binds to decorin and biglycan. J Biol Chem 276:47599–47607
33. French DM, Kaul RJ, D'Souza AL, Crowley CW, Bao M, Frantz GD, Filvaroff EH, Desnoyers L (2004) WISP-1 is an osteoblastic regulator expressed during skeletal development and fracture repair. Am J Pathol 165:855–867
34. Yu W, Gluer CC, Fuerst T, Grampp S, Li J, Lu Y, Genant HK (1995) Influence of degenerative joint disease on spinal bone mineral measurements in postmenopausal women. Calcif Tissue Int 57:169–174
35. Asai T, Ohkubo T, Katsuya T, Higaki J, Fu Y, Fukuda M, Hozawa A, Matsubara M, Kitaoka H, Tsuji I, Araki T, Satoh H, Hisamichi S, Imai Y, Ogihara T (2001) Endothelin-1 gene variant associates with blood pressure in obese Japanese subjects: the Ohasama Study. Hypertension 38:1321–1324
36. Baldwin CT, Farrer LA, Adair R, Dharmavaram R, Jimenez S, Anderson L (1995) Linkage of early-onset osteoarthritis and chondrocalcinosis to human chromosome 8q. Am J Hum Genet 56:692–697
37. Smith AJ, Gidley J, Sandy JR, Perry MJ, Elson CJ, Kirwan JR, Spector TD, Doherty M, Bidwell JL, Mansell JP (2005) Haplotypes of the low-density lipoprotein receptor-related protein 5 (LRP5) gene: are they a risk factor in osteoarthritis? Osteoarthritis Cartilage 13:608–613
38. Urano T, Shiraki M, Narusawa K, Usui T, Sasaki N, Hosoi T, Ouchi Y, Nakamura T, Inoue S. (2007) Q89R polymorphism in the LDL receptor-related protein 5 gene is associated with spinal osteoarthritis in postmenopausal Japanese women. Spine 32:25–29
39. Loughlin J, Dowling B, Chapman K, Marcelline L, Mustafa Z, Southam L, Ferreira A, Ciesielski C, Carson DA, Corr M (2004) Functional variants within the secreted frizzled-related protein 3 gene are associated with hip osteoarthritis in females. Proc Natl Acad Sci USA 101:9757–9762

40. Hurvitz JR, Suwairi WM, Van Hul W, El-Shanti H, Superti-Furga A, Roudier J, Holderbaum D, Pauli RM, Herd JK, Van Hul EV, Rezai-Delui H, Legius E, Le Merrer M, Al-Alami J, Bahabri SA, Warman ML (1999) Mutations in the CCN gene family member WISP3 cause progressive pseudorheumatoid dysplasia. Nat Genet 23:94–98
41. Lamb R, Thomson W, Ogilvie E, Donn R, British Society of Paediatric and Adolescent Rheumatology (2005) Wnt-1-inducible pathway protein 3 and susceptibility to juvenile idiopathic arthritis. Arthritis Rheum 52:3548–3553
42. Sen M, Cheng YH, Goldring MB, Lotz MK, Carson DA (2004) WISP3-dependent regulation of type II collagen and aggrecan production in chondrocytes. Arthritis Rheum 50:488–497
43. Tanaka I, Morikawa M, Okuse T, Shirakawa M, Imai K (2005) Expression and regulation of WISP2 in rheumatoid arthritic synovium. Biochem Biophys Res Commun 334:973–978

THE JOURNAL OF BIOLOGICAL CHEMISTRY VOL. 282, NO. 8, pp. 5736–5748, February 23, 2007

α-Synuclein Stimulates Differentiation of Osteosarcoma Cells
*RELEVANCE TO DOWN-REGULATION OF PROTEASOME ACTIVITY**

Received for publication, June 28, 2006, and in revised form, December 15, 2006 Published, JBC Papers in Press, December 22, 2006, DOI 10.1074/jbc.M606175200

Masayo Fujita[‡], Shuei Sugama[‡], Masaaki Nakai[‡], Takato Takenouchi[§], Jianshe Wei[‡], Tomohiko Urano[¶], Satoshi Inoue[¶], and Makoto Hashimoto[‡1]

From the [‡]Laboratory for Chemistry and Metabolism, Tokyo Metropolitan Institute for Neuroscience, Fuchu, Tokyo 183-8526, Japan, [§]Transgenic Animal Research Center, National Institute of Agrobiological Sciences, Tsukuba, Ibaraki 305-8634, Japan, and [¶]Department of Geriatrics and Gerontology, School of Medicine, University of Tokyo, Tokyo 113-8655, Japan

Because a limited study previously showed that α-synuclein (α-syn), the major pathogenic protein for Parkinson disease, was expressed in differentiating brain tumors as well as various peripheral cancers, the main objective of the present study was to determine whether α-syn might be involved in the regulation of tumor differentiation. For this purpose, α-syn and its non-amyloidogenic homologue β-syn were stably transfected to human osteosarcoma MG63 cell line. Compared with β-syn-overexpressing and vector-transfected cells, α-syn-overexpressing cells exhibited distinct features of differentiated osteoblastic phenotype, as shown by up-regulation of alkaline phosphatase and osteocalcin as well as inductive matrix mineralization. Further studies revealed that proteasome activity was significantly decreased in α-syn-overexpressing cells compared with other cell types, consistent with the fact that proteasome inhibitors stimulate differentiation of various osteoblastic cells. In α-syn-overexpressing cells, protein kinase C (PKC) activity was significantly decreased, and reactivation of PKC by phorbol ester significantly restored the proteasome activity and abrogated cellular differentiation. Moreover, activity of lysosome was up-regulated in α-syn-overexpressing cells, and treatment of these cells with autophagy-lysosomal inhibitors resulted in a decrease of proteasome activity associated with up-regulation of α-syn expression, leading to enhance cellular differentiation. Taken together, these results suggest that the stimulatory effect of α-syn on tumor differentiation may be attributed to down-regulation of proteasome, which is further modulated by alterations of various factors, such as protein kinase C signaling pathway and a autophagy-lysosomal degradation system. Thus, the mechanism of α-syn regulation of tumor differentiation and neuropathological effects of α-syn may considerably overlap with each other.

α-Synuclein (α-syn)[2] is a presynaptic protein that belongs to the syn family of peptides with two other members, β- and γ-syn (1, 2). These proteins are characterized by a native unfolded structure with a highly conserved N-terminal region and a divergent C-terminal acidic region (3). However, the most striking feature is that α-syn possesses a highly hydrophobic domain in the middle region that was previously purified from Alzheimer disease brain amyloid (4). Due to this hydrophobic domain, α-syn forms toxic protofibrils that might cause synaptic injury and dysfunction (5). The importance of α-syn in the pathogenesis of neurodegenerative disorders was further augmented by identification of missense mutations of α-syn in familial Parkinson disease (PD) (6–8). Subsequently, numerous histological studies have shown that α-syn is a major constituent in Lewy bodies and dystrophic neuritis in sporadic PD and diffuse Lewy body disease (2). Immunoreactivity of α-syn was also shown in glial cell inclusions in multiple system atrophy (2). By contrast, β-syn, which lacks the majority of the hydrophobic domain in the middle region, was protective against protofibrils of α-syn (9, 10). Thus, these results support the contention that α- and β-syn may play a central role in the pathogenesis of neurodegenerative diseases.

On the other hand, γ-syn, the less conserved third member of the syn family of peptides, was identified as a breast cancer-specific gene product (11) and has been extensively studied in a variety of cancers, such as breast cancer, ovarian cancer, liver cancer, pancreatic adenocarcinoma, and bladder cancer (11–15). Because expression levels of γ-syn were well correlated with the presence of metastatic lesions, it has been generally thought that γ-syn might regulate tumor invasiveness and metastasis (16, 17). Several studies indicated that γ-syn might be involved in the deregulation of cell cycle in cancer. For example, γ-syn interacted with a mitotic spindle checkpoint protein, BubR1, leading to decreased checkpoint function and tumor progression (18, 19). Moreover, γ-syn stimulated cell proliferation by augmenting estrogen receptor-mediated signaling in breast cancer cells (20). Thus, the role of γ-syn has been investigated mainly in the area of tumor biology.

* This work was supported in part by a grant-in-aid for Science Research from the Ministry of Education, Culture, Sports, Science, and Technology, Japan and a project grant from Tokyo Metropolitan Organization. The costs of publication of this article were defrayed in part by the payment of page charges. This article must therefore be hereby marked "*advertisement*" in accordance with 18 U.S.C. Section 1734 solely to indicate this fact.

[1] To whom correspondence should be addressed: Laboratory for Chemistry and Metabolism, Tokyo Metropolitan Institute for Neuroscience, 2–6 Musashidai, Fuchu, Tokyo 183-8526, Japan. Tel.: 81-42-325-3881; Fax: 81-42-321-8678; E-mail address: mhashimoto@tmin.ac.jp.

[2] The abbreviations used are: syn, synuclein; PD, Parkinson disease; UPS, ubiquitin-proteasome system; PKC, protein kinase C; PMA, 12-myristate 13-acetate; 4αPDD, 4α-phorbol 12,13-didecanoate; 3-MA, 3-methyladenine; Rb, retinoblastoma; RT, reverse transcriptase; CAPS, 3-(cyclohexylamino)-1-propanesulfonic acid; LSCM, laser-scanning confocal microscope; ALP, alkaline phosphatase; PBS, phosphate-buffered saline; LSCM, laser-scanning confocal microscope.

A recent study, however, suggests that molecular pathways shared by neurodegenerative disease and cancer may be considerably overlapped than thought before. Supporting this notion, it has been recently shown that several familial PD-causing factors are involved in the pathogenesis of cancer (21). First, overexpression of the PARK2 parkin, which functions as an E3 ligase in the ubiquitin-proteasome system (UPS), resulted in growth suppression in hepatocellular carcinoma cells (22). Furthermore, ectopic expression of parkin reportedly reduced *in vivo* tumorigenesis in nude mice (23). Second, the PARK5 ubiquitin C-terminal hydrolase light chain-1, which acts as a de-ubiquitinating enzyme in UPS, was shown to suppress proliferation of a lung cancer cells (24). Other evidence suggests that ubiquitin C-terminal hydrolase light chain-1 might be involved in the degradation of p27, a cyclin-dependent kinase inhibitor (25). Third, the PARK7 DJ-1 was first identified as an oncogene product that stimulated transformation of NIH3T3 cells in coordination with Ras (26). DJ-1 was recently shown to up-regulate the phosphatidylinositol 3-kinase pathway through inhibition of the tumor suppressor phosphatase PTEN, leading to enhance survival of cancer (27).

In the same context one may wonder if α- and β-syn, the central players in the pathogenesis of PD, might play some important roles for the regulation of cancer. Indeed, α-syn was widely expressed in a variety of brain tumors, such as medulloblastoma, neuroblastoma, pineoblastoma, and ganglioma (28, 29). Furthermore, both α- and β-syn were shown to be expressed in the peripheral cancers, including ovarian and breast cancers (30). Although the role of syn proteins in the pathogenesis of cancer is unclear, a limited number of studies suggest that α-syn might be involved in the regulation of tumor differentiation. Supporting this possibility, α-syn was preferentially expressed in brain tumors showing neuronal differentiation (28). In cell cultures expression of α-syn was increased during the hematopoietic differentiation of K562 myelogenous leukemia cells (31). Similarly, it was shown that α-syn was up-regulated during neural differentiation of pheochromocytoma PC12 cells (32). Thus, distinct from the possible role of γ-syn for tumor metastasis, α-syn might be involved in tumor differentiation.

Accordingly, the main objective of the present study was to determine whether α- and/or β-syn might regulate growth and differentiation of cancer cells. For this purpose, α- and β-syn were stably overexpressed in MG63 human osteosarcoma cells. We found that compared with vector-transfected and β-syn-overexpressing cells, α-syn-overexpressing cells exhibited distinct phenotype of differentiated osteoblastic cells. Mechanistically, α-syn may cause down-regulation of proteasome activity, leading to accelerate cellular differentiation. Further studies revealed that down-regulation of proteasome activity by α-syn was regulated by alteration of various factors, including PKC signaling activities and the autophagy-lysosomal pathway in α-syn-overexpressing cells.

EXPERIMENTAL PROCEDURES

Reagent—Chemical reagents include MG132 and lactacystin (purchased from EMD Biosciences, San Diego, CA), rotenone, 12-myristate 13-acetate (PMA), 4α-phorbol 12,13-didecanoate (4αPDD), leupeptin, chelerythrine chloride, and 3-methyladenine (3-MA) (obtained from Sigma), and caspase 1 inhibitor and III inhibitors (Ac-AAVALLPAVLLALLAP-YVAD-CHO, Ac-AAVALLPAVLLALLAP-DEVD-CHO) (Calbiochem) were applied to cell cultures at indicated concentrations.

Antibodies used are as follows. Monoclonal antibodies, anti-α-syn (syn-1), anti-β-syn, anti-PKCε, and anti-retinoblastoma (Rb) were purchased from BD Biosciences. Monoclonal anti-β-actin (AC-15) was obtained from Sigma. Monoclonal antibodies anti-p21 and anti-cyclin B1, rabbit polyclonal antibodies anti-p15, anti-cyclin D1, anti-cyclin-dependent kinase 4, and anti-phosphorylated Rb, and goat polyclonal anti-osteocalcin antibody were from Santa Cruz Biotechnology (Santa Cruz, CA). Monoclonal anti-ubiquitin antibody was from Chemicon (Temecula, CA). Monoclonal anti-19 S proteasome S6a subunit antibody was from Biomol (Plymouth Meeting, PA). Rabbit polyclonal anti-cathepsin B was from Calbiochem. Rabbit polyclonal antibodies, anti-C-terminal α-syn, and anti-β-syn were previously described (33, 34). Alexa fluor 488-conjugated anti-goat secondary antibody, Alexa fluor 488-conjugated anti-rabbit secondary antibody, and Alexa fluor 555-conjugated anti-mouse secondary antibody were from Invitrogen.

Cell Cultures and Transfection—MG63 and 293T cells were both cultured in Dulbecco's modified Eagle's medium (high glucose) containing 10% fetal calf serum (BioWest, Nuaille, France) and 1% v/v penicillin/streptomycin (Invitrogen) in a 5% CO_2, 95% air atmosphere. MG63 cells exhibited both α- and β-syn transcripts by RT-PCR analysis, but their protein expressions were hardly detectable by immunoblot analysis (data not shown). For stable transfection, MG63 cells were transfected with pCEP4 expression vector (Invitrogen) or pCEP4 containing either human α- or β-syn cDNA (34) using Lipofectamine 2000 (Invitrogen). After 2~3 weeks of incubation in the presence of 200 μg/ml hygromycin B (EMD Biosciences), the resistant colonies of cells (~20) were isolated. These stable cell lines were routinely maintained in the presence of 50 μg/ml hygromycin B. 293T cells were transiently transfected with p-Target expression vector (Promega, Madison, WI) containing human p21 cDNA insert.[3]

Reverse Transcriptase (RT)-PCR—Total RNA was isolated from cultured cells using the RNA extraction buffer ISOGEN (Nippon Gene, Tokyo, Japan). cDNA was synthesized from 2 μg of total RNA using the Superscript III First-Strand Synthesis system (Invitrogen) according to the manufacturer's instruction.

PCR amplification was carried out using Taq PCR polymerase (ABgene, Tokyo, Japan), and the amplified products were resolved by agarose gel electrophoresis. The following primers were used for PCR. Human α-syn (NM_000345): sense, 5′-ATGGATGTATTCATGAAAGGACTTTC-3′ (47–72-oligonucleotide position), antisense, 5′-GGCTTCAGGTTCGTAGTCTTGATAC-3′ (the 442–466 oligonucleotide position); human β-syn (BT006627): sense, 5′-ATGGACGTGTTCATGAAGGGC-3′ (1–21-oligonucleotide position), antisense, 5′-CTACGCCTCTGGCTCATACTC-3′ (385–405-oligonucleotide position); human cyclophilin A (NM_021130): sense, 5′-TACTATTAGCCATGGTCAAC-3′ (62–81-oligonucleotide position), antisense 5′-GTCTTGCCATTCCTGGACCC-3′ (508–527-oligonucleotide position); human liver/bone/kidney-type alkaline phosphatase (ALP) (AB011406): sense, 5′-GGGGGTGGCCGGAAATACAT-3′ (834–853-oligonucleotide position), antisense, 5′-GGGGGCCAGACCAAAGATAG-3′ (1357–1376-oligonucleotide position); human osteocalcin (X51699): sense, 5′-ATGAGAGCCCTCACACTCCTC-3′ (19–39-oligonucleotide position), antisense, 5′-GCCGTAGAAGCGCCGATAGGC-3′ (292–312-oligonucleotide position).

[3] T. Urano, unpublished information.

Immunoblot and Co-immunoprecipitation Analyses—Immunoblot analysis was performed as previously described (34). Briefly, cells were harvested and dissolved in lysis buffer (1% Nonidet P-40, 50 mM HEPES, 150 mM NaCl, 10% glycerol, 1.5 mM $MgCl_2$, 1 mM EGTA, 100 mM sodium fluoride, and protease inhibitor mixture (Nakarai Tesque, Kyoto, Japan)). Protein concentrations of the cell lysates were determined Bio-Rad protein assay reagent. Cell extracts (10 μg) were then resolved by SDS-PAGE (10 or 16%) and electroblotted onto nitrocellulose membranes (GE Healthcare) with CAPS buffer (pH 11.0). The membranes were blocked with 3% bovine serum albumin (BSA) in Tris-buffered saline (TBS: 25 mM Tris-HCl (pH 7.5), 150 mM NaCl) plus 0.2% Tween 20 followed by an incubation with primary antibodies in TBS containing 3% BSA. After washing, the membranes were further incubated with second antibody conjugated with horseradish peroxidase (GE Healthcare) in Tris-buffered saline (1:10,000). Finally, the target proteins were visualized with the ECL plus system (GE Healthcare). The intensity of the band was measured using BioMax 1D image analysis soft ware (Eastman Kodak Co.). In some experiments 293T cells were transfected with p-Target vector (Promega) with or without human p21 cDNA insert, and cell extracts were used for controls. Recombinant human α- and β-syn were also used for positive controls (9).

Immunoprecipitation was performed as previously described (35). Briefly, cell extracts (200 μg) were preabsorbed with protein G-Sepharose (GE Healthcare) for 1 h, and the precleared lysates were incubated with either syn-1 or mouse IgG control (each 1 μg) overnight at 4 °C followed by incubation with protein G-Sepharose. The immune complexes were then washed three times with the lysis buffer. The samples were then heated in the SDS sample buffer for 5 min and subjected to immunoblotting.

Immunofluorescence Study—Cells were seeded onto poly-L-lysine-coated glass coverslips, grown to 70% confluence, fixed in 4% paraformaldehyde for 30 min and pretreated with 0.1% Triton X-100 in phosphate-buffered saline (PBS) for 20 min. Fixed cells were blocked with PBS containing 3% goat serum and 5% bovine serum albumin at room temperature. For staining, cells were incubated overnight at 4 °C with primary antibody (or antibodies for double staining). After washing, cells were incubated with Alexa fluor-conjugated secondary antibody (or antibodies for double staining) (Invitrogen) for 1 h at room temperature. Control experiments included immunostaining in the absence of primary antibody. Coverslips were air-dried, mounted on slides with Gel/Mount (Biomeda Corp., Foster City, CA), and imaged with the laser-scanning confocal microscope (LSCM) (Olympus, FV1000, Tokyo, Japan).

Cell Cycle Analysis Using Flow Cytometry—Cells seeded at 1×10^5 cells in 6-well cell culture plates were incubated under low serum (0.1%) conditions for 24 h, treated with 10% serum for 6, 12, 18, 24, and 96 h, and harvested using trypsin-EDTA. After washing with PBS, cells were fixed by ice-cold ethanol to final concentration of 70%. The cells were then resuspended in PBS containing 0.5 mg/ml RNaseA (Nakarai Tesque), incubated for 30 min at 37 °C, and followed by staining with propidium iodide (10 μg/ml) for 10 min at room temperature. Before flow cytometry analysis, the stained cells were filtrated with nylon mesh. The fluorescence signals of 2×10^4 cells were recorded by EPICS ALTRA (Beckman Coulter, Fullerton, CA). The distribution of cell cycle phase was analyzed by Multicycle software (Phoenix Flow Systems, San Diego, CA).

Measurement of ALP Activity—Cellular activities of ALP were determined as described previously with some modifications (36). Briefly, cells were grown until confluency under the 10% serum conditions in 6-well cell culture plates. Cells were then washed twice, harvested into PBS, and sonicated by ultrasonic disruptor (TOMY, Tokyo, Japan) for 20 s. After centrifugation of the cell preparations at 15,000 rpm for 10 min, the supernatants were recovered and assessed for protein concentration. The supernatants (10 μg) were then incubated in the ALP assay buffer containing 10 mM *p*-nitrophenyl phosphate (Sigma), 100 mM glycine, 1 mM $ZnCl_2$, and 1 mM $MgCl_2$ (pH 10.4). After 90 min of incubation at 37 °C, ALP activity was determined by monitoring the amount of released *p*-nitrophenol at 415 nm. Dissolved *p*-nitrophenol in assay buffer was used to establish the standard for quantification. The released *p*-nitrophenol was adjusted by the amount of protein and described as nmol/min/mg of protein.

Increased levels of the cellular ALP activities were further confirmed by direct stain of the cells. The cells reached confluency were fixed with 70% ethanol, washed twice with Tris-buffered saline, and incubated with nitro blue tetrazolium chloride/5-bromo-4-chloro-3-indolyl phosphate *p*-toluidine salt ALP substrate solution (Roche Applied Science) for 2 h. The visualized image was then photographed.

Mineralization Assay—Mineralization of MG63 cells was performed as previously described (36) with some modifications. Briefly, cells were grown until confluency under the 10% serum conditions in 24-well cell culture plates. The cells were further incubated in α-minimal essential medium (Invitrogen) plus 10% serum in the presence of 10 mM β-glycerophosphate (Sigma) and 50 μg/ml ascorbic acid with or without the addition of various chemical reagents. The media were regularly changed twice a week. After 4 weeks, cells were evaluated for the extent of matrix mineralization by either alizarin red staining or von Kossa staining. For alizarin red staining, the cells were fixed with 70% ethanol for 30 min at room temperature. Then the cells were incubated with 40 mM alizarin red-S (Sigma) for 10 min and washed 4 times with distilled water. The visualized image was photographed. For von Kossa staining, the cells were fixed with 10% neutralized formaldehyde for 30 min at room temperature. The fixed cells were incubated with 5% silver nitrate for 5 min under the exposure to the sunlight. The reaction was stopped by the addition of 5% sodium thiosulfate.

The stained cells were washed four times with distilled water and imaged with microscope.

Evaluation of Proteasome and Cathepsin B Activity—Measurement of proteasome and cathepsin B activity was done as previously described with modifications (37). Briefly, cells reaching confluency in 6-well cell culture plates were incubated under the low serum (0.1%) conditions for 24 h and treated with 10% serum with or without treatment of various reagents. After the indicated times (0, 6, or 12 h), the cells were harvested in buffer containing 50 mM HEPES (pH 7.4), 10 mM EDTA, and 10 mM NaCl, subjected to freezing and thawing to rapture cell membranous structures, and then centrifuged at 15,000 rpm for 10 min. For the measurement of proteasome activity, 10 μg of the supernatants were incubated in assay buffer containing 50 mM HEPES (pH 7.4), 10 mM EDTA, 10 mM NaCl, and 40 μM benzyloxycarbonyl-Leu-Leu-Glu-amidomethylcoumarin fluorogenic proteasome substrate (Chemicon). For cathepsin B activity, 10 μg of the supernatants were incubated in buffer containing 50 mM HEPES (pH 6.0), 10 mM EDTA, 10 mM NaCl, and 40 μM benzyloxycarbonyl-Arg-Arg-amidomethylcoumarin fluorogenic cathepsin B substrate (Chemicon). These enzyme activities were assayed by continuous recording of the fluorescence activity released from fluorogenic substrate using Berthold Mithras LB940 microplate reader (Berthold, Bad Wildbad, Germany) for 1 h at 37 °C (excitation, 380 nm; emission, 460 nm), and the reaction rate was analyzed. These enzyme activities were described as arbitrary unit/min/mg of protein.

Evaluation of PKC Activity—PKC activity was determined using PepTag nonradioactive PKC assay kit (Promega) according to the manufacture's instruction. Briefly, cells reaching confluency in 6-well cell culture plates were treated with or without PMA for 20 min and harvested in extraction buffer (25 mM Tris-HCl (pH 7.4), 0.5 mM EDTA, 0.5 mM EGTA, 10 mM β-mercaptoethanol, 100 mM phenylmethylsulfonyl fluoride, and protease inhibitor mixture (Nakarai Tesque)). Cell extracts were then sonicated by ultrasonic disruptor (TOMY) for 20 s and centrifuged at 15,000 rpm for 15 min. The supernatants were used for the assay. The reaction was performed at 30 °C for 30 min in assay solution including, PepTag C1 peptide (0.4 μg/μl) and 5 μg of protein sample. The samples were separated on the 0.8% agarose gel and visualized on a transilluminator. The intensity of fluorescence of the phosphorylated peptides were quantified using BioMax 1D image analysis soft ware (Kodak).

Electron Microscopy—Electron microscopy analysis was performed as previously described with minor modifications (38). Briefly, cells were harvested using trypsin-EDTA and fixed by 2.5% glutaraldehyde in 0.1 M sodium cacodylate buffer at 4 °C for 2 h. After centrifugation, cells were washed with 0.1 M sodium cacodylate buffer 3 times. Cell pellets were obtained by centrifuge, post-fixed in 1% osmium tetroxide and 1% potassium ferrocyanide at room temperature for 2 h, and processed for embedding in Quetol 812 (Nisshin EM, Tokyo, Japan). Ultrathin sections were stained with uranyl acetate and lead nitrate and observed by a Hitachi H-7500 electron microscope.

Statistical Analysis—All values in the figures are expressed as means ± S.D. To determine statistical significance, the values were compared by two group *t* tests. The differences were considered as significant if *p* values were less than 0.05.

RESULTS

Overexpression of Syn in MG63 Osteosarcoma Cells—To investigate the effect of syn on growth and differentiation of tumor cells, MG63 osteosarcoma cells were stably transfected with α- or β-syn cDNA. Three high expressors of α-syn (clones α1, α5, and α15) and β-syn (clones β5, β8, and β13) were selected on the basis of immunoblot analysis together with empty vector-transfected cells (clones v2, v5, and v10) (Fig. 1*A*). For the majority of experiments, clone α1, the high expresser of α-syn, and clones β5 and v2 were used. Immunoblot analysis also showed that the immunoreactivities of both α- and β-syn were almost exclusively those of their monomers (Fig. 1*A*). To further analyze expression and distribution of syn proteins, double immunolabeling/LSCM was performed using at least two antibodies for each syn (Fig. 1*B*). The immunoreactivity of α-syn in α-syn-overexpressing cells (α1) was diffuse in the cell bodies as detected by both monoclonal syn-1 and polyclonal C-terminal antibodies (*a* and *b*). Immunoreactivity of β-syn in β-syn-overexpressing cells (β5) was also localized diffusely in the cell bodies by monoclonal anti-β-syn antibody (*e*) but was detected with a shift to perinuclear regions by polyclonal anti-β-syn antibody (*f*). In none of these cases, inclusion bodies were detected. Notably, expression levels of α-syn were heterogeneous (*c*), and similar patterns were consistently observed in all the three clones of α-syn-overexpressing cells (data not shown). By contrast, immunoreactivities of β-syn were homogeneous in β-syn-overexpressing cells (*g*). No immunoreactivities of syn proteins were detected in vector-transfected cells (v2) (*d* and *h*).

To determine whether cell proliferation was affected by overexpression of syn, the stable clones were evaluated for their cell growth rates. The doubling times of cells in log phase of growth under 10% serum conditions were 20–24 h for α-syn-overexpressing cells and 14–17.5 h for both β-syn-overexpressing and vector-transfected cells (data not shown). Cells were then incubated under the low serum (0.1%) for 24 h to synchronize at G_1 in cell cycle and then added with 10% serum followed by counting of cell numbers at the indicated times. The result showed that that the average cell numbers of α-syn-overexpressing cells at day 4 were significantly decreased compared with both β-syn-overexpressing and vector-transfected cells (Fig. 1*C*).

To determine whether decreased cell proliferation of α-syn-overexpressing cells is due to alteration of cell cycle profile, cell cycle analysis was performed using flow cytometry at varying time periods (0, 6, 12, 18, 24, and 96 h) after the addition of 10% serum to serum-deprived cells. The result showed that compared with both β-syn-overexpressing and vector-transfected cells, α-syn cells in G_0/G_1 phases were significantly increased ($p < 0.05$), whereas those in both S and G_2/M phase were decreased at 24 and 96 h ($p < 0.05$) (Fig. 1*D*). Essentially similar results were observed at 96 h. However, compared with the profile at 24 h, there were more cells in G_0/G_1 phase, fewer cells in S phase, and more cells in G_2/M at 96 h. One possible reason for the difference between 24 and 96 h could be that at 24 h many cells might have not yet reached G_2/M phase. Furthermore, a relatively high ratio of cells in G_0/G_1 phase at 96 h could

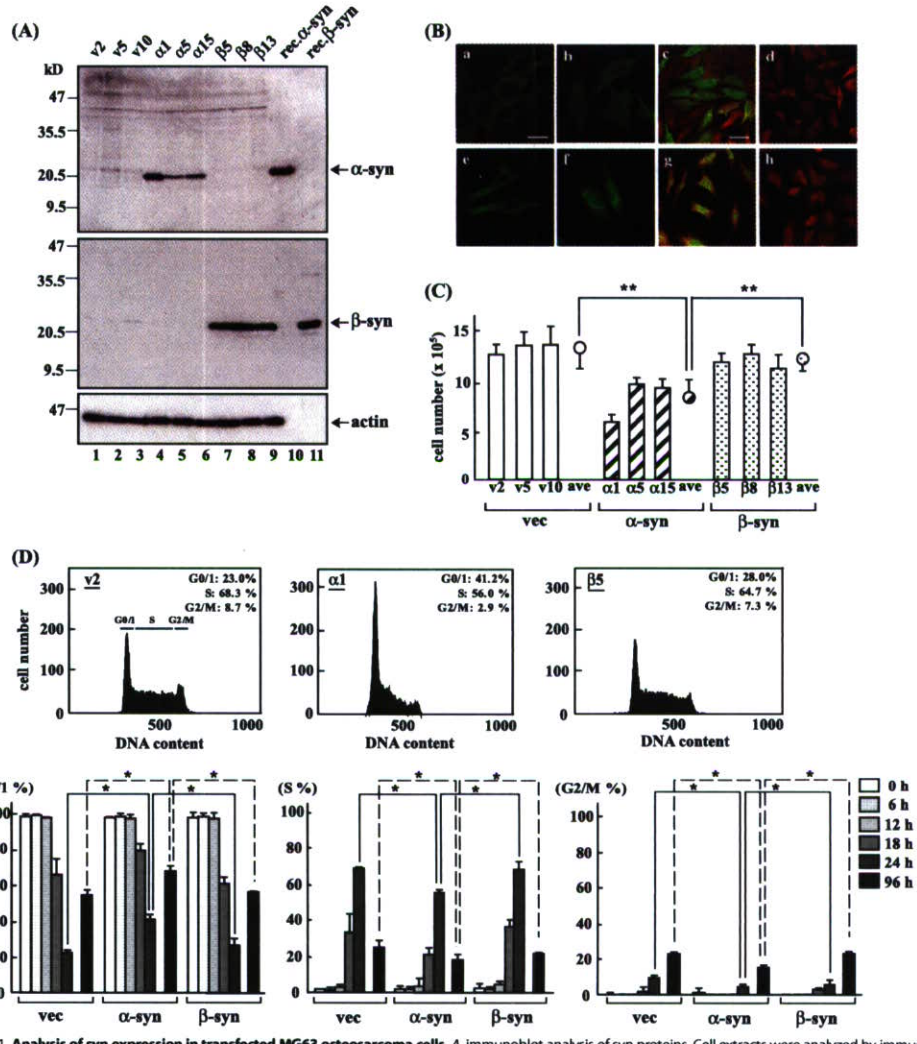

FIGURE 1. **Analysis of syn expression in transfected MG63 osteosarcoma cells.** *A*, immunoblot analysis of syn proteins. Cell extracts were analyzed by immunoblotting using syn-1 (*upper panel*), anti-β-syn monoclonal antibody (*middle panel*), and anti-actin antibody (*lower panel*). Three vector-transfected clones (v2, v5, v10, *lanes 1–3*), three high expresser clones for α-syn (α1, α5, α15, *lanes 4–6*), and β-syn (β5, β8, β13, *lanes 7–9*) are shown. Recombinant α- and β-syn proteins were used as positive controls (*lanes 10* and *11*). *B*, immunofluorescence/LSCM analysis of syn expression. α-Syn-overexpressing cells (α1) (*a–c*), β-syn-overexpressing cells (β5) (*e–g*), and vector-transfected cells (v2) (*d* and *h*) were immunostained with antibodies against α-syn (*green*, *a–d*), β-syn (*green*, *e–h*), and actin (*red*, *c*, *d*, *g*, and *h*) followed by observation by LSCM. α-Syn was diffusely distributed in the cell bodies with a slight shift to cell membrane as detected by both syn-1 (*a*) and polyclonal c-terminal antibody (*b*). β-Syn was similarly detected in the cell bodies by monoclonal anti-β-syn antibody (*e*), but strong stains of perinuclear regions were observed by polyclonal anti-β-syn antibody (*f*). Immunoreactivities of α-syn were heterogeneous (*c*), whereas those of β-syn were almost even in all cell populations (*g*). No immunoreactivities of syn proteins were detected in vector-transfected cells (*d* and *h*). *Bars* represent either 20 μm for high magnification (*a*, *b*, *e*, and *f*) or 50 μm for low magnification (*c*, *d*, *g*, and *h*). *C*, evaluation of cell proliferation. Cells (v2, v5, v10, α1, α5, α15, β5, β8, and β13) were incubated at 1×10^5 cells/well in the 6-well plates under the low serum (0.1%) conditions for 24 h to synchronize. Cells were then treated with 10% serum, and cell numbers were counted at 96 h. *Open circles* represent the group mean values. Data shown are the mean ± S.D. ($n = 3$). **, $p < 0.01$. *D*, flow cytometry for cell cycle analysis. Cells were prepared as described in *C*, and DNA contents were analyzed at the indicated times (0, 6, 12, 18, 24, and 96 h) after serum stimulation. The *upper figures* are a typical cell cycle profile at 24 h for v2, α1, and β5. The *x* axis represents the fluorescent intensities proportional to the amount of DNA, whereas the *y* axis indicates the cell number. The *lower column figures* show that G_0/G_1 phases at 24 and 96 h in α-syn cells were significantly increased, whereas those in both S and G_2/M phase were decreased compared with both β-syn-overexpressing and vector-transfected cells. Data presented are the mean ± S.D. of triple determinations. *, $p < 0.05$.

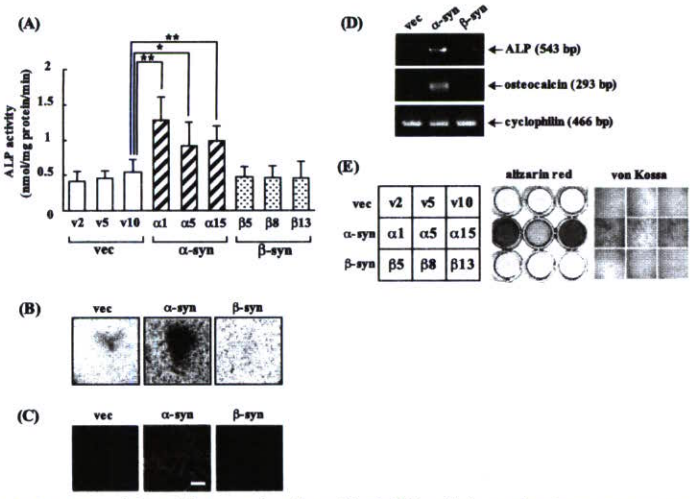

FIGURE 2. **Up-regulation of the expression of osteoblastic differentiation markers in α-syn-overexpressing MG63 cells.** *A*, measurement of ALP activity. Cells (v2, v5, v10, α1, α5, α15, β5, β8, and β13) under the confluent conditions were harvested, and cell extracts were incubated with *p*-nitrophenyl phosphate at 37 °C for 90 min. The amount of released nitrophenol was monitored by absorbance at 415 nm. α-Syn-overexpressing cells (α1) showed significantly higher ALP activity compared with other cell types (v2 and β5). Data shown are mean ± S.D. ($n = 5$). *, $p < 0.05$; **, $p < 0.01$. *B*, evaluation of ALP activity by staining. Cells (v2, α1, and β5) were stained with nitro blue tetrazolium chloride/5-bromo-4-chloro-3-indolyl phosphate solution and photographed. *C*, immunostaining of osteocalsin. Cells (v2, α1, and β5) were immunostained with anti-osteocalsin antibody followed by observation with LSCM. The *bar* represents 50 μm. *D*, RT-PCR analysis of ALP and osteocalcin mRNAs. Cyclophilin mRNA was used as an internal control. *E*, *in vitro* mineralization assay. Cells (v2, v5, v10, α1, α5, α15, β5, β8, and β13) were seeded onto 24-well cell culture plates (1×10^5 cells/ml) and maintained in α-minimal essential medium containing 10 mM β-glycerophosphate and 50 μg/ml ascorbic acid for 4 weeks. Matrix mineralization was evaluated by either alizarin red staining (*middle panel*) or von Kossa staining (*right panel*). Each clone number is indicated in the squire matrix (*left panel*). Please note that the strongest staining was observed in clone α1, the highest α-syn expresser.

be due to the decreased nutrients in the culture medium after long time culture. Taken together, these results suggested that overexpression of α-syn, but not of β-syn, suppressed cell proliferation in MG63 osteosarcoma cells.

α-Syn-overexpressing MG63 Cells Exhibit Enhanced Differentiation Phenotype—Based on the apparent decrease of growth rates and enhanced G_0/G_1 phases in cell cycle in α-syn-overexpressing MG63 cells compared with β-syn-overexpressing and vector-transfected cells, we speculated that the former cells might be shifted to cellular differentiation.

To test this possibility, we evaluated ALP since this molecule had been widely used as a marker for osteoblastic differentiation. As we suspected, all three clones of α-syn-overexpressing cells displayed significantly higher activity of ALP compared with both β-syn-overexpressing and vector-transfected cells (Fig. 2*A*). Activation of ALP was also assessed by direct stain of cells using nitro blue tetrazolium chloride/5-bromo-4-chloro-3-indolyl phosphate as substrate. The result showed that the intensity of the staining in α-syn-overexpressing cells was much stronger than those of β-syn-overexpressing and vector-transfected cells (Fig. 2*B*). Next, we analyzed expression of osteocalcin, another marker for osteoblastic differentiation. The immunofluorescence/LSCM study showed that immunoreactivity of osteocalcin was strongly observed in α-syn-overexpressing cells but not in other cell types (Fig. 2*C*). Furthermore, RT-PCR analysis revealed that up-regulation of ALP and osteocalcin in α-syn-overexpressed cells might be attributed to increased transcription (Fig. 2*D*). To further corroborate that cellular differentiation is accelerated in α-syn-overexpressing cells, we evaluated formation of mineral deposition in the matrix that may mimic the calcification by osteoblasts *in vivo*. For this purpose, cells were incubated in the presence of β-glycerophosphate and ascorbic acid for 4 weeks followed by staining with alizarin red to assess calcium incorporation. The result showed that mineralization was clearly detectable in α-syn-overexpressing cells but not in β-syn-overexpressing nor vector-transfected cells (Fig. 2*E*). Similar results were obtained by von Kossa staining for the assessment of bone nodule formation (Fig. 2*E*). Taken together, α-syn-overexpressing cells specifically exhibited a differentiated phenotype compared with both β-syn-overexpressing and vector-transfected cells.

Alteration of G_1 Cell Cycle Regulators and Decreased Proteasome Activity in α-Syn-overexpressing MG63 Cells—Because prolonged G_1 period in cell cycle is prerequisite for cell entry into G_0 and further differentiation, it was predicted that expressions and activities of various G_1 cell cycle regulators might be altered in α-syn-overexpressing cells.

To test this possibility, cells were incubated under the low serum (0.1%) conditions for 24 h to synchronize at G_1 followed by 10% serum treatment. Cells were then harvested, and expression of various cell cycle regulators were analyzed at the indicated times (Fig. 3*A*). Notably, expression of the cyclin-dependent kinase inhibitor p21, one of the key molecules which negatively regulate cell cycle progression from G_1 to S phase, was significantly up-regulated in α-syn-overexpressing cells. In these cells p21 was constitutively expressed without serum stimulation and was further increased in response to serum, reaching the maximum around 6- 12 h followed by gradual decrease. By contrast, in vector-transfected cells expression of p21 was transiently up-regulated at 6 h and immediately decreased. Consistent with this, phosphorylation of Rb protein was compromised in α-syn-expressing cells compared with vector-transfected cells. Furthermore, cyclin B1, a marker for G_2/M phase, was up-regulated earlier in vector-transfected cells than in α-syn-overexpressing cells. As for other cyclin-dependent kinase inhibitors, p15 level was slightly elevated at 24- and 48-h time points, whereas expression of p27 was not up-regulated in α-syn-overexpressing cells compared with vector-transfected cells (Fig. 3*A* and data not shown). Expression of other cell cycle regulators such as cyclin D1 and cyclin-dependent kinase 4 were not much different between both cell types. Similar expression patterns of p21 and phosphorylated Rb were observed between β-syn-overexpressing cells and vector-transfected cells (data not shown).

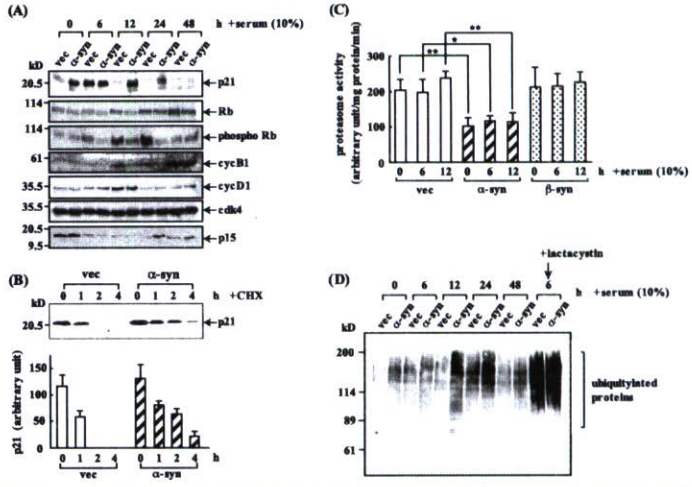

FIGURE 3. **Altered expression of cell cycle regulators and decrease of proteasome activity in α-syn-overexpressing MG63 cells.** *A*, immunoblot analysis of cell cycle regulators. Vector-transfected (v2) and α-syn-overexpressing cells (α1) were incubated under the low serum (0.1%) conditions for 24 h to synchronize and then treated with 10% serum for the indicated times (6, 12, 24, and 48 h). Cells were then harvested, and cell lysates were analyzed by immunoblotting with anti-p21, Rb, phospho Rb, cyclin (*cyc*) B, cyclin D1, cyclin-dependent kinase (*Cdk4*), p15, and ubiquitin. *B*, evaluation of the stability of p21 protein by cycloheximide experiments. The synchronized cells (v2 and α1) were treated with 10% serum with or without cycloheximide (*CHX*) for the indicated times (1, 2, and 4 h), and cell lysates were analyzed by immunoblotting (*upper panel*). Each band was quantified using BioMax 1D image analysis soft ware (*lower panel*). Data shown are the mean ± S.D. Similar results were obtained by three independent experiments. *C*, measurement of proteasome activity. Cells (v2, α1, and β5) were incubated under the low serum (0.1%) conditions for 24 h and then treated with 10% serum for the indicated times (6 and 12 h). To evaluate proteasome activity, cell extracts (10 μg) were incubated with fluorogenic substrate (benzyloxycarbonyl-Leu-Leu-Glu-amidomethylcoumarin) at 37 °C. Released fluorescence (excitation 380 nm, emission 460 nm) was monitored by 5 min intervals up to 60 min. The fluorogenic value at each time point was plotted, and the slope was calculated. Data shown are the mean ± S.D. ($n = 3$). *, $p < 0.05$; **, $p < 0.01$. *D*, immunoblot analysis of ubiquitylated proteins. Vector-transfected (v2) and α-syn-overexpressing cells (α1) were prepared as described in *A* and analyzed by immunoblotting using anti-ubiquitin antibody. Both types of cells treated with lactacystin for 6 h were included as positive controls.

Next, to determine whether up-regulation of p21 expression was due to the stabilization of p21 protein in α-syn-overexpressing cells, these cells were treated with cycloheximide to inhibit protein synthesis 6 h after serum stimulation. Under these conditions, expression levels of p21 protein quickly decreased within 2 h of treatment in vector-transfected cells, whereas expression levels in α-syn-overexpressing cells took longer to detect (Fig. 3*B*). Under the same experimental conditions, p21 mRNA was evaluated by real time PCR. However, no significant differences were observed between α-syn-overexpressing and vector-transfected cells (data not shown).

To further determine whether increased stability of p21 was due to compromised degradation by UPS in α-syn-overexpressing cells, syn-transfected cells were analyzed for proteasome activities. The result showed that the proteasome activities of α-syn-overexpressing cells were decreased to ~50% of those of vector-transfected cells, whereas those of β-syn-overexpressing cells were little affected (Fig. 3*C*). Under the same experimental conditions, immunoreactivities of polyubiquitylated proteins were significantly stronger in α-syn-overexpressing cells compared with those in vector-transfected and β-syn-overexpressing cells (Fig. 3*D* and data not shown). Taken together, expression of cell cycle regulators such as p21 and phosphorylated Rb were altered in α-syn-overexpressing cells, which might be attributed to the decreased proteasome activity.

Proteasome Inhibitors Stimulate Differentiation of Wild-type MG63 Cells—If suppression of proteasome activity by α-syn plays a causative role for stimulation of differentiation in MG63 osteosarcoma cells, then it is possible that down-regulation of proteasome activity by other experimental procedures might similarly stimulate differentiation in these cells.

To test this possibility, wild-type MG63 cells were treated with proteasome inhibitors, including MG132 and lactacystin followed by evaluation of cellular differentiation. Immunoblot analysis revealed that administration of these reagents at 10 μM clearly up-regulated p21 expression at 12 h (Fig. 4*A*). Under the same experimental conditions, ALP activity was significantly up-regulated, and immunoreactivity of osteocalcin became detectable (Fig. 4*B* and data not shown). In addition, the expression of ALP and osteocalcin mRNA was up-regulated in lactacystin-treated cells (Fig. 4*C*). Furthermore, cells were induced to form matrix mineralization with lower concentrations of proteasome inhibitors (0.01–0.1 μM for MG132 and 0.1–1.0 μM for lactacystin) in long-term cultures. High concentration (10 μM) treatment of these reagents caused prominent cell death within 48 h (data not shown). By contrast, sublethal concentrations (0.01–0.1 μM) of rotenone, an inhibitor of mitochondria complex I, caspase I, and III inhibitors (0.1–1.0 μM), and leupeptin (1–10 μM) had little effect on cellular differentiation (Fig. 4*D*). Taken together, treatment of wild-type MG63 cells with proteasome inhibitors resulted in stimulation of cellular differentiation.

Down-regulation of PKC Activity in α-Syn-overexpressing MG63 Cells—Our hypothesis was that alteration of signal transduction might be involved in the suppression of proteasome activity in α-syn-overexpressing cells. In this regard we especially focused on the potential role of PKC since it was recently shown that treatment of skeletal muscle by phorbol

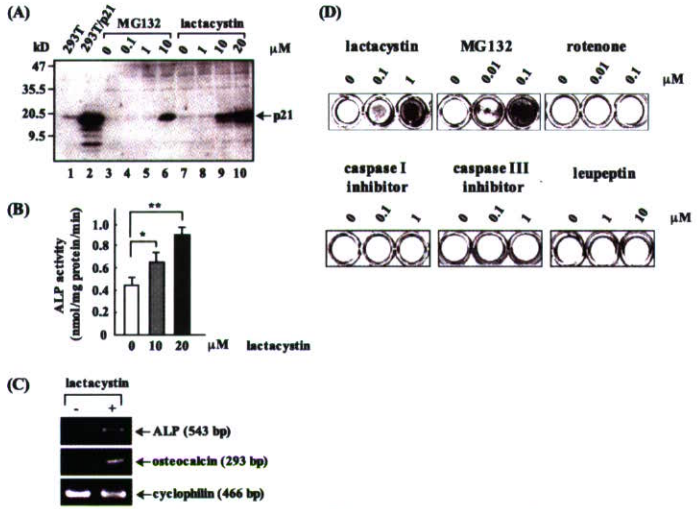

FIGURE 4. **Proteasome inhibitors induce cellular differentiation in wild-type MG63 cells.** Wild-type MG63 were incubated under the low serum (0.1%) conditions for 24 h and then treated with 10% serum in the presence of either MG132 or lactacystin. *A*, immunoblot analysis of p21. Cells were treated with various concentrations of either MG132 (0, 0.1, 1.0, 10 μM, *lanes 3–6*) or lactacystin (0, 1.0, 10, 20 μM, *lanes 7–10*) and harvested at 12 h. Cell lysates were analyzed by immunoblotting using anti-p21 antibody. Extracts of 293T cells transfected with or without p21 expression vector are shown as controls (*lanes 1* and *2*). *B*, measurement of ALP activity. Cells were treated with various concentrations (0, 10, 20 μM) of lactacystin for 12 h. To evaluate ALP activity, cell extracts were incubated with *p*-nitrophenyl phosphate at 37 °C for 90 min. The amount of released nitrophenol was monitored by the absorbance at 415 nm. Data shown in the *left panel* are the mean ± S.D. ($n = 3$). *, $p < 0.05$; **, $p < 0.01$. *C*, RT-PCR analysis of ALP and osteocalcin mRNAs. Cells were treated with lactacystin (10 μM) for 24 h. Cyclophilin mRNA was used as an internal control. *D*, *in vitro* mineralization assay. Cells were treated with various reagents, including MG132 (0, 0.01, 0.1 μM), lactacystin (0, 0.1, 1.0 μM), rotenone (0, 0.1, 0.1 μM), caspase I inhibitor (0, 0.1, 1.0 μM), caspase III inhibitor (0, 0.1, 1.0 μM), and leupeptin (0, 1, 10 μM) for 4 weeks. Matrix mineralization was evaluated by alizarin red staining. Please note that positive staining was observed for cells treated with proteasome inhibitors. Acridine orange/ethidium bromide staining revealed that cells were alive during mineralization (not shown).

ester resulted in stimulation of proteasome activity (39) and it was previously shown that α-syn bound with PKC and down-regulated the activity of PKC in α-syn overexpressing neuroblastoma cells (40).

To determine whether α-syn associates with PKC, a co-immunoprecipitation experiment was performed (Fig. 5*A*). Cell extracts of α-syn-overexpressing cells were immunoprecipitated with syn-1 followed by immunoblotting analysis with mouse anti- PKCε antibody. In agreement with a previous study by Ostrerova *et al.* (40), the result showed that PKCε was specifically co-immunoprecipitated with α-syn.

Next, to further determine whether α-syn colocalize with PKC, cells were double-immunolabeled with anti-α-syn rabbit polyclonal antibody and anti-PKCε antibody followed by observation with LSCM. As shown in Fig. 5*B*, immunoreactivities of α-syn and PKCε considerably overlapped in the cytoplasm of α-syn-overexpressing cells. We observed that PKCε and PKCλ were highly expressed in addition to moderate expression of other PKC family of peptides in MG63 cells (data not shown). Similar results were obtained by both co-immunoprecipitation and double immunolabeling/LSCM studies for PKCλ (data not shown).

Finally, to determine whether PKC activity was compromised in α-syn-overexpressing cells, the syn-transfected cells were treated with or without PMA and analyzed for their PKC activities (Fig. 5*C*). The result showed that proteasome activities of α-syn-overexpressing cells were significantly lower than those of β-syn-overexpressing and vector-transfected cells. Importantly, PMA treatment of α-syn-overexpressing cells restored the PKC activity to the basal levels of those in other cell types. Taken together, these results suggested that α-syn might directly suppress the PKC activity in α-syn-overexpressing cells.

Because previous studies suggested an alternative possibility that α-syn bound with S6 subunit of 19 S proteasome, leading to interference with proteasome functions (41–43), we investigated the association of α-syn with S6a. The results of co-immunoprecipitation experiment confirmed the association of these molecules (Fig. 5*A*). Double immunolabeling/LSCM showed that overlapping of the immunoreactivities of these molecules was partially detected in the cell bodies, since S6a was considerably localized in the nucleus (Fig. 5*B*).

Phorbol Ester Treatment of α-Syn-overexpressing MG63 Cells Restores Proteasome Activity and Suppresses Cellular Differentiation—If suppression of PKC activity by α-syn is causative for down-regulation of proteasome activity and enhanced differentiation in α-syn-overexpressing cells, then stimulation of PKC might restore the proteasome activity and abrogate cellular differentiation in these cells.

Accordingly, α-syn-overexpressing cells were treated with phorbol ester followed by evaluation of proteasome activity. The results showed that the compromised activity of proteasome in α-syn-overexpressing cells was significantly improved by treatment with PMA both at 10 and 50 nM but not with an inactive analogue 4αPDD (Fig. 6*A*). On the other hand, although proteasome activity of vector-transfected cells was increased by treatment with 50 nM PMA, there were little effects observed at 10 nM PMA (Fig. 6*A*). Thus, α-syn-overexpressing cells responded more sensitively to PMA treatment, suggesting the effect of PMA on proteasome was more specific for α-syn-overexpressing cells, which showed decreased proteasome activity. The stimulatory effects of PMA on the proteasome activity in α-syn-overexpressing cells reached the maximum at 50 nM (data not shown) and were completely abro-

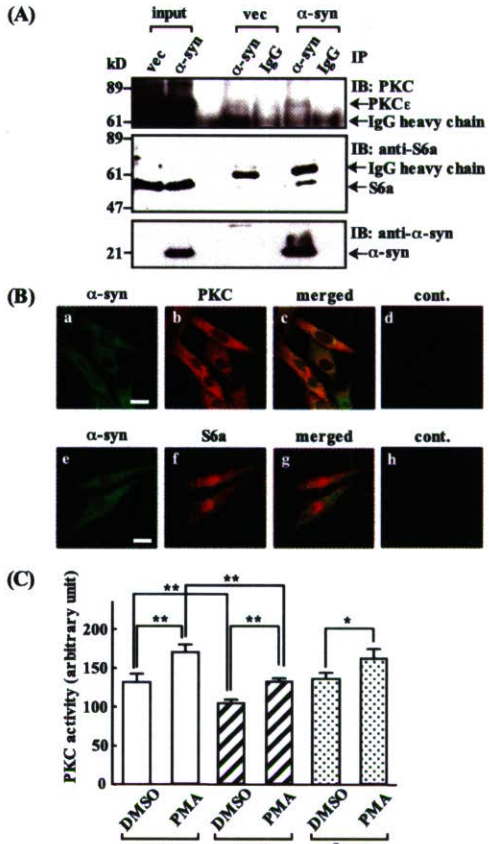

FIGURE 5. **Association of α-syn with PKC and down-regulation of PKC activity in α-syn-overexpressing MG63 cells.** *A*, coimmunoprecipitation (*IP*) of α-syn with either PKCε (*upper*) or S6a (*middle*). Vector-transfected (v2) and α-syn-overexpressing cells (α1) were harvested, and cell extracts (300 μg) were immunoprecipitated with anti-α-syn antibody or mouse IgG control followed by immunoblotting (*IB*)with either anti-PKCε (*upper*), anti-S6a (*middle*), or syn-1 (*low*). Cell extracts (5% of input) were used as positive controls. *B*, immunofluorescence/LSCM of α-syn association with either PKCε or S6a in α-syn-overexpressing cells. Cells (α1) were doubly stained with anti-α-syn antibody (*green*) and either anti-PKCε or S6a (*red*) and observed by LSCM. Please note that α-syn (*red*) and PKCε (*green*) were well co-localized in the cell bodies (*c*). *Bars* represent 50 μm. *C*, measurement of PKC activity. Exponentially growing cells (v2, α1, and β5) were treated with or without PMA for 20 min, and cell extracts (10 μg) were analyzed for PKC activity using fluorogenic peptides as substrates as described under "Experimental Procedures." Data shown are the mean ± S.D. ($n = 3$). *, $p < 0.05$; **, $p < 0.01$. *DMSO*, dimethyl sulfoxide.

gated in the presence of PKC inhibitor, chelerythrine chloride (Fig. 6*A*), implying that PMA stimulated proteasome activity through phosphorylation but not through depletion of PKC.

Next, to determine whether PKC stimulation of proteasome activity modifies differentiation in α-syn-overexpressing cells, cellular differentiation markers were analyzed. Compared with

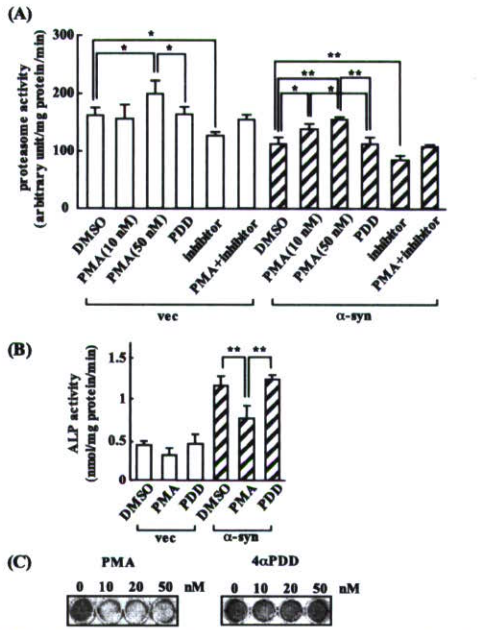

FIGURE 6. **Phorbol ester treatment restores proteasome activity and abrogates differentiation in α-syn-overexpressing MG63 cells.** *A*, measurement of proteasome activity. Vector-transfected (v2) and α-syn-overexpressing cells (α1) were incubated under the low serum (0.1%) conditions for 24 h and then treated with 10% serum in the presence of any of vehicle (0.1% Me_2SO (*DMSO*)), PMA (10 and 50 nM), 4αPDD (50 nM), chelerythrine chloride (PKC inhibitor, 50 nM), or PMA (50 nM) plus chelerythrine chloride (50 nM). Cell extracts (5 μg) were harvested at 12 h after treatment and incubated with fluorogenic proteasome substrate at 37 °C. Released fluorescence (excitation, 380 nm; emission, 460 nm) was monitored each 5 min up to 60 min. Fluorogenic intensity of each time point was plotted, and the slope was calculated. Data shown are the mean ± S.D. ($n = 3$). **, $p < 0.01$. *B*, measurement of ALP activity. Vector-transfected (v2) and α-syn-overexpressing cells (α1) were treated as described in *A*. Cell extracts at 12 h treatment were incubated with *p*-nitrophenyl phosphate at 37 °C for 90 min. The amount of released nitrophenol was monitored by the absorbance at 415 nm. Data shown are the mean ± S.D. ($n = 3$). *, $p < 0.05$; **, $p < 0.01$. *C*, *in vitro* mineralization assay. α-Syn-overexpressing cells (α1) were treated with either PMA or 4αPDD at the indicated concentrations (0, 10, 20, 50 nM). Matrix mineralization was then evaluated by alizarin red staining. Please note that the staining was mitigated by PMA but not by 4αPDD. Similar results were obtained by three independent experiments.

treatment with either vehicle or inactive 4αPDD, PMA efficiently reduced ALP activity in α-syn-overexpressing cells (Fig. 6*B*). Immunoreactivity of osteocalcin was also decreased by PMA but not by 4αPDD in these cells (data not shown). Finally, it was confirmed that PMA, but not 4αPDD, significantly reduced matrix mineralization in α-syn-overexpressing cells as demonstrated by decreased stains of alizarin red (Fig. 6*C*). Taken together, PMA treatment of α-syn-overexpressing cells restored proteasome activity and abrogation of cellular differentiation in these cells.

Up-regulation of Lysosomal Activity in α-Syn-overexpressing MG63 Cells—Because a recent study has shown that autophagy-lysosomal pathway may play an important role for aggre-

gate-prone proteins, including α-syn and Huntingtin (44), it is reasonable to speculate that down-regulation of proteasome activity by α-syn might be further modulated by this pathway.

In this context we wondered if lysosomal activity might be altered due to increased level of α-syn expression in α-syn-overexpressing cells. To test this hypothesis, cysteine protease cathepsin B, one of the major protease in lysosome, was evaluated. The results showed that cathepsin B was significantly up-regulated in α-syn-overexpressing cells compared with vector-transfected and β-syn-overexpressing cells (Fig. 7*A*). Consistent with this, expression of cathepsin B was up-regulated at protein and mRNA levels in α-syn-overexpressing cells (Fig. 7*B*, data not shown). To investigate the ultrastructure of lysosome, an electron microscopic study was performed. The results revealed extensive lysosomal pathology, such as autolysosome and myelinosome, in α-syn-overexpressing cells (Fig. 7*C*, *a*, *c*, *e*, and *f*). On the contrary, fewer lysosomes were observed in vector-transfected and β-syn-overexpressing cells (Fig. 7*C*, *b* and *d*). Taken together, these results suggested that lysosomal activity was up-regulated in α-syn-overexpressing cells.

Autophagy-lysosomal Inhibitor Treatment Results in Down-regulation of Proteasome Activity, Leading to Acceleration of Cellular Differentiation in α-Syn-overexpressing MG63 Cells—If up-regulation of lysosomal activity in α-syn-overexpressing cells may reflect the compensatory mechanism against the increased level of α-syn, then suppression of autophagy-lysosomal pathways may result in compromised clearance of α-syn, leading to decrease proteasome activity and accelerate cellular differentiation in those cells.

We first evaluated expression levels of α- and β-syn proteins in the presence of autophagy-lysosomal inhibitors. The results of immunoblot analysis showed that α- and β-syn proteins were up-regulated by macroautophagy inhibitor 3-MA as well as by ammonium chloride, which inhibits lysosomal activity independently of the form of autophagy. By contrast, proteasome inhibitor lactacystin had little effect on the expression of both α- and β-syn proteins (Fig. 8*A*). Thus, these results suggested that α- and β-syn were preferentially degraded by autophagy-lysosomal pathway.

Then, to determine whether down-regulation of autophagy-lysosomal activity affects proteasome function, proteasome activity was evaluated by treatment with autophagy-lysosomal inhibitors. The result showed that treatments with autophagy-lysosomal inhibitors significantly decreased proteasome activities in α-syn-overexpressing cells but not in other cell types (Fig. 8*B*). By contrast, inhibition of proteasome by lactacystin had little effect on cathepsin B activity (data not shown). Similarly, treatment of PMA, which was shown to stimulate proteasome activity (Fig. 6), had little effects on cathepsin B activity (data not shown).

Finally, it was shown that treatment with both 3-MA and ammonium chloride significantly stimulated ALP activity, osteocalcin expression, and matrix mineralization in α-syn-overexpressing cells compared with other cell types (Fig. 8, *C* and *D*, data not shown). Taken together, inhibition of autophagy-lysosomal activity in α-syn-overexpressing cells resulted in down-regulation of proteasome activity, leading to stimulate cellular differentiation. Thus, these results suggest that autophagy-lysosomal pathway may mitigate the down-regulation of proteasome activity by α-syn, therefore leading to abrogate cellular differentiation by α-syn.

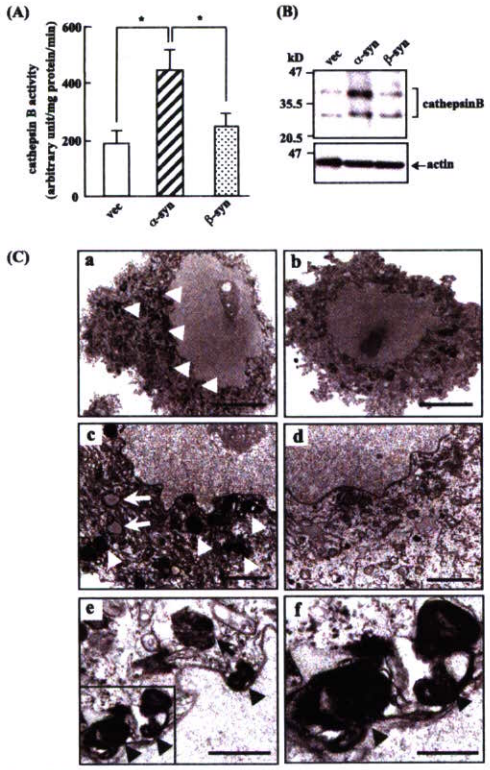

FIGURE 7. **Up-regulation of lysosomal activity in α-syn-overexpressing MG63 cells.** *A*, measurement of cathepsin B activity. Cell extracts (10 μg) were prepared as described under "Experimental Procedures" were analyzed for cathepsin B activity using fluorogenic substrates. Released fluorescence (excitation, 380 nm; emission, 460 nm) was monitored each 5 min up to 60 min. Fluorogenic intensity of each time point was plotted, and slope was calculated. Data shown are the mean ± S.D. ($n = 3$). *, $p < 0.05$; **, $p < 0.01$. *B*, immunoblot analysis of cathepsin B. Cell extracts (v2, α1, and β5) were analyzed by immunoblotting using anti-cathepsin B antibody (*upper panel*) and anti-actin antibody (*lower panel*). *C*, electron microscopic analysis. Typically, α-syn-overexpressing cells (α1: *a*, *c*, *e*, and *f*) exhibited numerous enlarged electron-dense lysosomes (*white arrowheads*), vacuoles that might have already discharged their contents (*white arrows*), autolysosome-like body (*black arrow*), and myelinosome-like structures (*black arrowheads*). The enclosed area in *panel e* is magnified in *panel f*. Fewer lysosomal structures were found in vector-transfected cells (v2, *b*) and β-syn-overexpressing cells (β5, *d*). *Bars* represent 8 μm (*a* and *b*, x1500), 2 μm (*c* and *d*, ×5000), 1 μm (*e*, ×13000), or 0.5 μm (*f*, ×26000).

DISCUSSION

Although α-syn was previously shown to be expressed in the brain tumors that preferentially displayed differentiation rather than proliferation, little has been documented regarding the role of

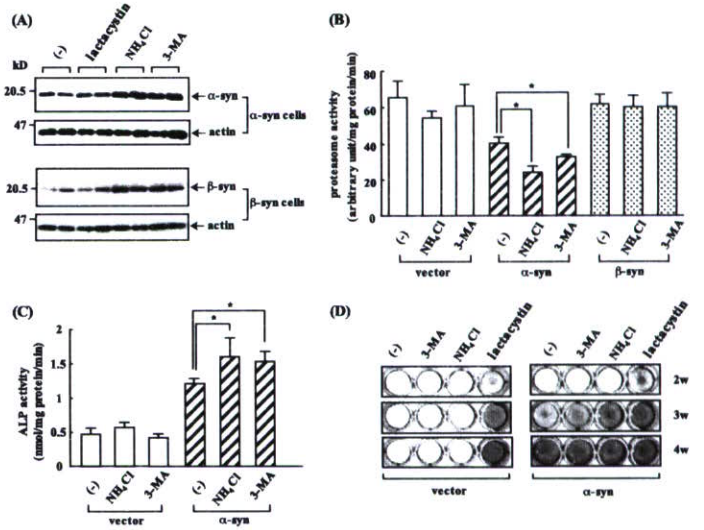

FIGURE 8. **Autophagy-lysosome inhibitor treatment decreases proteasome activity and stimulates cellular differentiation in α-syn-overexpressing MG63 cells.** *A*, immunoblot analysis of syn proteins. Cells (α1, and β5) were incubated under the low serum (0.1%) conditions for 24 h and then treated with 10% serum in the presence of lactacystin (10 μM), ammonium chloride (NH_4Cl) (20 mM), and 3-MA (10 mM) for 24 h. Cell lysates were analyzed by immunoblotting using syn-1 (*upper panel*) and anti-β-syn monoclonal antibody (*low panel*). Blots were reprobed with anti-actin antibody. Similar results were obtained by three independent experiments. *B*, measurement of proteasome activity. Cells (v2, α1, and β5) were prepared as described in *A*. Cell extracts (5 μg) were harvested and incubated with fluorogenic proteasome substrate at 37 °C. Released fluorescence (excitation, 380 nm; emission, 460 nm) was monitored each 5 min up to 60 min. Fluorogenic intensity of each time point was plotted, and slope was calculated. Data shown are the mean ± S.D. ($n = 3$). Please note that proteasome activity was significantly decreased in α-syn-overexpressing cells by ammonium chloride treatment (*, $p < 0.05$). *C*, measurement of ALP activity. Vector-transfected (v2) and α-syn-overexpressing cells (α1) were prepared as described in *A*. Cell extracts at 12 h of treatment were incubated with *p*-nitrophenyl phosphate at 37 °C for 90 min. The amount of released nitrophenol was monitored by the absorbance at 415 nm. Data shown are the mean ± S.D. ($n = 3$). *, $p < 0.05$; **, $p < 0.01$. *D*, *in vitro* mineralization assay. Vector-transfected (v2) and α-syn-overexpressing cells (α1) were treated with ammonium chloride (10 mM), 3-MA, (10 mM), or lactacystin (1 μM) for 2–4 weeks (*2W–4W*). Matrix mineralization was then evaluated by alizarin red staining. Please note that the staining was stimulated by ammonium chloride and to a lesser extent by 3-MA in α-syn-overexpressing cells but not in vector-transfected cells. Similar results were obtained by three independent experiments.

α-syn for tumor differentiation. The present study showed that α-syn-overexpressing MG63 osteosarcoma cells specifically exhibited phenotype of osteoblastic differentiation. Compared with both β-syn-overexpressing and vector-transfected cells, α-syn-overexpressing cells were characterized by decreased growth rates, associated with increased expression of p21 and reduced phosphorylated Rb (Figs. 1 and 3), indicating that the progression from G_1 to S phase was compromised in these cells. The prolonged G_1 phase would be prerequisite for transition from G_1 to G_0 and subsequent cellular differentiation. Consistent with this view, osteoblastic differentiation markers, including ALP and osteocalcin, were significantly up-regulated in α-syn-overexpressing cells compared with other cell types (Fig. 2). Furthermore, α-syn-overexpressing cells, but not other cell types, were induced to form matrix mineralization during long-term cultures (Fig. 2). Taken together, our results using osteosarcoma cells support the contention that α-syn might stimulate tumor differentiation.

Because proteasome activity was significantly lower in α-syn-overexpressing cells compared with both β-syn-overexpressing and vector-transfected cells (Fig. 3), it was assumed that down-regulation of proteasome activity by α-syn could be at play for accelerated cellular differentiation in α-syn-overexpressing cells. Supporting this notion, expression levels of p21 were up-regulated due to increased stability at the protein level. Furthermore, high molecular weight proteins with polyubiquitylation were also significantly accumulated (Fig. 3). Thus, it was interpreted that decreased proteasome activity might result in prolonged G_1 phase of cell cycle, which could be prerequisite for proliferating cells to escape from cell cycle and proceed to differentiation. Indeed, it has been well described that proteasome inhibitors stimulated cellular differentiation in a variety of cell types, including osteoblastic cells (45), PC12 cells (46, 47), and oligodendrocytes (48). For example, proteasome inhibitors induced osteoblastic differentiation and bone formation *in vitro* and *in vivo*, which were associated with up-regulation of bone morphogenetic protein-2 (45). It was also shown that proteasome inhibitors stimulated neurite outgrowth in PC12 cells through activation of c-Jun NH_2-terminal kinase signaling pathway (46, 47). We also confirmed that treatment of wild-type MG63 cells with proteasome inhibitors, such as MG132 and lactacystin, resulted in similar differentiation phenotype as characterized by increased expression of p21, up-regulation of ALP and osteocalcin, and enhanced matrix mineralization (Fig. 4).

Then, what is the mechanism through which α-syn suppresses proteasome activity? In this regard several reports have already documented a possibility that α-syn may directly interfere with the proteasome. Based on two-hybrid screening, α-syn was shown to bind to S6′, a component of the 19 S subunit in the 26 S proteasome, in cell cultures (41). Subsequently, it was shown that aggregated α-syn, but not its monomeric form, efficiently inhibited the activity of the 26 S proteasome under the cell-free conditions (42, 43, 49). Using α-syn-overexpressing MG63 cells, we observed that S6a was co-precipitated with α-syn by co-immunoprecipitation experiment, although immunofluorescence/LSCM study revealed that these molecules were partially colocalized in the cytoplasm (Fig. 5). Although we failed to observe any evidence of aggregated α-syn by both immunoblotting and immunofluorescence/LSCM (Fig. 1*B*, *a* and *b*), one possible explanation for supporting the pos-

sibility of the direct suppression of proteasome by α-syn could be that misfolded monomer of α-syn rather than SDS-resistant oligomers/high molecular aggregates might be at play for the suppression of proteasome functions in α-syn-overexpressing MG63 cells. In contrast to α-syn, β-syn, a less aggregate-prone protein that is non-amyloidogenic under the physiological conditions, had little effect on proteasome activity. The result is consistent with the previous report by Snyder *et al.* (49).

An alternative possibility that we favor is that alteration of signal transduction might play an important role for suppression of proteasome activity in α-syn-overexpressing cells. Indeed, it has been shown that various signaling molecules in mitogen-activated protein kinase and phosphatidylinositol 3-kinase pathways were altered by accumulation of α-syn in a variety of cell cultures (35, 50). In the present study the role of the PKC signaling pathway was addressed for the regulation of proteasome activity because it was recently shown that treatment of skeletal muscle with phorbol ester stimulated proteasome activity (39). Consistent with a previous study using neuroblastoma cells and human brains (40), α-syn was shown to bind with PKC, thereby down-regulating the activity of this molecule in α-syn-overexpressing MG63 cells (Fig. 5). Furthermore, treatment of α-syn-overexpressing cells with PMA significantly restored the proteasome activity and abrogated differentiation in these cells (Fig. 6). Thus, proteasome activities were inversely correlated with the extent of differentiation, reinforcing the concept that suppression of proteasome activity by α-syn may accelerate differentiation. Although the precise mechanism by which the proteasome is activated by PKC stimulation requires further investigation, it is possible that phosphorylation might be involved. Supporting this notion, it was recently shown that phosphorylation of α subunits of 20 S proteasome by various stimuli, such as γ-interferon and casein kinase II, was important for the regulation of the stability of 26 S proteasome complexes in mammalian cells (51). Taken together, proteasome activity may be regulated through phosphorylation by signal transduction pathways, including PKC, which may be down-regulated by accumulation of α-syn.

Given the emerging role of autophagy-lysosomal pathway for the degradation of α-syn (52, 53), it is probable that alteration of this pathway may affect α-syn-mediated suppression of proteasome activity. Indeed, the present study showed that the lysosomal activity was significantly up-regulated in α-syn-overexpressing cells compared with other cells (Fig. 7). Furthermore, in α-syn-overexpressing cells, inhibition of the autophagy-lysosomal pathway resulted in down-regulation of proteasome activity associated with up-regulation of α-syn, whereas inhibition of proteasome activity had little effect on autophagy-lysosomal activity with little change of α-syn, suggesting that autophagy-lysosomal pathway is dominant to negatively regulate proteasome activities in these cells (Fig. 8). Together, these results suggest that lysosomal activity was up-regulated due to the compensatory mechanisms against increased level of α-syn. It has been recently shown that the autophagy-lysosomal pathway has pleiotropic roles in the regulation of cancer (54). For example, this pathway may be indispensable to tumors that must frequently survive under the nutrient-poor environments. Conversely, loss of function of this pathway might be beneficial because of accumulation of genotoxic substances in the cytoplasm that could promote mutation and, hence, tumorigenesis. The present study may provide a novel mechanism that the autophagy-lysosomal degradation pathway might negatively modulate the UPS-regulated cellular differentiation in α-syn-overexpressing tumors.

Because the identification of gene mutations of parkin in recessive familial PD and further characterization of this molecule as a ubiquitin E3 ligase, it has been extensively shown that dysfunction of UPS may be one major pathogenic pathway for PD and related neurodegenerative disorders. In this context, much literature has described that overexpression of α-syn was shown to result in decreased proteasome activities in a variety of biological system, including yeast (55) and the inducible expression system in PC12 cells (56), whereas some studies described that suppression of proteasome activity was not observed either in transgenic mice or in some cell cultures, including PC12 and 293 cells (37). Our results are in line with the former reports and further suggest that down-regulation of UPS by α-syn may play an important role for cells to escape from cell cycle and commit to cellular differentiation. Although little has been documented regarding the role of α-syn for cell cycle, Lee *et al.* (57) previously showed that inducible expression of α-syn in PC12 cells resulted in enhanced proliferation rates through stimulation of ERK pathway whereby cells were enriched in the S phase associated with increased accumulation of cyclin B and down-regulation of Rb (57). The reason for the apparent discrepancy between the report by Lee *et al.* (57) and our present study is obscure. However, one possible explanation is that effects of α-syn on growth and differentiation might be cell type-specific. Indeed, it was shown that inducible expression of α-syn in neuro2A cells resulted in inactivation of ERK and other mitogen-activated protein kinase signals (58). Taken together, although our results using MG63 osteosarcoma cells suggest a role of α-syn for tumor differentiation, further investigation is required to confirm our current findings *in vivo*.

In conclusion, our results showed that accumulation of α-syn might result in down-regulation of proteasome activity, leading to accelerate cellular differentiation in osteosarcoma cells. This process is further modulated by various factors, including PKC signaling pathway as well as autophagy-lysosomal activity. Moreover, because a recent study has shown that many of other PD-related molecules are directly or indirectly involved in the regulation of UPS (59), it is possible that the PD-related molecules might converge to regulate the activity of UPS in tumor differentiation. Thus, comprehensive understanding of the common pathway shared by both neurodegenerative disease and cancer have a great potential to provide a novel insight into the mechanism of these distinct categories of diseases.

Acknowledgments—We thank Dr. Koji Okamoto (National Cancer Center Research Institute, Tokyo) for critical reading of the manuscript and Drs. Hidetaka Yakura and Kazuya Mizuno (Tokyo Metropolitan Institute for Neuroscience) for instructions on flow cytometry. We are also indebted to Hideki Itabashi for help in preparing the photographs.

REFERENCES

1. Hashimoto, M., and Masliah, E. (1999) *Brain Pathol.* **9,** 707–720
2. Trojanowski, J., Goedert, M., Iwatsubo, T., and Lee, V. (1998) *Cell Death Differ.* **5,** 832–837
3. Jakes, R., Spillantini, M., and Goedert, M. (1994) *FEBS Lett.* **345,** 27–32
4. Ueda, K., Fukushima, H., Masliah, E., Xia, Y., Iwai, A., Yoshimoto, M., Otero, D. A., Kondo, J., Ihara, Y., and Saitoh, T. (1993) *Proc. Natl. Acad. Sci. U. S. A.* **90,** 11282–11286
5. Lansbury, P. T., Jr. (1999) *Proc. Natl. Acad. Sci. U. S. A.* **96,** 3342–3344
6. Polymeropoulos, M. H., Lavedan, C., Leroy, E., Ide, S. E., Dehejia, A., Dutra, A., Pike, B., Root, H., Rubenstein, J., Boyer, R., Stenroos, E. S., Chandrasekharappa, S., Athanassiadou, A., Papapetropoulos, T., Johnson, W. G., Lazzarini, A. M., Duvoisin, R. C., Di Iorio, G., Golbe, L. I., and Nussbaum, R. L. (1997) *Science* **276,** 2045–2047
7. Kruger, R., Kuhn, W., Muller, T., Woitalla, D., Graeber, M., Kosel, S., Przuntek, H., Epplen, J. T., Schols, L., and Riess, O. (1998) *Nat. Genet.* **18,** 106–108
8. Zarranz, J. J., Alegre, J., Gomez-Esteban, J. C., Lezcano, E., Ros, R., Ampuero, I., Vidal, L., Hoenicka, J., Rodriguez, O., Atares, B., Llorens, V., Gomez Tortosa, E., del Ser, T., Munoz, D. G., and de Yebenes, J. G. (2004) *Ann. Neurol.* **55,** 164–173
9. Hashimoto, M., Rockenstein, E., Mante, M., Mallory, M., and Masliah, E. (2001) *Neuron* **32,** 213–223
10. Park, J. Y., and Lansbury, P. T., Jr. (2003) *Biochemistry* **42,** 3696–3700
11. Ji, H., Liu, Y. E., Jia, T., Wang, M., Liu, J., Xiao, G., Joseph, B. K., Rosen, C., and Shi, Y. E. (1997) *Cancer Res.* **57,** 759–764
12. Lavedan, C., Leroy, E., Dehejia, A., Buchholtz, S., Dutra, A., Nussbaum, R. L., and Polymeropoulos, M. H. (1998) *Hum. Genet.* **103,** 106–112
13. Zhao, W., Liu, H., Liu, W., Wu, Y., Chen, W., Jiang, B., Zhou, Y., Xue, R., Luo, C., Wang, L., Jiang, J. D., and Liu, J. (2006) *Int. J. Oncol.* **28,** 1081–1088
14. Li, Z., Sclabas, G. M., Peng, B., Hess, K. R., Abbruzzese, J. L., Evans, D. B., and Chiao, P. J. (2004) *Cancer* **101,** 58–65
15. Iwaki, H., Kageyama, S., Isono, T., Wakabayashi, Y., Okada, Y., Yoshimura, K., Terai, A., Arai, Y., Iwamura, H., Kawakita, M., and Yoshiki, T. (2004) *Cancer Sci.* **95,** 955–961
16. Jia, T., Liu, Y. E., Liu, J., and Shi, Y. E. (1999) *Cancer Res.* **59,** 742–747
17. Liu, H., Liu, W., Wu, Y., Zhou, Y., Xue, R., Luo, C., Wang, L., Zhao, W., Jiang, J. D., and Liu, J. (2005) *Cancer Res.* **65,** 7635–7643
18. Gupta, A., Inaba, S., Wong, O. K., Fang, G., and Liu, J. (2003) *Oncogene* **22,** 7593–7599
19. Inaba, S., Li, C., Shi, Y. E., Song, D. Q., Jiang, J. D., and Liu, J. (2005) *Breast Cancer Res. Treat.* **94,** 25–35
20. Jiang, Y., Liu, Y. E., Lu, A., Gupta, A., Goldberg, I. D., Liu, J., and Shi, Y. E. (2003) *Cancer Res.* **63,** 3899–3903
21. West, A. B., Dawson, V. L., and Dawson, T. M. (2005) *Trends Neurosci.* **28,** 348–352
22. Wang, F., Denison, S., Lai, J. P., Philips, L. A., Montoya, D., Kock, N., Schule, B., Klein, C., Shridhar, V., Roberts, L. R., and Smith, D. I. (2004) *Genes Chromosomes Cancer* **40,** 85–96
23. Picchio, M. C., Martin, E. S., Cesari, R., Calin, G. A., Yendamuri, S., Kuroki, T., Pentimalli, F., Sarti, M., Yoder, K., Kaiser, L. R., Fishel, R., and Croce, C. M. (2004) *Clin. Cancer Res.* **10,** 2720–2724
24. Liu, Y., Lashuel, H. A., Choi, S., Xing, X., Case, A., Ni, J., Yeh, L. A., Cuny, G. D., Stein, R. L., and Lansbury, P. T., Jr. (2003) *Chem. Biol.* **10,** 837–846
25. Caballero, O. L., Resto, V., Patturajan, M., Meerzaman, D., Guo, M. Z., Engles, J., Yochem, R., Ratovitski, E., Sidransky, D., and Jen, J. (2002) *Oncogene* **21,** 3003–3010
26. Nagakubo, D., Taira, T., Kitaura, H., Ikeda, M., Tamai, K., Iguchi-Ariga, S. M., and Ariga, H. (1997) *Biochem. Biophys. Res. Commun.* **231,** 509–513
27. Kim, R. H., Peters, M., Jang, Y., Shi, W., Pintilie, M., Fletcher, G. C., DeLuca, C., Liepa, J., Zhou, L., Snow, B., Binari, R. C., Manoukian, A. S., Bray, M. R., Liu, F. F., Tsao, M. S., and Mak, T. W. (2005) *Cancer Cell* **7,** 263–273
28. Kawashima, M., Suzuki, S. O., Doh-ura, K., and Iwaki, T. (2000) *Acta Neuropathol. (Berl.)* **99,** 154–160
29. Fung, K. M., Rorke, L. B., Giasson, B., Lee, V. M., and Trojanowski, J. Q. (2003) *Acta Neuropathol. (Berl.)* **106,** 167–175
30. Bruening, W., Giasson, B. I., Klein-Szanto, A. J., Lee, V. M., Trojanowski, J. Q., and Godwin, A. K. (2000) *Cancer* **88,** 2154–2163
31. Hashimoto, M., Yoshimoto, M., Sisk, A., Hsu, L. J., Sundsmo, M., Kittel, A., Saitoh, T., Miller, A., and Masliah, E. (1997) *Biochem. Biophys. Res. Commun.* **237,** 611–616
32. Stefanis, L., Kholodilov, N., Rideout, H. J., Burke, R. E., and Greene, L. A. (2001) *J. Neurochem.* **76,** 1165–1176
33. Takeda, A., Hashimoto, M., Mallory, M., Sundsumo, M., Hansen, L., and Masliah, E. (2000) *Acta Neuropathol. (Berl)* **99,** 296–304
34. Takenouchi, T., Hashimoto, M., Hsu, L. J., Mackowski, B., Rockenstein, E., Mallory, M., and Masliah, E. (2001) *Mol. Cell. Neurosci.* **17,** 141–150
35. Hashimoto, M., Takenouchi, T., Rockenstein, E., and Masliah, E. (2003) *J. Neurochem.* **85,** 1468–1479
36. Tanimoto, Y., Yokozeki, M., Hiura, K., Matsumoto, K., Nakanishi, H., Matsumoto, T., Marie, P. J., and Moriyama, K. (2004) *J. Biol. Chem.* **279,** 45926–45934
37. Martin-Clemente, B., Alvarez-Castelao, B., Mayo, I., Sierra, A. B., Diaz, V., Milan, M., Farinas, I., Gomez-Isla, T., Ferrer, I., and Castano, J. G. (2004) *J. Biol. Chem.* **279,** 52984–52990
38. Nakai, M., Toshimori, K., Yoshinaga, K., Nasu, T., and Hess, R. A. (1998) *Cell Tissue Res.* **294,** 145–152
39. Wyke, S. M., and Tisdale, M. J. (2006) *Life Sci.* **78,** 2898–2910
40. Ostrerova, N., Petrucelli, L., Farrer, M., Mehta, M., Choi, P., Hardy, J., and Wolozin, B. (1999) *J. Neurosci.* **19,** 5782–5791
41. Ghee, M., Fournier, A., and Mallet, J. (2000) *J. Neurochem.* **75,** 2221–2224
42. Snyder, H., Mensah, K., Theisler, C., Lee, J., Matouschek, A., and Wolozin, B. (2003) *J. Biol. Chem.* **278,** 11753–11759
43. Lindersson, E., Beedholm, R., Hojrup, P., Moos, T., Gai, W., Hendil, K. B., and Jensen, P. H. (2004) *J. Biol. Chem.* **279,** 12924–12934
44. Rubinsztein, D. C. (2006) *Nature* **443,** 780–786
45. Garrett, I. R., Chen, D., Gutierrez, G., Zhao, M., Escobedo, A., Rossini, G., Harris, S. E., Gallwitz, W., Kim, K. B., Hu, S., Crews, C. M., and Mundy, G. R. (2003) *J. Clin. Investig.* **111,** 1771–1782
46. Obin, M., Mesco, E., Gong, X., Haas, A. L., Joseph, J., and Taylor, A. (1999) *J. Biol. Chem.* **274,** 11789–11795
47. Giasson, B. I., Bruening, W., Durham, H. D., and Mushynski, W. E. (1999) *J. Neurochem.* **72,** 1081–1087
48. Pasquini, L. A., Paez, P. M., Moreno, M. A., Pasquini, J. M., and Soto, E. F. (2003) *J. Neurosci.* **23,** 4635–4644
49. Snyder, H., Mensah, K., Hsu, C., Hashimoto, M., Surgucheva, I. G., Festoff, B., Surguchov, A., Masliah, E., Matouschek, A., and Wolozin, B. (2005) *J. Biol. Chem.* **280,** 7562–7569
50. Seo, J. H., Rah, J. C., Choi, S. H., Shin, J. K., Min, K., Kim, H. S., Park, C. H., Kim, S., Kim, E. M., Lee, S. H., Lee, S., Suh, S. W., and Suh, Y. H. (2002) *FASEB J.* **16,** 1826–1828
51. Bose, S., Stratford, F. L., Broadfoot, K. I., Mason, G. G., and Rivett, A. J. (2004) *Biochem. J.* **378,** 177–184
52. Webb, J. L., Ravikumar, B., Atkins, J., Skepper, J. N., and Rubinsztein, D. C. (2003) *J. Biol. Chem.* **278,** 25009–25013
53. Cuervo, A. M., Stefanis, L., Fredenburg, R., Lansbury, P. T., and Sulzer, D. (2004) *Science* **305,** 1292–1295
54. Mizushima, N. (2005) *Cell Death Differ.* **12,** Suppl. 2, 1535–1541
55. Chen, Q., Thorpe, J., and Keller, J. N. (2005) *J. Biol. Chem.* **280,** 30009–30017
56. Tanaka, Y., Engelender, S., Igarashi, S., Rao, R. K., Wanner, T., Tanzi, R. E., Sawa, A., V. L. D., Dawson, T. M., and Ross, C. A. (2001) *Hum. Mol. Genet.* **10,** 919–926
57. Lee, S. S., Kim, Y. M., Junn, E., Lee, G., Park, K. H., Tanaka, M., Ronchetti, R. D., Quezado, M. M., and Mouradian, M. M. (2003) *Neurobiol. Aging* **24,** 687–696
58. Iwata, A., Maruyama, M., Kanazawa, I., and Nukina, N. (2001) *J. Biol. Chem.* **276,** 45320–45329
59. Abou-Sleiman, P. M., Muqit, M. M., and Wood, N. W. (2006) *Nat. Rev. Neurosci.* **7,** 207–219

ELSEVIER

Bone 40 (2007) 997–1005

BONE

www.elsevier.com/locate/bone

Association of a single-nucleotide variation (A1330V) in the low-density lipoprotein receptor-related protein 5 gene (*LRP5*) with bone mineral density in adult Japanese women

Yoichi Ezura [a,*], Toshiaki Nakajima [a], Tomohiko Urano [b], Yoshihiro Sudo [a], Mitsuko Kajita [a], Hideyo Yoshida [c], Takao Suzuki [c], Takayuki Hosoi [d], Satoshi Inoue [b], Masataka Shiraki [e], Mitsuru Emi [a]

[a] *Department of Molecular Biology, Institute of Gerontology, Nippon Medical School, 1-396, Kosugi-cho, Nakahara-ku, Kawasaki 211-8533, Japan*
[b] *Department Geriatric Medicine, Faculty of Medicine, University of Tokyo, Tokyo, Japan*
[c] *Department Epidemiology, Tokyo Metropolitan Institute of Gerontology, Tokyo, Japan*
[d] *Department Internal Medicine, Tokyo Metropolitan Geriatric Hospital, Tokyo, Japan*
[e] *Research Institute and Practice for Involutional Diseases, Nagano, Japan*

Received 20 October 2004; revised 29 May 2005; accepted 13 June 2005
Available online 15 February 2007

Abstract

Low-density lipoprotein receptor-related protein 5 (LRP5), a co-receptor of Wnt signaling, is an important regulator of bone development and maintenance. Recently we identified correlation between an intronic single-nucleotide polymorphism (SNP) in the *LRP5* gene and vertebral bone mineral density (BMD), indicating that a genetic ground exists at this locus for determination of BMD. In the study reported here, we searched for nucleotide variation(s) that might confer susceptibility to osteoporosis among an extended panel of 387 healthy subjects recruited from the same hospital (Group-A), as well as among 384 subjects from the general population in eastern Japan (Group-B). We basically focused on two potentially functional variations, Q89R (c.266A > G) and A1330V (c.3989C > T), whose functional effects by the amino-acid changes were estimated by the SIFT software program; it predicted the 1330 V allele as deleterious ("intolerant") although the minor allele of Q89R was questionable. By analyzing associations between the variant alleles and the BMD, reproducible association of the minor variant of A1330V to lower adjusted BMD levels was detected; i.e., In Group-A subjects 1330-V significantly associated with the spinal BMD *Z*-score ($P = 0.034$), and in Group-B it associated with low radial BMD ($P = 0.019$). From haplotype and linkage disequilibrium (LD) analysis for 29 SNPs, we detected two separate LD blocks within the entire 137-kb *LRP5* locus, basically consistent with a previous report on Caucasians. One of the second block haplotype significantly associated with adjusted BMD ($r = 0.15$, $P = 0.004$). Possible combined effect of Q89R and A1330V belonging to different LD blocks was denied by multiple regression analyses. Our results indicate that genetic variations in *LRP5* are important factors affecting BMD in adult women and that 1330 V may contribute to osteoporosis susceptibility, at least in Japanese.

Keywords: Single-nucleotide polymorphism; LRP5; Low-density lipoprotein receptor-related protein; Bone mineral density; Association study; Quantitative trait

Introduction

Osteoporosis is a common, multi-factorial disease characterized by reduced bone mass, microarchitectual deterioration of bone tissue, and increased risk of fragility fractures. Achievement of high peak bone mass before maturation, as well as avoidance of postmenopausal bone loss, is important for prevention of osteoporosis [1]. Since complicated processes during periods of development, maturation, and aging are regulated through multiple endocrine and local systems, many aspects of the mechanisms affecting control of bone mass remain to be clarified.

Wnt signaling is likely to be one of the most important systems involved in regulating developmental and homeostatic control of the skeletal system [2–4]. Low-density lipoprotein receptor-related protein 5 (LRP5) is a co-receptor for Wnt [5,6], and by studies on osteoporosis pseudoglioma syndrome (OPPG) family, causative mutations were identified in the *LRP5* gene [7,8]. On the other hand, certain mutations in *LRP5* cause an inherited trait of high bone mass in some families [9,10], and autosomal-dominant osteopetrosis in others [11]. These observations strongly suggest an important general role of LRP5 in acquisition and/or maintenance bone mass.

Genes responsible for monogenic inherited diseases sometimes also play roles in the phenotypic manifestations of common diseases [12–14], and thus are first-choice candidates for testing associations. Previously we suggested a possible contribution of LRP5 in determination of BMD, after detecting an intronic nucleotide variation of the *LRP5* gene (IVS17-1677C > A) associated with age-adjusted values of spinal BMD (*Z*-score) in a set of adult Japanese women. Although no definitive responsible variation(s) were established at that time [15], three other groups subsequently reported association of different missense nucleotide variations in *LRP5* with bone mineral density among Asian populations (Korean and Japanese; Q89R and A1330V [16,17]) and in Caucasians (V667M [18]). Although the significance levels and the suggested responsible variations were different, the reports were consistent in implicating the *LRP5* locus.

To examine in more detail the possibly responsible variation(s) of that gene in terms of BMD, we investigated multiple genetic variations within the *LRP5* locus in two independently recruited subject groups, comprising a total of 771 adult women in Japan. We constructed haplotypes, analyzed linkage disequilibrium (LD), and searched for mutations in these subjects.

* Corresponding author. Present address: 2-3-10 Kanda-Surugadai, Chiyoda-ku, Tokyo, Tokyo Medical and Dental University, Medical Research Institute, Department of Molecular Pharmacology. Fax: +81 3 5280 8067.
E-mail address: ezura.mph@mri.tmd.ac.jp (Y. Ezura).

8756-3282/$ - see front matter © 2007 Published by Elsevier Inc.
doi:10.1016/j.bone.2005.06.025

Materials and methods

Subjects

The 308 subjects recruited for the previous report [15] were from an outpatient clinic in Nagano prefecture (Research Institute and Practice for Involutional Diseases). Although BMD levels distributed in a wide range without skewness, these subjects were not from a population-based panel, and thus adjustment by multiple regression was not applicable. However instead, quantitative association analysis was possible using spinal BMD *Z*-scores, and we detected significant association with an intronic variant of *LRP5*. To verify that association, extended panel of 387 adult female was recruited from the same clinic (Group-A); these are basically healthy individuals who visited the same clinic up to December 2003. Mean ages and body mass indices (BMI) with standard deviations (SD) were 64.6 ± 10.8 (range 25–89) years and 22.2 ± 2.9 (range 14.3–32.9) kg/m^2, respectively. The BMD of lumbar vertebral bodies (from L2 to L4; expressed in g/cm^2) was measured in each participant by DXA using DPX-L (GE Medical Systems Lunar Corporation, Madison WI). Coefficients of variation (CV) for the anteroposterior view of the lumbar BMD was 0.5 ± 0.5% (CV ± SD) as described [40]. *Z*-scores were calculated using installed software (Lunar DPX-L) on the basis of data from 20,000 Japanese women [19]. Eight of the subjects had remarkably high BMD (*Z*-scores > 3.0),

Table 1
Summary of LRP5 polymorphisms analyzed among 384 adult women in the general Japanese population

No.	SNP name	nt.	cSNP characteristics †	dbSNP-ID ‡	Allele frequency (%-Heterozygosity)	*n* §	Distance (bp) *	Genotyping method
1	IVS1 + 4689C > G	G/C		rs312014	0.53:0.47 (45)	378	9469	TaqMan
2	IVS1 + 14158G > A	G/A		rs312024	0.44:0.56 (46)	383	310	Invader
3	IVS1 + 14468T > C	T/C		rs634008	0.26:0.74 (41)	367	7259	Sd-PCR
4	IVS1-13315A > G	G/A		rs606989	0.91:0.09 (16)	378	9089	TaqMan
5	IVS1-4226T/C	T/C		rs74744	0.09:0.91 (18)	384	3832	Invader
6	IVS1-394A/G	A/G		rs312782	0.09:0.91 (17)	369	567	Sd-PCR
7	Q89R	A/G	(c.266A > G)	–	0.93:0.07 (13)	383	3075	Invader
8	IVS2 + 2852T > C	T/C		rs312783	0.09:0.91 (18)	381	197	Sd-PCR
9	IVS2 + 3049T > C	T/C		rs312784	0.11:0.89 (21)	375	3535	Sd-PCR
10	IVS2 + 2823T > G	T/G		rs312788	0.09:0.91 (18)	384	9317	Invader
11	IVS4 + 201G > A	A/G		rs178352	0.91:0.09 (18)	377	21,779	TaqMan
12	IVS5-393C > T	C/T		rs3781592	0.06:0.94 (11)	381	5761	Sd-PCR
13	IVS7 + 1632G > A	G/A		rs3781590	0.09:0.91 (16)	374	11,224	Invader
14	IVS7-575T > C	T/C		rs685095	0.30:0.70 (40)	382	7134	Sd-PCR
15	c.2220C > T	C/T	Silent	rs2306862	0.26:0.74 (36)	372	218	Sd-PCR
16	IVS10 + 120T > C			rs667126	0.30:0.70 (40)	384	907	Invader
17	IVS10-269C > T	C/T		rs583545	0.33:0.67 (45)	370	33	Sd-PCR
18	IVS10-236A > G	A/G		rs23691	0.34:0.66 (42)	381	498	Invader
19	IVS11 + 78G > A	G/A		rs689179	0.30:0.70 (41)	378	13,524	Sd-PCR
20	c.3357A > G	A/G	Silent	rs556442	0.42:0.58 (51)	373	6662	Sd-PCR
21	IVS17-1718G/del	G/del		rs3837372	0.39:0.61 (46)	383	41	Invader
22	IVS17-1677C > A	C/A		rs3781586	0.28:0.72 (41)	375	941	Sd-PCR
23	IVS17-376G > A	G/A		rs3781585	0.05:0.95 (10)	379	110	Sd-PCR
24	IVS17-626G > A	G/A		rs3781584	0.05:0.95 (10)	383	101	Invader
25	IVS17-525C > T	C/T		rs3781583	0.05:0.95 (10)	384	750	Invader
26	A1330V	C/T	(c.3989C > T)	rs3736228	0.26:0.71 (40)	384	1285	Invader
27	IVS18 + 1274A > G	A/G		rs638076	0.39:0.61 (44)	377	2998	Sd-PCR
28	IVS19-336T > C	T/C		rs901823	0.36:0.64 (44)	370	4140	Sd-PCR
29	IVS21 + 2334T > C	T/C		rs3781579	0.19:0.83 (28)	375	–	Sd-PCR

* Number of nucleotides to the next SNP (bp).
† Nucleotide positions in the coding sequence are indicated for missense cSNPs.
‡ IDs are from dbSNP of NCBI (http://www.ncbi.nlm.nih.gov/SNP/).
§ Number of genotyped subjects.

Table 2
Association analysis of adjusted BMD in Groups-A and -B

SNP	Genotype	Group-A (n = 387) (spinal BMD Z-score)		P value[a]	Group-B (n = 384) (radial-adjusted BMD)		P value[a]
		Mean ± SD	n		Mean ± SD	n	
Q89R	Q	−0.15 ± 1.50	332	0.85	0.401 ± 0.055	333	0.052
	QR	−0.14 ± 1.54	35		0.387 ± 0.049	48	
	R	−0.57 ± 1.10	3		0.360 ± 0.059	2	
A1330V	A	−0.04 ± 1.61	178	0.034*	0.405 ± 0.053	195	0.019*
	AV	−0.35 ± 1.38	174		0.395 ± 0.059	155	
	VV	−0.47 ± 1.47	35		0.385 ± 0.041	34	
MC17-1677C > A	CC	−0.01 ± 1.42	166	0.005**	0.405 ± 0.053	194	0.055
(before expansion)	CA	−0.35 ± 1.44	118		0.395 ± 0.059	152	
	A	−0.78 ± 1.36	24		0.390 ± 0.040	29	

±Data were from the previous study before subject expansion.
[a] P values were calculated for the linear regression.
* $P < 0.05$.
** $P < 0.01$.

and four had remarkably low BMD (Z-scores < −3.0). For distribution analysis, we selected 91 subjects with Z-scores > +1.0 and 139 with Z-scores < −1.0. Among those women, the Z-score was greater than 2.0 in 33 and smaller than −2.0 in 34 of them. Biochemical markers of bone turnover including serum intact osteocalcin, urinary pyridinoline, and deoxypyridinoline were measured in most of the 387 subjects ascertained from the Institute; each had given informed consent prior to the study.

DNA samples for a population-based analysis were obtained from peripheral blood of 384 adult Japanese women [20,21]. In this group (Group-B), mean ages and body mass indices (BMI) with standard deviations (SD) were 58.4 ± 8.6 (range 32–69) years and 23.7 ± 3.61 (range 14.7–38.5) kg/m^2, respectively. The BMD of radial bone (expressed in g/cm^2) of each participant was measured by dual energy X-ray absorptiometry (DXA) using DTX-200 (Osteometer Meditech Inc., Hawthorne, CA, USA) and was normalized for differences in age, height, and weight by multiple linear regression analysis [21]. Forearm BMD in the distal radius was measured according to the Guidelines for Osteoporosis Screening in a health check-up program in Japan [22]; the instruments (DTX-200) were calibrated at every measurement, and the coefficients of variation were kept within the 1.0 ± 0.5% (CV ± SD). No participant had medical complications or was undergoing treatment for conditions known to affect bone metabolism [21]. All were non-related volunteers, and written informed consent was obtained from each of them. The ethical committee of the Institutional Review Board approved the entire project.

Mutation search, SNP selection, and genotyping

Mutation analysis of all 23 exons and flanking regions was carried out in DNA from the 12 subjects with the highest (>3.0, n = 8) and lowest (<−3.0, n = 4) Z-scores by direct sequencing of PCR products in the ABI Prism 377 DNA system (Applied Biosystems).

As potentially functional SNPs, two previously reported missense coding-SNPs, A1330V (c.3989C > T) and Q89R (c.266A > G), were selected for testing association of BMD levels, but a third, V667M, was eliminated because it was undetectable among our subjects (Table 1). Another intronic variation previously reported to associate with low BMD also was tested for association. For LD analysis, we first tested more than 40 variations within the *LRP5* locus, including all 38 polymorphic variations archived in the JSNP-database (http://snp.ims.u-tokyo.ac.jp/index.html), dbSNP, and from the literature [11,23]. However, since some of the variations showed minor allele frequencies of <0.05 among our Group-B 384 subjects, we chose to use only 29 SNPs for LD analysis.

Genotypes for these 29 selected SNPs were determined either by the Sd-PCR method [20], Invader assay (Third Wave Technologies, Madison, WI) [24], or TaqMan Assay (Applied Biosystems). The Sd-PCR method was used for 16 SNPs, according to a protocol described previously [20]. In brief, the Sd-PCR reaction was carried out using two allele-specific primers (AS-primers) and one reverse primer in a standard reaction mixture containing fluorescence-labeled dCTP. Discrimination of alleles, on the basis of by five-base differences between the AS-primers, was achieved using an ABI Prism 377 DNA system [21]. The Invader assay was applied for 10 other SNPs, according to the manufacturer's protocol. In brief, 1 μl of the diluted PCR product (1:333 in distilled water) of the region flanking each SNP was used as template in a 6-μl reaction mixture in 384-well plates, and fluorescent signals for FAM and Redmond Red were detected by a plate-reader after standard 1-h incubation [25]. The other three SNPs were genotyped by TaqMan Assay according to the manufacturer's protocol.

Table 3
Physical and clinical characteristics of the subjects in Group-A (healthy subjects from a clinic)

Group-A subjects (n = 387)	A1330V			P value*
	AA	AV	VV	
Number	178	174	35	–
Age (Years)	65.6 ± 10.1 (41–86)	64.1 ± 10.4 (33–89)	59.3 ± 15.0 (25–87)	0.012
Weight (kg)	51.1 ± 7.9 (34–74)	50.0 ± 7.9 (33–76)	50.2 ± 8.1 (34–70)	NS
BMI (kg/m^2)	22.5 ± 3.0 (16.4–32.9)	21.9 ± 2.7 (14.3–31.8)	21.9 ± 3.2 (15.3–29.5)	NS
Height (cm)	150.8 ± 6.2 (135–167)	150.8 ± 6.7 (134–172)	151.1 ± 5.4 (140–162)	NS
Spine BMD (g/cm^2)	0.914 ± 0.215 (0.387–1.732)	0.878 ± 0.188 (0.400–1.506)	0.898 ± 0.196 (0.518–1.310)	NS
BMD Z-score	−0.03 ± 1.62 (−3.1–7.1)	−0.35 ± 1.38 (−3.5–5.3)	−0.45 ± 1.47 (−2.9–3.1)	0.034
Intact-OC (ng/ml)[†]	7.18 ± 3.16 (n = 117)	8.40 ± 3.82 (n = 118)	8.87 ± 3.81 (n = 18)	0.004
Pyridinoline (pmol/μmol crea.)	34.2 ± 11.1 (n = 138)	33.6 ± 11.2 (n = 133)	34.5 ± 11.4 (n = 20)	NS
Deoxypyridinoline (pmol/μmol crea.)	7.20 ± 2.50 (n = 139)	7.29 ± 2.42 (n = 133)	7.85 ± 3.01 (n = 20)	NS

* P values are calculated for regression analysis with ANOVA F-test.
[†] Serum intact osteocalcin level.

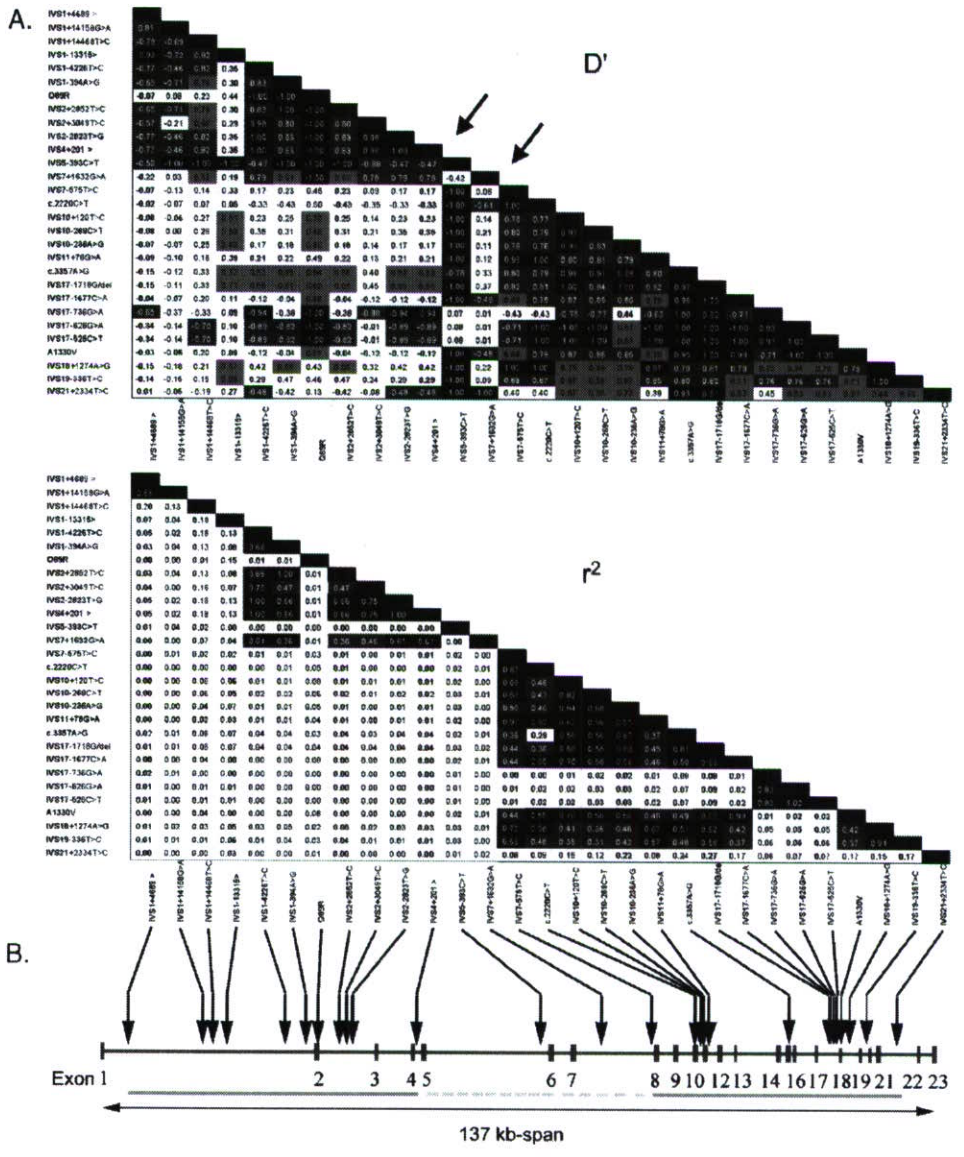

Fig. 1. Linkage disequilibrium analysis among 29 SNPs within the *LRP5* locus. (A) Indices of linkage disequilibrium D' (upper half) and r^2 (lower half), calculated from the predicted haplotype frequencies and presented as separate tables. D' values greater than 0.5 and r^2 values greater than 0.1 are highlighted by gray-to-black gradients. Arrows indicate a possible hot spot for recombination. (B) Schematic diagram of the *LRP5* gene showing locations of the 23 exons. Locations of the 29 tested SNPs are indicated by downward arrows.

Table 4
Contingency table analysis on Group-A subjects

Group-A	n	A1330V			P value [a]
		AA	AV	VV	
Z-score > 3.0	8	5	2	1	NA
Z-score < −3.0	4	1	3	0	
Z-score > 2.0	33	22	8	3	0.025 *
Z-score < −2.0	34	13	14	7	
Z-score > 1.0	91	52	33	6	0.046 *
Z-score < −1.0	139	61	63	15	

NA: not applicable.
[a] P values are calculated in chi-square test for trend.
* $P < 0.05$.

Haplotyping, LD analysis, and statistical analysis

Maximum likelihood haplotype frequencies among the 582 chromosomes of 291 subjects from Group-B were estimated by an EM algorithm using SNPAlyze v3.1 (DYNA-COM, Chiba, Japan). The LD for all possible two-way combinations of SNPs was tested with D, D', and r^2 [26,27]. After defining LD blocks and tag-SNPs in each block, each individual diplotype was estimated by SNPAlyze v3.1 software.

Quantitative associations between genotypes and adjusted BMD values (g/cm^2) were examined by analysis of variance (ANOVA), with regression analysis as a post hoc test using Instat 3 software (GraphPad Software, San Diego, CA). The three genotypic categories of each SNP were converted into incremental values (0, 1, and 2), which represent the number of chromosomes carrying the major allele. Significant association was defined when the given P value of the ANOVA F-test was less than 5% ($P < 0.05$). Similarly, quantitative association was tested for major 5- and 4-haplotypes (frequency >5%) defined for each LD block in the *LRP5* gene locus. Chi-square tests were used to ascertain Hardy–Weinberg equilibrium among genotypes ($P > 0.05$). Multiple linear regression analysis was applied for examining potential combined effects of Q89R and A1330V alleles, using Instat 3 software. Distribution analysis of the genotype frequencies among phenotypically divided groups, i.e., BMD Z-scores > 1.0 ($n = 91$) and Z-scores < −1.0 ($n = 139$) was conducted by chi-square tests as in our previous experiments [21]. Predictive analysis of protein function for the two missense coding SNPs was conducted using the SIFT (Sorting Intolerant From Tolerant) program (http://blocks.fhcrc.org/sift/SIFT.html) [28]. When the given score was less than 0.05, the alteration was deemed to be intolerant (i.e., deleterious).

Results

To identify the genetic ground involved in a previously detected association of an intronic *LRP5* polymorphism with low BMD in Group-A subjects [15], we first searched for a causative mutation anywhere among the 23 exons of the gene. However, among 12 subjects who had extremely high or low BMD Z-scores (>3.0 or <−3.0), no mutations were detected apart from two already known missense variations (Q89R and A1330V). We analyzed the effect of these amino acid alterations, using predictive computer program SIFT [28]; this program estimated a deleterious effect of 1330-V (score = 0.03) and possible mild effect of 89-R (score = 0.19). Although the lowest score was predicted for another missense variation V667M (score = 0.01), this variant was not detected in our test population. Based on the notion that strong candidate for the causative polymorphism would be missense variation, we investigated association of these SNPs among the entire Group-A subjects.

To analyze the effects on BMD, all the extended 387 subjects were genotyped for these two SNPs as well as previously tested IVS17-1677C > A (Table 2). No association of the Q89R genotypes was detected for BMD Z-score ($r = 0.03$, NS). However, we detected significant correlation of the A1330V genotype with spinal BMD Z-score ($r = 0.11$, $P = 0.034$); homozygous carriers of the minor T-allele (V/V) had the lowest BMD Z-scores (−0.47 ± 1.47, $n = 35$), heterozygous individuals (A/V) were intermediate (−0.35 ± 1.38; $n = 174$), and homozygous carriers of the C-allele (A/A) had the highest BMD Z-scores (−0.03 ± 1.62; $n = 178$) (Tables 2 and 3). The result was consistent with previously detected results for the intron SNP IVS17-1677C > A [15], as indicated (Table 2). We noticed that these SNPs were in strong linkage disequilibrium (see Fig. 1). Consistent results were achieved in a distribution analysis of phenotypically divided subjects (high BMD Z-scores: $n = 91$ and low BMD Z-scores: $n = 139$), using 2 × 3 chi-square tests for detecting trends ($P = 0.046$) (Table 4). A similar result was obtained by analyzing subjects with more prominent phenotypes (Z-scores > +2.0: $n = 33$, and Z-scores < −2.0: $n = 34$; $P = 0.025$) (Table 4).

No significant differences were detected in physical characteristics (body weight, height, or BMI) between groups genotypically classified according to A1330V alleles. Although we detected a significant correlation of A1330V with levels of intact osteocalcin in serum ($P = 0.004$), this might be affected by a correlation detected for age distribution ($P = 0.01$) (Table 3).

To examine the reproducibility of that correlation, 384 adult Japanese women recruited from general Japanese population were analyzed (Group-B) on adjusted values of radial BMD by ANOVA with linear regression. As a result, significant correlation of the A1330V genotype with adjusted BMD was replicated (Tables 2 and 5). Homozygous carriers of the minor

Table 5
Physical and clinical characteristics of the subjects in Group-B (cohort subjects)

Group-B subjects (n = 384)	A1330V			P value *
	AA	AV	VV	
Number	195	155	34	–
Age (Years)	58.4 ± 8.72 (34–69)	58.3 ± 8.14 (32–69)	58.9 ± 9.93 (32–69)	NS
Weight (kg)	53.2 ± 9.01 (34.8 ± 84.8)	55.1 ± 8.73 (28.8–89.0)	55.9 ± 8.7 (44.6–80.0)	0.027
BMI (kg/m^2)	23.3 ± 3.63 (16.2–37.7)	23.9 ± 3.61 (14.7–38.5)	24.6 ± 3.29 (17.5–31.3)	0.018
Height (cm)	151.2 ± 6.04 (130.5–169.0)	151.7 ± 5.41 (139.0–166.0)	150.6 ± 6.65 (140.0–163.4)	NS
Radial BMD (g/cm^2)	0.402 ± 0.082 (0.222–0.635)	0.398 ± 0.084 (0.178–0.613)	0.390 ± 0.079 (0.270–0.566)	NS
Adjusted BMD (g/cm^2)	0.405 ± 0.053 (0.275–0.551)	0.395 ± 0.059 (0.225–0.554)	0.385 ± 0.041 (0.298–0.448)	0.019

* P values are calculated for regression analysis with ANOVA F-test.

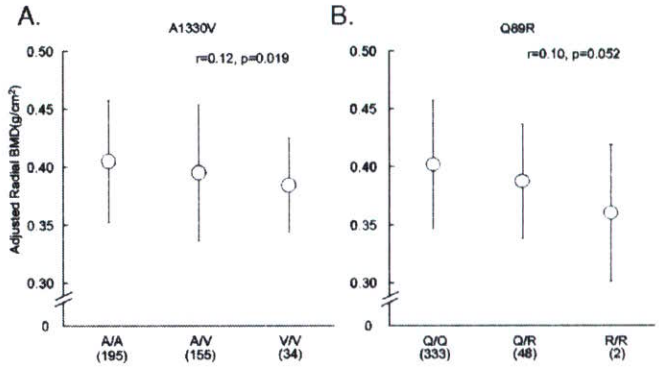

Fig. 2. Reproducible association of two missense *LRP5* variations (Q89R and A1330V) with adjusted BMD. (A) Plots of adjusted BMD values for three genotypically classified subgroups by A1330V among 384 subjects from the general population. (B) Plots of adjusted BMD values for three genotypically classified subgroups by Q89R. Open circles indicate mean values and error bars indicate standard deviations. Correlations between the number of minor allele possessed and the adjusted BMD were tested by linear regression analysis.

T-allele (V/V) had the lowest adjusted BMDs (0.385 ± 0.041 g/cm^2, $n = 34$); heterozygous individuals (A/V) were intermediate (0.395 ± 0.059 g/cm^2; $n = 155$); and homozygous C-allele carriers (A/A) had the highest adjusted BMDs (0.405 ± 0.053 g/cm^2; $n = 195$), indicating a possible codominant effect of the minor T-allele (corresponding to the second nucleotide for a valine codon, gTg) on lowering adjusted BMD levels (Fig. 2A; $r = 0.12$, $P = 0.019$; $n = 384$). Interestingly in these subjects, we observed a tendency for association of Q89R minor G-allele (corresponds to arginine; cGg) to low adjusted BMD, although this tendency did not quite reach statistical significance (Fig. 2B; $r = 0.10$, $P = 0.052$). We also examined if any patient characteristics correlated with the genotype; however, no significant differences were detected except in body weight ($r = 0.11$, $P = 0.03$) or BMI ($r = 0.12$, $P = 0.02$). A contribution of A1330V to control of body mass appeared to be a possibility (Table 5). For analysis of possible combined effects of Q89R and A1330V on BMD determination, multivariate linear regression analysis estimated a fitting equation explained about 2% of BMD variances ($r^2 = 0.023$, $P = 0.01$). However only the A1330V genotype contributed significantly to the equation ($P = 0.004$).

We then analyzed LD in the LRP5 locus by genotyping these subjects for informative 29 SNPs (minor allele frequencies >0.05) (Table 1). Average distance between neighboring SNPs was 4.6 kb (median, 3.0 kb; range, 33–21,779 bp). Genotype, allelic frequency, and heterozygosity were clarified successfully for each SNP, and no deviation was detected from Hardy–Weinberg equilibrium. Indices of pairwise LD (D' and r^2) were calculated by estimating the maximum-likelihood haplotypes and their frequencies from 293 Group-G subjects genotyped for all 29 SNPs. These procedures detected two LD blocks separated by a region of about 11 kb, from intron 5 to intron 7 (Fig. 1). In the second block, the indices of pairwise LD between the A1330V and IVS17-1677C > A variants were remarkably high ($D' = 0.99$, $r^2 = 0.98$). More important, the two missense SNPs, Q89R (c.266A > G) and A1330V (c.3989C > T), appeared to localize in different LD blocks, although the indices of pairwise LD between the two SNPs were slightly higher than the neighboring intronic SNPs ($D' = 0.64$, $r^2 = 0.07$). By analyzing haplotype frequency estimated by all the belonging SNPs for each LD block (11 and 18, respectively), representative 4 and 5 SNPs were selected (Tables 6 and 7). By estimating diplotype in each individual,

Table 6
Representative haplotypes for LD block-1

Hap-No	IVS1 + 4689C > G	IVS1 + 14158G > A	IVS1 + 14468T > C	IVS2 + 2852T > C	Frequency (%)	SUM (%)
#1–1	0	0	0	0	37.6	
#1–2	1	1	0	0	26.4	
#1–3	1	1	1	0	15.0	
#1–4	1	1	1	1	6.5	
#1–5	0	1	0	0	6.3	
#1–6	1	0	1	0	2.1	
#1–7	1	0	0	0	2.1	
#1–8	0	0	1	0	1.0	
#1–9	0	0	0	1	0.9	98.0

0 and 1 represent major and minor alleles, respectively.

Table 7
Representative haplotypes for LD block-2

Hap-No	IVS7-575T > C	c.3357A > G	IVS 17-626G > A	A1330V	IVS21 + 2334T > C	Frequency (%)	SUM (%)
#2–1	0	0	0	0	0	53.0	
#2–2	1	1	0	1	0	13.9	
#2–3	1	1	0	1	1	9.2	
#2–4	0	1	0	0	0	3.8	
#2–5	1	1	0	0	0	3.5	
#2–6	0	1	0	1	0	3.4	
#2–7	1	0	0	0	0	3.2	
#2–8	0	1	1	0	1	2.9	
#2–9	0	1	0	1	1	1.8	
#2–10	0	1	1	0	0	1.6	
#2–11	0	1	0	0	1	1.4	97.6

0 and 1 represent major and minor alleles, respectively.

association was examined for 9 haplotypes (5 and 4 haplotypes for each block). Significant association was represented by haplotype-#2–3 (C-G-G-V-C) for the second LD block (r = 0.15, P = 0.0041); homozygous and heterozygous haplotype#3 carriers had lower adjusted BMD (0.384 ± 0.049, n = 6 and 0.379 ± 0.057, n = 57) compared to non-carriers (0.402 ± 0.053, n = 299).

Discussion

In the study reported here, we investigated a possible contribution of *LRP5* polymorphisms to determination of bone-mineral density in Japanese women. A search for mutations, an LD analysis, and a study for association between two candidate SNPs and adjusted BMD values in two independently collected groups revealed reproducible association of the *LRP5* variations with BMD levels. During the preparation and submitting this manuscript, five independent groups reported similar results. One reported consistent correlation of A1330V with radial BMD in adult Japanese women [16], and the other reported a similar tendency of Q89R to be associated with hip BMD in young Korean males [17]. Although another study, involving Caucasians, reported a c.2047G > A variation (V667M: nucleotide numbering is from the cap site of mRNA in that report [18]), that variant appeared to be so rare in our test subjects that we excluded it from our investigations. Recent two articles further supported consistent association of A1330V, although both reports emphasized association of other intron SNPs in strong LD with A1330V [29,30]. We propose that *LRP5* variations may be important determinants of BMD in the general population, and believe that the A1330V polymorphism is the most likely LRP5 determinant of bone mass as well, at least in adult Japanese women.

Although the molecular basis for the function of LRP5 in determining BMD is not fully clarified, evidence is accumulating. Several mutations in the *LRP5* gene have been identified as causing inherited diseases with bone phenotypes, including OPPG and autosomal-dominant types of osteopetrosis [8–11]. Functional molecular analyses, including gene targeting experiments and analysis of mutated LRP5 products, have revealed a mechanistic basis for bi-directional phenotypic expression, where a key is the Wnt pathway and binding of its antagonists to the YWTD motif in the extracellular domains of this co-receptor [4,10,31]. So far, however, the cellular and in vivo mechanisms causing reduction of bone mass are not well understood. Therefore, functional differences focusing on the alanine residue at 1330 and the LDLR class-A domain should be investigated, and binding affinity for Wnt ligands or other co-binding regulators like dickkopfs (Dkks) [6] should be examined. In our experiments, a predictive informatics program (SIFT [28]) for functional alterations caused by the two missense variations in *LRP5* estimated an intolerable alteration of alanine to valine at A1330V (score = 0.03) but not for glutamine to arginine in Q89R (score = 0.19). Those estimates were consistent with our assumption from association analysis that the effect of Q89R might be weaker than that of A1330V. However, a cross-sectional study conducted elsewhere had indicated a selective influence of a V667M variant on vertebral bone mass among Caucasians where the SIFT program predicted an intolerant effect of 667M (score = 0.01). Longitudinal human studies, or an in vivo animal study, may clarify the developmental period(s) during which *LRP5* variants affect BMD most strongly.

The feasibility of a candidate-gene association study generally depends on control of confounding factors resulting from population bias, unreliability of diagnosis or phenotypic evaluation, interaction with environmental factors, or deficiencies in statistical power [32–34]. In our study, a reliable measurement of BMD, a quantitative trait with significant heredity, was evaluated with adjustment for age and BMI among unbiased population with no evidence of the stratification. Moreover, the reproducibly demonstrated association of the 1330 V variant with low BMD among independent groups of subjects, in other studies and ours [16,17], seems to provide comprehensive evidence for a functional contribution of this variant, even though in all of the studies cited, the significance levels were moderate without adjustment for multiple testing [16–18]. Supportive data from linkage analysis includes a quantitative trait locus (QTL) for spinal BMD at 11q12–13 that has been identified in general populations [35]. A possible combined effect of the multiple coding SNP(s) tested in our multiple regression analysis should be re-evaluated in a larger cohort study.

The existence of overlapping mechanisms for lipid metabolism, body mass regulation, and bone metabolism is a classically discussed issue [36–38]. These processes are under systemic control of leptin and neuro-endocrinological systems [37–39], but are influenced by apolipoprotein E polymorphisms [40], subject to developmental controls of mesenchymal-cell differentiation by transcription factors like PPAR-gamma [41], and affected by statins [42]. In addition, the Wnt-LRP system may affect regulation of both bone and body mass [43]. Our data support that notion because body weight and BMI, as well as adjusted BMD, correlated with A1330V genotypes among 384 adult women from the general Japanese population. Other effector molecules in the Wnt signaling system might contribute as well.

In summary, our data suggest a functional effect of polymorphic variants in a candidate osteoporosis-susceptibility gene, *LRP5*, whose common polymorphisms significantly correlated with bone mineral density of women recruited from two independent populations. Because osteoporosis is a multifactorial disease, other genes, especially genes acting through the Wnt pathway, may have to be examined for potential contributions to disease susceptibility. That information will help to clarify the complex mechanism of BMD determination in vivo, and may explain, at least in part, the pathogenesis of postmenopausal osteoporosis. Such studies should provide a novel viewpoint for establishing suitable treatment designs and preventive strategies for the disease.

Acknowledgments

We thank Dr. Tatsuhiko Tsunoda at RIKEN SNP Research Center for critical reading of our manuscript, and Mina Kodaira, Miho Kawagoe, and Tamami Uchida for technical assistance. This work was supported by a grant for Strategic Research from the Ministry of Education, Science, Sports and Culture of Japan; by a Research Grant for Research from the Ministry of Health and Welfare of Japan; and by a Research for the Future Program Grant of The Japan Society for the Promotion of Science.

References

[1] Riggs BL, Melton III LJ. Involutional osteoporosis. N Engl J Med 1986;314:1676–86.
[2] Hartmann C, Tabin DJ. Wnt-14 plays a pivotal role in inducing synovial joint formation in the developing appendicular skeleton. Cell 2001;140: 341–51.
[3] Yang Y, Topol L, Lee H, Wu J. Wnt5a and Wnt5b exhibit distinct activities in coordinating chondrocyte proliferation and differentiation. Development 2003;130:1003–15.
[4] Kato M, Patel MS, Levasseur R, Lobov I, Chang BHJ, Glass II DA, et al. Cbfa1-independent decrease in osteoblast proliferation, osteopenia, and persistent embryonic eye vascularization in mice deficient in Lrp5, a Wnt coreceptor. J Cell Biol 2002;157:303–14.
[5] Mao J, Wang J, Liu B, Pan W, Farr III GH, Flynn C, et al. Low-density lipoprotein receptor-related protein-5 binds to axin and regulates the canonical Wnt signaling pathway. Mol Cell 2001;7:801–9.
[6] Zorn AM. Wnt signaling: antagonistic Dickkopfs. Curr Biol 2001;11: R592–5.
[7] Gong Y, Vikkula M, Boon L, Liu J, Beighton P, Ramesar R, et al. Osteoporosis-pseudoglioma syndrome, a disorder affecting skeletal strength and vision, is assigned to chromosome region 11q12–13. Am J Hum Genet 1996;59:146–51.
[8] Gong Y, Slee RB, Fukai N, Rawadi G, Roman-Roman S, Reginato AM, et al. LDL receptor-related protein 5 (LRP5) affects bone accrual and eye development. Cell 2001;107:513–23.
[9] Little RD, Carulli JP, Del Mastro RG, Dupuis J, Osborne M, Folz C, et al. A mutation in the LDL receptor-related protein 5 gene results in the autosomal dominant high-bone-mass trait. Am J Hum Genet 2002;70: 11–9.
[10] Boyden LM, Mao J, Belsky J, Mitzner L, Farhi A, Mitnick MA, et al. High bone density due to a mutation in LDL-receptor-related protein 5. N Engl J Med 2002;346:1513–21.
[11] Van Wesenbeeck L, Cleiren E, Gram J, Beals RK, Benichou O, Scopelliti D, et al. Six novel missense mutations in the LDL receptor-related protein 5 (LRP5) gene in different conditions with an increased bone density. Am J Hum Genet 2003;72:763–71.
[12] Grant SFA, Reid DM, Blake G, Herd R, Fogelman I, Ralston SH. Reduced bone density and osteoporosis associated with a polymorphic Sp1 binding site in the collagen type I α 1 gene. Nat Genet 1996; 14:203–5.
[13] Tavtigian SV, Simard J, Teng DH, Abtin V, Baumgard M, Beck A, et al. A candidate prostate cancer susceptibility gene at chromosome 17p. Nat Genet 2001;27:172–224.
[14] Rebbeck TR, Walker AH, Zeigler-Johnson C, Weisburg S, Martin AM, Nathanson KL, et al. Association of HPC2/ELAC2 genotypes and prostate cancer. Am J Hum Genet 2000;67:1014–9.
[15] Urano T, Shiraki M, Ezura Y, Fujita M, Sekine E, Hoshino S, et al. Association of a single-nucleotide polymorphism in low-density lipoprotein receptor-related protein 5 gene with bone mineral density. J Bone Miner Metab 2004;22:341–5.
[16] Mizuguchi T, Furuta I, Watanabe Y, Tsukamoto K, Tomita H, Tsujihata M, et al. LRP5, low-density-lipoprotein-receptor-related protein 5, is a determinant for bone mineral density. J Hum Genet 2004;49:80–6.
[17] Koh JM, Jung MH, Hong JS, Park HJ, Chang JS, Shin HD, et al. Association between bone mineral density and LDL receptor-related protein 5 gene polymorphisms in young Korean men. J Korean Med Sci 2004;19:407–12.
[18] Ferrari SL, Deutsh S, Choudhury U, Chevalley T, Bonjour JP, Dermitzakis ET, et al. Polymorphisms in the low-density lipoprotein receptor-related protein 5 (LRP5) gene are associated with variation in vertebral bone mass, vertebral bone size, and stature in whites. Am J Hum Genet 2004; 74:866–75.
[19] Orimo H, Hayashi Y, Fukunaga M, Sone T, Fujiwara M, Shiraki M, et al. Diagnostic criteria for primary osteoporosis: year 2000 revision. J Bone Miner Metab 2001;19:331–7.
[20] Ezura Y, Nakajima T, Kajita M, Ishida R, Inoue S, Yoshida H, et al. Association of molecular variants, haplotypes, and linkage disequilibrium within the human vitamin D-binding protein (DBP) gene with postmenopausal bone mineral density. J Bone Miner Res 2003;18:1642–9.
[21] Iwasaki H, Emi M, Ezura Y, Ishida R, Kajita M, Kodaira M, et al. Association of a Trp16Ser variation in the gonadotropin releasing hormone (GnRH) signal peptide with bone mineral density, revealed by SNP-dependent PCR (Sd-PCR) typing. Bone 2002;32:185–90.
[22] Ogawa S, Hosoi T, Shiraki M, Orimo H, Emi M, Muramatsu M, et al. Association of estrogen receptor b gene polymorphism with bone mineral density. Biochem Biophys Res Commun 2000;269:537–41.
[23] Okubo M, Horinishi A, Kim DH, Yamamoto TT, Murase T. Seven novel sequence variations in the human low density lipoprotein receptor related protein 5 (LRP5) gene. Hum Mutat 2002;19:186.
[24] Mein CA, Barratt BJ, Dunn MG, Siegmund T, Smith AN, Esposito L, et al. Evaluation of single nucleotide polymorphism typing with invader on PCR amplicons and its automation. Genome Res 2000;10:330–43.
[25] Haga H, Yamada R, Ohnishi Y, Nakamura Y, Tanaka T. Gene-based SNP discovery as part of the Japanese Millennium Genome Project:

identification of 190 562 genetic variations in the human genome. J Hum Genet 2002;47:605–10.
[26] Miller PT, Sardina IB, Saccone NL, Putzel J, Laitinen T, Cao A, et al. Juxtaposed regions of extensive minimal linkage disequilibrium in human Xq25 and Xq28. Nat Genet 2000;25:324–8.
[27] Thompson EA, Deeb S, Walker D, Motulsky AG. The detection of linkage disequilibrium between closely linked markers: RFLPs at the AI-CIII apolipoprotein genes. Am J Hum Genet 1988;42:113–24.
[28] Ng PC, Henikoff S. Accounting for human polymorphisms predicted to affect protein function. Genome Res 2002;12:436–46.
[29] Koay MA, Woon PY, Zhang Y, Miles LJ, Duncan EL, Ralston SH, et al. Influence of LRP5 polymorphisms on normal variation in BMD. J Bone Miner Res 2004;19:1619–27.
[30] Koller DL, Ichikawa S, Johnson ML, Lai D, Xuei X, Edenberg HJ, et al. Contribution of the LRP5 gene to normal variation in peak BMD in women. J Bone Miner Res 2005;20:75–80.
[31] Babij P, Zhao W, Small C, Kharode Y, Yaworsky PJ, Bouxsein ML, et al. High bone mass in mice expressing a mutant LRP5 gene. J Bone Miner Res 2003;18:960–74.
[32] Eisman JA. Genetics of osteoporosis. Endocr Rev 1999;20:788–804.
[33] Peacock M, Turner CH, Econs MJ, Foroud T. Genetics of osteoporosis. Endocr Rev 2002;23:303–26.
[34] Hobson EE, Ralston SH. Role of genetic factors in the pathophysiology and management of osteoporosis. Clin Endocrinol 2001;54:1–9.
[35] Koller DL, Econs MJ, Morin PA, Christian JC, Hui SL, Parry P, et al. Genome screen for QTLs contributing to normal variation in bone mineral density and osteoporosis. J Clin Endocrinol Metab 2000; 85:3116–20.
[36] Reid IR. Relationships among body mass, its components, and bone. Bone 2002;31:547–55.
[37] Amling M, Takeda S, Karsenty G. A neuro(endo)crine regulation of bone remodeling. BioEssays 2000;22:970–5.
[38] Whipple T, Sharkey N, Demers L, Williams N. Leptin and the skeleton. Clin Endocrinol 2002;57:701–11.
[39] Takeda S, Elefteriou F, Levasseur R, Liu X, Zhao L, Parker KL, et al. Leptin regulates bone formation via the sympathetic nervous system. Cell 2002;111:305–3017.
[40] Shiraki M, Shiraki Y, Aoki C, Hosoi T, Inoue S, Kaneki M, et al. Association of bone mineral density with apolipoprotein E phenotype. J Bone Miner Res 1997;12:1438–45.
[41] Lecka-Czernik B, Moerman EJ, Grant DF, Lehmann JM, Manolagas SC, Jilka RL. Divergent effects of selective peroxisome proliferator-activated receptor-gamma 2 ligands on adipocyte versus osteoblast differentiation. Endocrinology 2002;143:2376–84.
[42] McFarlane SI, Muniyappa R, Francisco R, Sowers JR. Pleiotropic effects of statins: lipid reduction and beyond. J Clin Endocr Metab 2002;87: 1451–8.
[43] Johnson ML, Harnish K, Nusse R, Van Hul W. LRP5 and Wnt signaling: a union made for bone. J Bone Miner Res 2005;19:1749–57.

Geriatr Gerontol Int 2007; 7: 48–53

ORIGINAL ARTICLE

Association of a single nucleotide polymorphism in *Wnt10b* gene with bone mineral density

Takahiko Usui,[1] Tomohiko Urano,[1,2] Masataka Shiraki,[3] Yasuyoshi Ouchi[1] and Satoshi Inoue[1,2,4]

[1]*Department of Geriatric Medicine and* [2]*Department of Coca-Cola Anti-Aging Medicine, Graduate School of Medicine, University of Tokyo, Tokyo,* [3]*Research Institute and Practice for Involutional Diseases, Nagano, and* [4]*Research Center for Genomic Medicine, Saitama Medical School, Saitama, Japan*

Background: Wnt signaling pathway regulates bone mineral density (BMD) through the lipoprotein receptor-related protein (LRP)5, a receptor of this signaling. Recently, we and several groups have shown that genetic variations at the *LRP5* gene locus are associated with osteoporosis. These data suggest that genetic variations in Wnt signaling genes may affect the pathogenesis of osteoporosis. To explore whether the Wnt signaling molecules are involved in the maturation of osteoblasts, we analyzed the expression levels of Wnt signaling genes, including LRP5, LRP6 and Wnt10b, in rat primary osteoblasts. Then, we studied an association of a single nucleotide polymorphism (SNP) in *Wnt10b* gene with BMD.

Methods: Expression levels of LRP5, LRP6 and Wnt10b mRNA were analyzed during the culture course of rat primary osteoblasts by real-time reverse transcription polymerase chain reaction (RT-PCR). Association of the *Wnt10b* gene polymorphism at 1059C/T (His353His), that is the only coding SNP found in J-SNP database with BMD, was examined in 221 postmenopausal Japanese women.

Results: LRP5, LRP6 and Wnt10b mRNA were detected during the differentiation of rat primary osteoblasts. As an association study of the SNP in the *Wnt10b* gene, the subjects without the T allele (CC; $n = 59$) had significantly higher total body and lumbar BMD than the subjects bearing at least one T allele (TT + TC; $n = 162$) (total body, $P = 0.0091$; lumber spine. $P = 0.0052$).

Conclusion: Wnt10b mRNA was expressed and regulated in rat primary osteoblasts. A genetic variation at the *Wnt10b* gene locus is associated with BMD, suggesting an involvement of the *Wnt10b* gene in the bone metabolism. SNP of Wnt signaling genes would serve to facilitate early diagnosis, treatment and prevention of osteoporosis.

Keywords: bone mineral density (BMD), LRP5, LRP6, osteoporosis, single nucleotide polymorphism (SNP), Wnt10b.

Introduction

Osteoporosis is a skeletal disorder characterized by low bone mineral density (BMD) and micro-architectural deterioration of bone tissue leading to an increased risk of fracture.[1] BMD is a complex trait that is influenced by both genetic and environmental factors. Heritability studies in twins and family studies have shown that genetic factors account for 50–90% of the variance in BMD.[2–6] In studies on osteoporosis-related genes, significant associations of the vitamin D receptor (*VDR*) gene,[7] estrogen receptor α (*ERα*) gene,[8] collagen type Iα1 (*COLIA1*) gene[9] and low density lipoprotein receptor-related protein 5 (*LRP5*) gene[10] polymorphisms with

Accepted for publication 11 August 2006.

Correspondence: Dr Satoshi Inoue MD PhD, Department of Coca-Cola Anti-Aging Medicine, Graduate School of Medicine, University of Tokyo, 7-3-1 Hongo, Bunkyo-ku, Tokyo, 113-8655, Japan. Email: inoue-ger@h.u-tokyo.ac.jp

BMD in postmenopausal women have already been described. Identification of candidate genes, of which polymorphisms affect bone mass, will be useful for early detection of individuals who are at risk for osteoporosis and early institution of preventive measures.

The Wnt proteins represent a large group of secreted signaling proteins that are involved in cell proliferation, differentiation and morphogenesis.[11] Wnt proteins activate signal transduction through Frizzled which acts as receptors for Wnt proteins[12] and induce stabilization of cytoplasmic β-catenin protein. Meanwhile, low-density lipoprotein (LDL) receptor-related protein 5 and 6 (LRP5/6) were also found to be required for Wnt co-receptors.[13,14] Recent reports demonstrated that the Wnt signaling pathway regulates bone density through the LRP5.[15-18] We and several groups have shown that their is a significant association between BMD and polymorphisms in the *LRP5* gene.[10,19-21] We also have shown that a genetic variation of the *sFRP4* gene,[22] which is an inhibitor of Wnt signaling, affects the BMD among postmenopausal Japanese women. These data suggest that the single nucleotide polymorphism (SNP) in other Wnt signaling genes may affect the BMD.

Although these and other studies suggest that endogenous Wnt signaling regulates osteoblastogenesis and bone formation, Wnt molecules that are responsible for activation of this pathway in bone cells have to be determined. Recently, Wnt10b has demonstrated to regulate bone formation *in vivo*.[23] In this report, FABP4-Wnt10b mice, which overexpress Wnt10b in bone marrow, have shown increased bone.[23] It has also shown that Wnt10b$^{-/-}$ mice have decreased trabecular bone and serum osteocalcin.[23] These data suggest that Wnt10b may be a promising Wnt molecule as a determinant of BMD through the regulation of osteogenesis.

In the present study, we examined the expression of the Wnt10b in rat primary osteoblasts and the association of a polymorphism in the *Wnt10b* gene with BMD in Japanese women to investigate possible contribution of the Wnt10b in bone metabolism.

Materials and methods

Cell culture

Rat primary osteoblasts were isolated from calvaria of 5-day-old neonatal rats by enzymatic digestion as described previously[24] with some modification. Briefly, calvaria were minced and incubated at 37°C for 20 min in magnesium-free phosphate-buffered saline containing 0.1% collagenase and 0.2% dispase. The enzymatic digestion was repeated twice. The second digestion was performed for 70 min. Cells isolated at second digestion were cultured in α-minimum essential medium (MEM) containing 10% fetal bovine serum (FBS) and antibiotics (100 IU/mL penicillin and 100 mg/mL streptomycin). Cells at the second passage were used for experiments.

Total RNA isolation and cDNA synthesis

Osteoblasts were cultured in 6-cm dishes with α-MEM containing 10% FBS, 50 μg/mL ascorbic acid and 5 mmol/L β-glycerophosphate for 3, 5, 8, 11, 13, 15 or 18 days. Total RNA were extracted from these cells using a ToTALLY RNA Kit (Ambion, Austin, TX, USA). cDNA was synthesized from 1 μg of total RNA of primary osteoblasts using a first strand cDNA synthesis kit (Amersham, Chicago, IL, USA).

SYBR green real time PCR

Primers were designed using PRIMER EXPRESS 1.0 software (Applied Biosystems, Foster City, CA, USA). Definitive primers were: rat glyceraldehyde-3-phosphate dehydrogenase (GAPDH) forward 5′-GGC ACAGTCAAGGCTGAGAAT-3′, reverse 5′-TCGCGC TCCTGGAAGATG-3′, rat alkaline phosphatase (ALP) forward 5′-TGACCACCACTCGGGTGAA-3′, reverse 5′-GCATCTCATTGTCCGAGTACCA-3′, rat LRP5 forward 5′-TGGATGGGCGTCAGAACA-3′, reverse5′-TGGGAGAGGTCAGCATGGA-3′, rat LRP6 forward 5′-AGCGTCCTCAAGCAGCTCTTC-3′, reverse5′-CGATGGTGGTGGGTTCAAA-3′ and rat Wnt10b forward 5′-TCTCTCGGGATTTCTTGGATTC-3′, reverse 5′-TGTTGTGGATCCGCATTCTC-3′. Quantitative polymerase chain reaction (PCR) was carried out using a 2× master mix composed from the SYBR Green PCR Core Reagents (Applied Biosystems) and 50 nmol/L primers. PCR reactions were performed using an ABI Prism 7000 system (Applied Biosystems) with the following sequence: 2 min at 50°C, 10 min at 95°C and 40 cycle of 15 s at 95°C and 1 min at 60°C. ALP, LRP5, LRP6 or Wnt10b signals were normalized to GAPDH signals.

Subjects

Genotypes were analyzed in DNA samples obtained from 221 healthy postmenopausal Japanese women. We chose postmenopausal women who were older than 50 years from volunteers (mean age ± SD; 61.8 ± 6.6). All women were non-related volunteers who lived in the Chubu district of Japan and provided informed consent before this study. Exclusion criteria included endocrine disorders and a metabolic bone disease other than primary osteoporosis such as hyperthyroidism, hyperparathyroidism, diabetes mellitus, liver disease, renal disease or unusual gynecological history. Women taking medicine related to bone metabolism such as active vitamin D, vitamin K, a vitamin K antagonist, estrogen, bisphosphonate, corticosteroids, anticonvulsants and heparin sodium were also excluded. Ethical approval for the study was obtained from ethics committees of University of Tokyo and Research Institute and Practice for Involutional Diseases.

Measurement of BMD and biochemical markers

The lumbar-spine BMD and total body BMD (g/cm^2) of each participant were measured by dual-energy X-ray absorptiometry using fast-scan mode (DPX-L; Lunar, Madison, WI, USA). We measured serum concentration of calcium (Ca), ALP, intact-osteocalcin (I-OC, ELISA; Teijin, Tokyo, Japan), intact parathyroid hormone (PTH), calcitonin (CT) and 1,25(OH)$_2$D$_3$. We also measured urinary ratios of urinary deoxypyridinoline (DPD, high-performance liquid chromatography method) to creatinine. The BMD data were recorded as "Z scores"; that is, deviation from the weight-adjusted average BMD for each age. Z scores were calculated using installed software (Lunar DPX-L) on the basis of data from 20 000 Japanese women.

Determination of a single nucleotide polymorphism in the Wnt10b gene

Because there was only one coding SNP in the *Wnt10b* gene in the Japanese-SNP database (J-SNP), we examined association of this SNP in the *Wnt10b* gene at 1059C/T (His353His) with BMD in 221 postmenopausal Japanese women. We also extracted this variation in the Wnt10b gene from the Assays-on-Demand SNP Genotyping Products database (Applied Biosystems) and, according to its localization on the gene, denoted it 1059C/T. We determined the 1059C/T polymorphism of the *Wnt10b* gene using the TaqMan (Applied Biosystems) PCR method.[22] To determine the *Wnt10b* SNP we used Assays-on-Demand SNP Genotyping Products C_7470505_1 (Applied BioSystems), which contains sequence-specific forward and reverse primers and two TaqMan MGB probes for detecting alleles. During the PCR cycle, two TaqMan probes competitively hybridize to a specific sequence of the target DNA and the reporter dye is separated from the quencher dye, resulting in an increase in fluorescence of the reporter dye. The fluorescence levels of the PCR products were measured with the ABI PRISM 7000, resulting in clear identification of three genotypes of the SNP.

Statistical analysis

Comparisons of Z scores and biochemical markers between the group of individuals possessing one or two chromosomes of the T-allele and the group with only C-allele encoded at that locus were subjected to statistical analysis (Student's *t*-test; StatView-J 4.5). A *P*-value less than 0.05 was considered statistically significant.

Results

Wnt10b mRNA expression is regulated during the course of primary osteoblast differentiation

At the inception of this study, we measured the Wnt10b mRNA levels during the course of differentiation in rat primary osteoblasts. In the presence of ascorbic acid and β-glycerophosphate, primary osteoblasts proceed to differentiation normally with the deposition of a collagenous extracellular matrix that mineralizes.[25,26] The continual maturation of the osteoblasts was reflected by the increase of ALP mRNA (Fig. 1A). The Wnt10b mRNA was detected at day 2 and then decreased in primary osteoblasts (Fig. 1B). Inversely, the LRP5 mRNA increased persistently during the time-course of osteoblastic differentiation until day 28 (Fig. 1C). The levels of LRP6 mRNA were almost parallel to those of LRP5 mRNA (Fig. 1D).

Association of the Wnt10b gene polymorphism with BMD

We examined a *Wnt10b* polymorphism at 1059C/T (His353His) in postmenopausal Japanese women, using the TaqMan methods. Among 221 postmenopausal women, 42 were TT homozygotes, 120 were CT heterozygotes, and 59 were CC homozygotes. The genotype distribution was found to be in the Hardy–Weinberg equilibrium.

We compared Z scores for BMD of total body and lumbar spine between the subjects bearing at least one T allele (TT + TC) and subjects without the T allele (CC). Those with the T allele had significantly lower Z scores for total body BMD (Z score; 0.24 ± 0.99 vs 0.65 ± 1.11; $P = 0.0091$) (Figs 2A and 1A) and lumbar spine BMD (Z score; −0.42 ± 1.35 vs 0.16 ± 1.41; $P = 0.0052$) (Fig. 2B). The background and biochemical data were not statistically different between these two groups (Table 1).

Discussion

During the course of primary osteoblast differentiation, Wnt10b mRNA levels showed gradual decrease and sustained at certain levels during the observation period. Recent reports demonstrated that during the course of adipogenetic differentiation in 3T3L1 cells, Wnt10b rapidly falls to an undetectable level by the first 0–1 day.[27,28] The differential expression of Wnt10b in osteoblasts and adipocytes may imply a different role of Wnt10b in the cell differentiation. The increase of LRP5 and LRP6 expression was accompanied by the increase of ALP expression, which is a marker of osteoblast differentiation.[29] A previous report also demonstrated that BMP2 induced the osteoblastic differentiation markers,

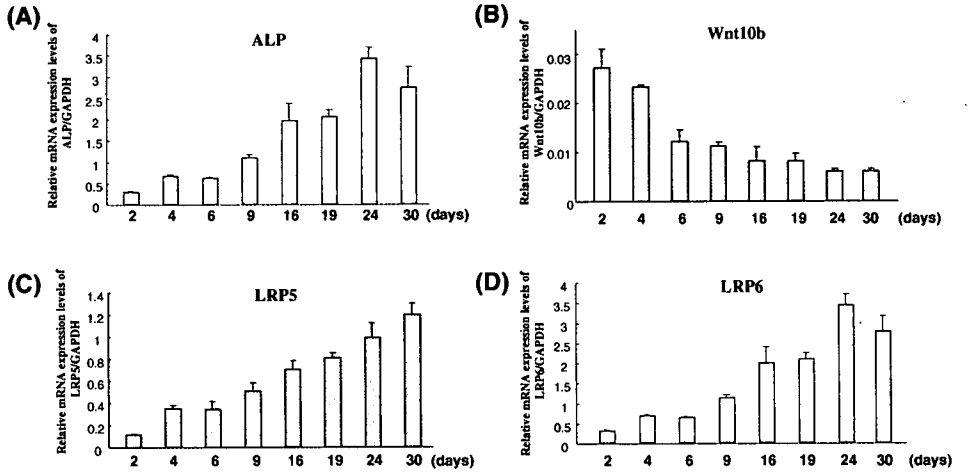

Figure 1 Expressions of the alkaline phosphatase (ALP), Wnt10b, lipoprotein receptor-related protein (LRP)5 and LRP6 mRNA during culture course of rat primary osteoblasts were analyzed by real-time reverse transcription polymerase chain reaction (RT-PCR). Rat primary osteoblasts were cultured with α-minimum essential medium (MEM) containing 10% fetal bovine serum (FBS), 50 μg/mL ascorbic acid and 5 mmol/L β-glycerophosphate up to 18 days. At the indicated times, RNA were extracted and the expression levels of ALP (A), Wnt10b (B), LRP5 (C) and LRP6 (D) were analyzed by real-time RT-PCR, normalized to glyceraldehyde-3-phosphate dehydrogenase (GAPDH) expression ($n = 4$ for each group). Values are shown as means ± SD.

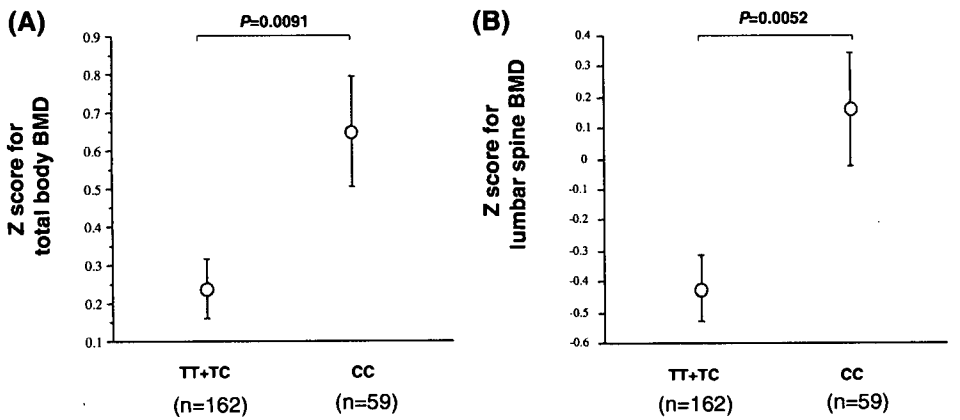

Figure 2 "Z score" values of total body and lumbar spine bone mineral density (BMD) in the groups of genotype TT + TC and genotype CC of the *Wnt10b* polymorphism in exon 6 (1059C/T). (A) Z score values for total BMD are shown for genotype TT + TC and for genotype CC. Values are expressed as mean ± SE. Numbers of subjects are shown in parentheses. (B) Z scores for lumbar BMD are shown in the same manner as (A).

followed by the increase of the LRP5 and LRP6 expression in ST2 cells.[15] Thus, the increase of LRP5 and LRP6 expression may have some roles in osteoblastic differentiation.

To our knowledge, the present study is the first to investigate the influence of a polymorphism of the Wnt10b gene on BMD. We demonstrated that the Japanese postmenopausal women who had one or two

Table 1 Comparison of background, bone mineral density and biochemical data between subjects bearing at least one T allele (TT + TC) and subjects with no T allele (CC) in the *Wnt10b* gene (1059C/T)

Items	Genotype (mean ± SD)		*P*-value
	TT + TC	CC	
No. of subjects	162	59	
Age (years)	61.4 ± 6.5	62.9 ± 6.7	NS
Height (cm)	152.3 ± 5.8	151.6 ± 5.8	NS
Bodyweight (kg)	52.2 ± 7.8	52.2 ± 7.0	NS
Lumber spine BMD (Z score)	−0.42 ± 1.35	0.16 ± 1.41	0.0052
Total body BMD (Z score)	0.24 ± 0.99	0.65 ± 1.11	0.0091
ALP (IU/L)	187.6 ± 58.8	182.3 ± 64.5	NS
I-OC (ng/mL)	8.2 ± 3.9	7.2 ± 3.2	NS
DPD (pmol/μmol/Cr)	6.3 ± 4.0	6.1 ± 3.3	NS
Intact PTH (pg/mL)	33.1 ± 10.7	36.4 ± 19.7	NS
Calcitonin (pg/mL)	23.0 ± 12.9	22.3 ± 7.9	NS
1,25 $(OH)_2D_3$ (pg/mL)	34.7 ± 10.2	35.2 ± 11.7	NS
% fat	32.6 ± 7.3	33.0 ± 7.0	NS
BMI	22.5 ± 3.1	22.7 ± 3.1	NS

ALP, alkaline phosphatase; BMD, bone mineral density; BMI, body mass index; DPD, deoxypyridinoline; I-OC, intact-osteocalcin; NS, not significant; PTH, parathyroid hormone. Statistical analysis was performed according to the method described in the text.

allele(s) of a synonymous change of C-T transition showed significant total body and lower lumbar BMD. Lower BMD in postmenopausal women could be considered as results of abnormally rapid bone loss and/or lower peak bone mass. The SNP analyzed in the present study would be useful as a genetic marker for low BMD and susceptibility to osteoporosis. Although the biological meanings of this polymorphism should be revealed by functional studies, several hypotheses could be proposed at present. First, this silent polymorphism may be linked with other mutations in exons, which contributes to the change of the Wnt10b protein function, such as in case of the *PADI4* polymorphisms in rheumatoid arthritis.[30] Second, the SNP may be linked with a mutation in regulatory elements affecting the levels of expression through variable transcriptional regulation, such as in case of the *LTA* exon 1 polymorphisms in myocardial infarction.[31] Third, this SNP in the *Wnt10b* gene may be linked with a mutation of another undefined gene adjacent to the *Wnt10b* gene that causes low BMD directly or indirectly, such as in case of the *ECM2* and *ASPN* polymorphisms in osteoarthritis.[32]

Because of the limited sample size and the number of SNP utilized in the present study, we need larger scale studies on this coding SNP and other polymorphisms in the Wnt10b gene in the future. The association study between multiple SNP and BMD using a statistical correction as well as functional analysis of SNP would be helpful.

The Wnt pathway has recently been implicated in the control of bone mass in adults in human and mice.[15–18] Activation of this pathway increases bone mass through a number of mechanisms including renewal of stem cells, stimulation of preosteoblast replication, induction of osteoblastgenesis, and inhibition of osteoblast and osteocyte apoptosis.[33] Taken together, these studies suggest that endogenous Wnt signaling plays an important role in osteogenesis and bone formation. However, the Wnt that are involved directly in the bone metabolism have to be identified among 19 members of the Wnt family. Recently, it was demonstrated that expression of Wnt10b in bone marrow increased bone mass and strength in mice.[22] Taking together with these data, our present finding of an association of a polymorphism in *Wnt10b* gene with BMD suggests that Wnt10b may be a specific ligand responsible for BMD among several Wnt.

In conclusion, our findings suggest that the *Wnt10b* gene may be a genetic determinant of BMD in postmenopausal women as is the case with its related co-receptor, *LRP5*. Examining the variation in the *Wnt10b* gene will hopefully enable us to elucidate one of mechanisms of involutional osteoporosis. Furthermore, the variation may be a potential genetic susceptibility factor that need to be further evaluated with regard to the condition of other metabolisms in which the Wnt signaling have been clearly implicated, including cholesterol, glucose and fat metabolisms.[34,35]

Acknowledgments

We thank Ms N. Sasaki and Ms. K. Sue for expert technical assistance. This work was partly supported by grants from the Japanese Ministry of Health, Labor, Welfare and Japan Society for the Promotion of Science. This work was also partly supported by a grant of the

Genome Network Project from the Ministry of Education, Culture, Sports, Science and Technology of Japan.

References

1 Osteoporosis prevention, diagnosis, and therapy. *NIH Consens Statement* 2000; **17**: 1–36.
2 Flicker L, Hopper JL, Rodgers L *et al.* Bone density determinants in elderly women: a twin study. *J Bone Miner Res* 1995; **10**: 1607–1613.
3 Smith DM, Nance WE, Kang KW *et al.* Genetic factors in determining bone mass. *J Clin Invest* 1973; **2**: 2800–2808.
4 Young D, Hopper JL, Nowson CA *et al.* Determinants of bone mass in 10- to 26-year-old females: a twin study. *J Bone Miner Res* 1995; **10**: 558–567.
5 Nelson DA, Kleerekoper M. The search for the osteoporosis gene. *J Clin Endocrinol Metab* 1997; **82**: 989–990.
6 Liu YZ, Liu YJ, Recker RR *et al.* Molecular studies of identification of genes for osteoporosis: the 2002 update. *J Endocrinol* 2003; **177**: 147–196.
7 Morrison NA, Qi JC, Tokita A *et al.* Prediction of bone density from vitamin D receptor alleles. *Nature* 1994; **367**: 284–287.
8 Kobayashi S, Inoue S, Hosoi T *et al.* Association of bone mineral density with polymorphism of the estrogen receptor gene. *J Bone Miner Res* 1996; **11**: 306–311.
9 Uitterlinden AG, Burger H, Huang Q *et al.* Relation of alleles of the collagen type Ialpha1 gene to bone density and the risk of osteoporotic fractures in postmenopausal women. *N Engl J Med* 1998; **338**: 1016–1021.
10 Urano T, Shiraki M, Ezura Y *et al.* Association of a single-nucleotide polymorphism in low-density lipoprotein receptor-related protein 5 gene with bone mineral density. *J Bone Miner Metab* 2004; **22**: 341–345.
11 Nusse R, Varmus HE. Wnt genes. *Cell* 1992; **69**: 1073–1087.
12 Cadigan KM, Nusse R. Wnt signaling: a common theme in animal development. *Genes Dev* 1999; **11**: 3286–3305.
13 Tamai K, Semenov M, Kato Y *et al.* LDL-receptor-related proteins in Wnt signal transduction. *Nature* 2000; **407**: 530–535.
14 Mao J, Wang J, Liu B *et al.* Low-density lipoprotein receptor-related protein-5 binds to Axin and regulates the canonical Wnt signaling pathway. *Mol Cell* 2001; **7**: 801–809.
15 Gong Y, Slee RB, Fukai N *et al.* LDL receptor-related protein 5 (LRP5) affects bone accrual and eye development. *Cell* 2001; **107**: 513–523.
16 Kato M, Patel MS, Levasseur R *et al.* Cbfa1-independent decrease in osteoblast proliferation, osteopenia, and persistent embryonic eye vascularization in mice deficient in Lrp5, a Wnt coreceptor. *J Cell Biol* 2002; **157**: 303–314.
17 Boyden LM, Mao J, Belsky J *et al.* High bone density due to a mutation in LDL-receptor-related protein 5. *N Engl J Med* 2002; **346**: 1513–1521.
18 Little RD, Carulli JP, Del Mastro RG *et al.* A mutation in the LDL receptor-related protein 5 gene results in the autosomal dominant high-bone-mass trait. *Am J Hum Genet* 2002; **70**: 11–19.
19 Mizuguchi T, Furuta I, Watanabe Y *et al.* LRP5, low-density-lipoprotein-receptor-related protein 5, is a determinant for bone mineral density. *J Hum Genet* 2004; **49**: 80–86.
20 Ferrari SL, Deutsch S, Choudhury U *et al.* Polymorphisms in the low-density lipoprotein receptor-related protein 5 (LRP5) gene are associated with variation in vertebral bone mass, vertebral bone size, and stature in whites. *Am J Hum Genet* 2004; **74**: 866–875.
21 Koay MA, Brown MA. Genetic disorders of the LRP5-Wnt signalling pathway affecting the skeleton. *Trends Mol Med* 2005; **11**: 129–137.
22 Fujita M, Urano T, Shiraki M *et al.* Association of a single nucleotide polymorphism in the secreted frizzled related protein 4 (sFRP4) gene with bone mineral density. *Geriatric Gerontol Int* 2004; **4**: 175–180.
23 Bennett CN, Longo KA, Wright WS *et al.* Regulation of osteoblastogenesis and bone mass by Wnt10b. *Proc Natl Acad Sci USA* 2005; **102**: 3324–3329.
24 Urano T, Yashiroda H, Muraoka M *et al.* p57 (Kip2) is degraded through the proteasome in osteoblasts stimulated to proliferation by transforming growth factor beta1. *J Biol Chem* 1999; **274**: 12197–12200.
25 Nefussi JR, Boy-Lefevre ML, Boulekbache H *et al.* Mineralization in vitro of matrix formed by osteoblasts isolated by collagenase digestion. *Differentiation* 1985; **29**: 160–168.
26 Bellows CG, Aubin JE, Heersche JN *et al.* Mineralized bone nodules formed in vitro from enzymatically released rat calvaria cell populations. *Calcif Tissue Int* 1986; **38**: 143–154.
27 Ross SE, Hemati N, Longo KA *et al.* Inhibition of adipogenesis by Wnt signaling. *Science* 2000; **289**: 950–953.
28 Bennett CN, Ross SE, Longo KA *et al.* Regulation of Wnt signaling during adipogenesis. *J Biol Chem* 2002; **277**: 30998–31004.
29 Aubin JE. Advances in the osteoblast lineage. *Biochem Cell Biol* 1998; **76**: 899–910.
30 Suzuki A, Yamada R, Chang X *et al.* Functional haplotypes of PADI4, encoding citrullinating enzyme peptidylarginine deminase 4, are associated with rheumatoid arthritis. *Nat Genet* 2003; **34**: 395–402.
31 Ozaki K, Tanaka T. Genome-wide association study to identify SNPs conferring risk of myocardial infarction and their functional analysis. *Cell Mol Life Sci* 2005; **62**: 1804–1813.
32 Kizawa H, Kou I, Iida A *et al.* An aspartic acid repeat polymorphism in asporin inhibits chondrogenesis and increases susceptibility to osteoarthritis. *Nat Genet* 2005; **37**: 138–144.
33 Krishnan V, Bryant HU, MacDougald OA. Regulation of bone mass by Wnt signaling. *J Clin Invest* 2006; **116**: 1202–1209.
34 Longo KA, Wright WS, Kang S *et al.* Wnt10b inhibits development of white and brown adipose tissues. *J Biol Chem* 2004; **279**: 35503–35509.
35 Fujino T, Asaba H, Kang MJ *et al.* Low-density lipoprotein receptor-related protein 5 (LRP5) is essential for normal cholesterol metabolism and glucose-induced insulin secretion. *Proc Natl Acad Sci USA* 2003; **100**: 229–234.

Int. J. Cancer: **120**, 2325–2330 (2007)

Increased expression of estrogen-related receptor α (ERRα) is a negative prognostic predictor in human prostate cancer

Tetsuya Fujimura[1], Satoru Takahashi[1,2]*, Tomohiko Urano[3], Jinpei Kumagai[1], Tetsuo Ogushi[1], Kuniko Horie-Inoue[4], Yasuyoshi Ouchi[3], Tadaichi Kitamura[1], Masami Muramatsu[4] and Satoshi Inoue[3,4]

[1]*Department of Urology, Faculty of Medicine, The University of Tokyo, Bunkyo-ku, Tokyo, Japan*
[2]*Department of Urology, Nihon University Hospital, Itabashi-ku, Tokyo, Japan*
[3]*Department of Geriatric Medicine, Faculty of Medicine, The University of Tokyo, Bunkyo-ku, Tokyo, Japan*
[4]*Research Center for Genomic Medicine, Saitama Medical School, Moroyama-machi, Iruma-gun, Saitama, Japan*

The nuclear receptor ERRα (estrogen-related receptor α) is known to modulate the estrogen-signaling pathway, but the biological significance of ERRα in the prostate remains unclear. We investigated the expression of ERRα in human prostate tissues and cancer cell lines to evaluate the potential roles of the receptor in prostate cancer (PC). Western blot analysis of ERRα was performed in three cell lines of human PC (LNCaP, DU145 and PC-3). The expressions of ERRα in cancerous lesions (n = 106) and benign foci (n = 99) of 106 surgically obtained prostate specimens were evaluated by immunohistochemistry. The relationships between the ERRα expression and clinicopathological features were evaluated. Western blot analysis using the polyclonal anti-ERRα antibody detected a 52 kD band in all three PC cell lines. Positive immunostaining of ERRα in the nuclei was found in 73 (69%) cancerous and 47 (47.5%) benign epithelium, whereas the stromal tissues were negative for ERRα. The mean immunoreactivity score (IR score) of the cancerous lesions (3.5 ± 2.6) was significantly higher than that of the benign foci (1.8 ± 2.1) (p < 0.0001). The IR score of the cancerous lesions significantly correlated with the Gleason score (p = 0.0135). Univariate and multivariate hazard analyses revealed significant correlations between elevated ERRα expression and poor cancer-specific survival (p = 0.0141 and 0.0367, respectively). The enhanced expression of ERRα might play a role in the development of human PC and serve as a significant prognostic factor for the disease.
© *2007 Wiley-Liss, Inc.*

Key words: estrogen related receptor α (ERRα); prognostic predictor; prostate cancer

Estrogens have been widely used for the treatment of advanced prostate cancer (PC).[1] The direct effect of estrogens on normal prostate and PC is assumed to be mediated through estrogen receptors (ERs) α and β.[2,3] ERα is predominantly localized in the stromal cells of the prostate.[3–6] In light of this, the ERα-mediated effects of estrogens on the prostate epithelium are thought to be conferred via paracrine pathways. ERβ, on the other hand, is localized predominantly in the epithelial cell compartment of the normal human prostate, and the expression of ERβ is decreased in PC compared with benign epithelium.[2,3] Thus, ERβ may exert a protective effect against aberrant cell proliferation and carcinogenesis.[7–10]

Recent studies have focused on an additional estrogen signaling pathway mediated by estrogen-related receptors (ERRs) in the estrogen-targeted organs.[11–13] ERRs belong to the nuclear receptor super family and consist of three closely related members (α, β and γ).[11–13] The cDNA for ERRα was isolated by screening cDNA libraries using probes corresponding to the DNA-binding domain of human ERα.[11] Evidence suggests that there may be an overlap between ERRα and ER biology. While ERRα shows no direct response to 17β-estradiol, it has been found to bind to functional estrogen response elements (EREs) in ER target genes such as lactoferrin and aromatase.[12–14] ERRα may participate in processes such as bone development, skeleton formation and fat metabolism.[15–18] Further, ERRα is now established to be associated with unfavorable biomarkers in human breast cancer.[19–21] Much less is known, however, about the extent or pattern of ERRα expression in the prostate.[22] The present study evaluated ERRα expression in human prostate tissues and PC cell lines by immunohistochemistry and Western blot analysis to assess its clinical significance.

Material and methods

Tissue selections and patient characteristics

Formalin-fixed, paraffin-embedded sections were obtained from 106 patients who underwent radical prostatectomy for prostatic adenocarcinoma between 1987 and 2001. We obtained informed consent from all the patients. The age of the patients ranged from 52 to 78 years (mean 66.8 ± 6.0), and pretreatment serum PSA level ranged from 2.2 to 136 ng/ml (mean 16.9 ± 19.5). The pathological stages included B (n = 33), C (n = 59) and D_1 (n = 14). Prostate tissue sections submitted for this study contained 99 benign and 106 cancerous foci. The cancerous lesions consisted of tumors with Gleason score (GS) 6 (n = 22), 7 (n = 41), 8 (n = 20), 9 (n = 22) and 10 (n = 1), which was evaluated by 2 trained pathologists. Thirty-five patients (33%) were treated with surgery alone, whereas the remaining patients received adjuvant anti-androgen therapy. Patients were followed postoperatively by their surgeons at 3-month intervals to 5 years and yearly thereafter. Mean patient follow-up period was 82 ± 39 months (range 10–192). During the follow-up period, 77 patients (73%) are alive with no evidence of the disease, and 12 (11%) are alive with biochemical or clinical recurrence. Eleven patients (10%) died of PC, and 6 (6%) died of other diseases during the follow-up period.

Cell culture

The human prostatic cancer cell lines (PC-3, DU145 and LNCaP) and COS7 cells were obtained from American Type Culture Collection (Rockville, MD) and maintained in the RPMI 1640 with 10% FBS. All cell lines were maintained at 37°C in 5% CO_2. Transfections of hERRα were performed using 3.5×10^6 COS7 cells, 5 μg of pcDNA3-hERRα vector and FuGENE® 6 transfection kit (Roche Applied Science, Indianapolis, IN) according to the manufacture's protocol. After 48 hr cell extracts were analyzed.

Antibodies

Rabbit polyclonal antibody for ERR1 (PA1-314) was purchased from Affinity Bio Reagents (Golden, CO). The characterization of this antibody was confirmed by Western blot analysis in hERRα-transfected COS7 cells.

***Correspondence to:** Department of Urology, Nihon University Hospital, 30-1 Oyaguchi, Itabashi-ku, Tokyo 173-8610, Japan.
Fax: +81-3-3972-8111. E-mail: tsatoru@med.nihon-u.ac.jp
Received 30 January 2006; Accepted after revision 9 August 2006
DOI 10.1002/ijc.22363
Published online 9 February 2007 in Wiley InterScience (www.interscience.wiley.com).

Publication of the International Union Against Cancer

Western blot analyses

Western blot analysis was performed using total cell extracts obtained from 3 strains of LNCaP, DU145, PC-3 and hERRα-transfected COS7 cells as previously described.[23] Cells were rinsed twice with ice-cold phosphate-buffered saline (PBS) and lysed in Nonidet P-40 lysis buffer (50 mM Tris-HCl [pH 7.4], 150 mM NaCl, 10 mM NaF, 5 mM EDTA, 5 mM EGTA, 2 mM sodium vanadate, 0.5% sodium deoxycholate, 1 mM diethiothreitol [DTT], 1 mM phenylmethylsulfonyl fluoride [PMSF], 2 mg/ml aprotinin and 0.1% no diet P-40), and the lysates were cleared by centrifugation at 15,000 for 15 min at 4°C. Total protein lysate (20 μg) of each cell line was fractionated on sodium dodecyl sulfate (SDS)-12.5% polyacryl-amide gels and electrophoretically transferred onto polyvinylidene difluoride (PVDF) membranes (Immobilin, Millipore, Bedford, MA). The membranes were blocked in Tris-buffered saline (TBS) with 5% skim milk before incubating with the anti-ERRα antibodies diluted (1:500), followed by a horseradish peroxidase-conjugated donkey anti-rabbit immunoglobulin IgG (Amersham-Pharmacia Biotech, Arlington Heights, IL). Bands were visualized with the chemiluminescence's -based ECL plus detection system (Amersham-Pharmacia Biotech).

Immunohistochemistry

We performed immunohistochemical analysis of ERRα employing the streptavidin-biotin amplification method using a peroxidase catalyzed signal amplification system: CSA system (DAKO, Carpentaria, CA) following the manufacturer-supplied protocol. Tissue-sections (6 μm) were deparaffinized, dehydrated through a graded ethanol series and rinsed in phosphate-buffered saline (PBS). For antigen retrieval, the sections were autoclaved at 120°C for 15 min in citric acid buffer (2 mM citric acid and 9 mM trisodium citrate dehydrate, pH 6.0). After blocking endogenous peroxidase with 0.3% H_2O_2, the sections were incubated in 10% bovine serum for 10 min. Application of the polyclonal antibody for ERRα (1:100 dilution) followed by sequential 15-min incubations with biotinylated link antibody, streptavidin-biotin-peroxidase complex, amplification reagent and streptavidin-peroxidase. The antigen-antibody complex was visualized with 3,3′-diaminobenzidine (DAB) solution (1 mM DAB, 50 mM Tris-HCl buffer pH 7.6 and 0.006% H_2O_2).

As positive controls, sections of human heart tissues (BioChain Institute, Inc, Hayward, CA) were immunoassayed with the primary antibodies in the same manner as described above.

In addition to the standard negative controls with rabbit IgG, we performed peptide blocking of anti-ERRα antibody using its neutralizing peptide purchased from Affinity Bio Reagents (Golden, CO) in order to confirm the specificity of the antibody.

Immunohistochemical assessment

Immunostained slides were evaluated for the proportion (0, none; 1, <1/100; 2, 1/100 to 1/10; 3, 1/10 to 1/3; 4, 1/3 to 2/3; and 5, >2/3) and the intensity (0, none; 1, weak; 2, moderate; and 3, strong) of positively stained cells.[24] The total scores of immunoreactivity (0–8) were obtained as the sum of the proportion and the intensity. For immunohistochemical assessment, two investigators (T. F. and J. K.) evaluated the tissue sections independently. If IR score was different between two investigators, third investigator (S.T.) counted and we adopted the average IR score. To determine potential correlation between expression of ERRα in the malignant epithelium and clinicopathological characteristics, we considered the sections with 2 of IR score as positive for ERRα immunoreactivity. Since almost all benign foci showed <5 of IR scores for ERRα, we defined IR score 5 as a cutoff for strong immunoreactivity of ERRα.

Statistical analysis

Correlations between the immunoreactivity score (IR score) and clinicopathological characteristics (age, pretreatment serum PSA level, pathological stage and the Gleason score) were evaluated using the *t*-test or chi-square test. Cancer-specific survival curves were obtained by the Kaplan-Meier method and verified by the Log rank (Mantel-Cox) test. We analyzed statistical assessment by Stat View-J 5.0 software (SAS Institute, Cary, NC), and regarded *p*-values < 0.05 as statistically significant.

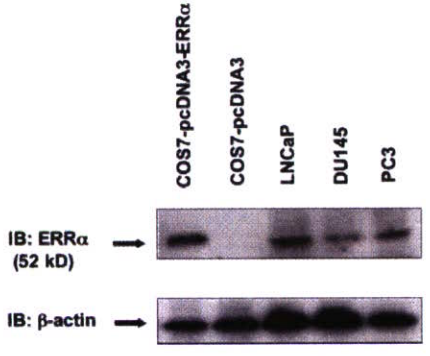

FIGURE 1 – Western blot analysis of the ERRα proteins in pcDNA3-ERRα and PC cell lines (LNCaP, DU145 and PC-3). Total cell extracts were subjected to immunoblotting with both the anti-ERRα and β-actin antibody. Anti-ERRα antibody detected a 52 kD band in COS7-pcDNA3-ERRα and human PC cell lines (LNCaP, DU145 and PC-3).

Results

Western blot analysis

Using the polyclonal anti-ERRα antibody, a 52 kD band, which corresponded to the molecular weight of ERRα, was detected in COS7-pcDNA3-ERRα. Positive signals were also observed in all three PC cell lines (LNCaP, DU145 and PC-3) (Fig. 1).

Immunoreactivity of ERRα in benign and malignant prostate tissues

Table I shows a summary of ERRα immunoreactivities in surgically obtained human prostate tissues. Strong immunoreactivity of ERRα was identified in the nuclei of human myocardium (Fig. 2*a*). Although ERRα immunoreactivity was focally detected in benign epithelium in some cases, the strong immunoreactivity (IR score: 5 or more) was rarely observed (Table I and Fig. 2*c*). No significant immunoreactivity was identified in stromal cells. In contrast, increased ERRα immunoreactivity was observed in low-grade PC (Fig. 2*e*). Extensive ERRα expression was often identified in high-grade cancer (Table I and Fig. 2*g*). Immunostaining with the ERRα antibody pre-absorbed with immunizing peptide did not identify any significant signals in all the samples examined (Figs. 2*b*,2*d*,2*f* and 2*h*). ERRα immunoreactivities were positive in 47 of 99 cases (47.5%) in benign epithelium and in 73 of 106 cancer cases (69%). The cancerous lesions showed significantly higher ERRα IR scores (3.5 ± 2.6) than 1.8 ± 2.1 of the benign foci ($p < 0.0001$). Higher-GS (8–10) cancers showed significantly higher IR score (4.3 ± 2.7), compared with the lower-GS (2–7) tumors (3.0 ± 2.6) ($p = 0.0194$)(Table I).

TABLE I – EXPRESSION OF ESTROGEN RELATED RECEPTOR α (ERRα) PROTEIN IN HUMAN PROSTATE ($N = 106$)

	Immunoreactive (IR) score[1] (%)									
	0	2	3	4	5	6	7	8	Mean ± S.D.	*p*-value
Benign ($n = 99$)	52 (52.5)	3 (3)	10 (10.1)	23 (23.2)	8 (8.1)	3 (3)	0	0	1.8 ± 2.1	<0.0001
Malignant ($n = 106$)										
Low Grade[2] ($n = 63$)	23 (36.5)	0	8 (12.7)	12 (19.0)	6 (9.5)	10 (15.9)	3 (4.8)	1 (1.6)	3.0 ± 2.6	0.0194
High Grade[2] ($n = 43$)	10 (23.2)	0	2 (4.7)	8 (18.6)	5 (11.6)	8 (18.6)	8 (18.6)	2 (4.7)	4.3 ± 2.71	

[1]Immunoreactivity (IR) score (0 to 8) was obtained as the sum of the proportion and the intensity of immunoreactivity. Proportion (0, none; 1, <1/100; 2, 1/100 to 1/10; 3, 1/10 to 113; 4, 1/3 to 2/3; and 5, >213), Intensity (0, none; 1, weak; 2, moderate; and 3, strong).–[2]Low Grade: Gleason score; 2–7, High Grade: Gleason score; 8–10.

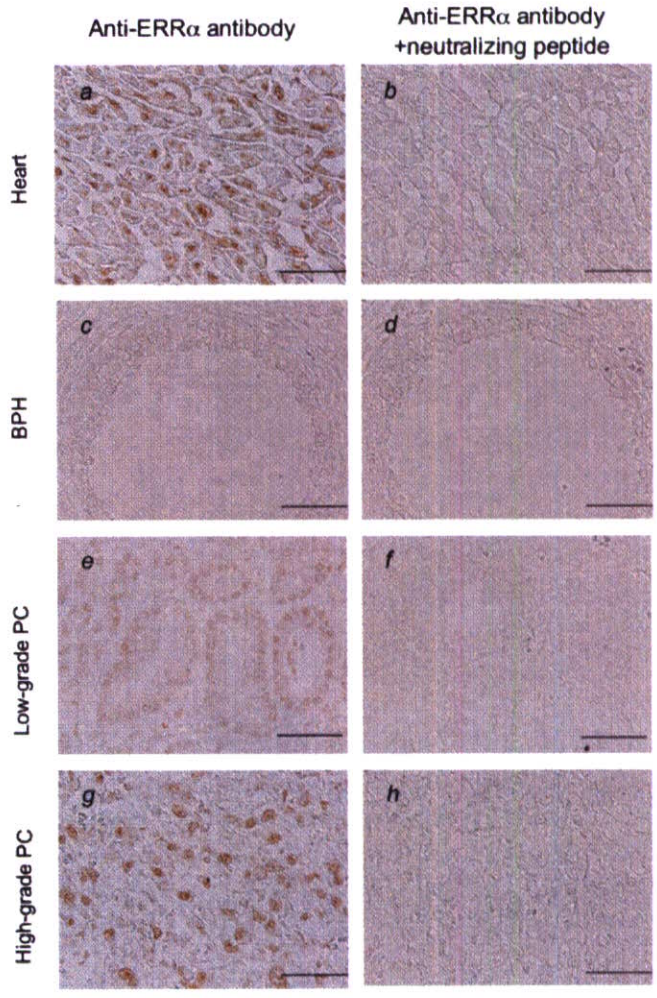

FIGURE 2 – Immunohistochemical staining (*a*, *c*, *e* and *g*) for ERRα and neutralizing peptide blocking (*b*, *d*, *f* and *h*) in human prostate and myocardium. Strong staining (IR score: 8) of ERRα was identified in the nuclei of human myocardium (*a*) Immunoreactivity was not detected in benign epithelium (*c*). Moderately increased immunoreactivity of ERRα (IR score: 6) was observed in low-grade PC (GS 6) (*e*). Extensive expression (IR score: 8) of ERRα was identified in high-grade cancer (GS 9) (*g*). Immunostaining with the ERRα antibody pre-absorbed with immunizing peptide did not identify any significant signals in all the samples examined (*b*, *d*, *f* and *h*). Original magnification: ×400, Scale bar = 50 μm.

Clinical significance of ERRα expression in human PC

Since most of benign foci showed <5 of IR scores for ERRα, we defined IR score 5 as a cutoff for strong immunoreactivity of ERRα. Table II shows correlation of ERRα expression and clinicopathological characteristics. Cases with high serum PSA level showed a trend of strong expression of ERRα, although it did not reach statistical significance ($p = 0.07$). GS correlated with the status of ERRα expression. ERRα expression in higher-GS cancer

(8–10) was significantly higher than that in lower GS (2–7) cancer ($p = 0.0135$).

Figure 3 demonstrates a cancer-specific survival curve prepared by the Kaplan-Meier method. Eleven (10%) cases died of PC during the follow-up period. Cancer-specific survival of patients with higher ERRα expression (IR score ≥5) was significantly worse than cases with lower expression (IR score < 5) ($p = 0.0055$). Table III indicates the results of univariate and multivariate proportional analyses of cancer-specific survival with status of ERRα expression and clinicopathological parameters. ERRα expression, GS and pathological stages were significant prognostic predictors in univariable analysis ($p = 0.0141$, 0.0123 and 0.0352, respectively). Multivariate analysis showed that ERRα expression and GS are independent predictors ($p = 0.0367$ and 0.0264, respectively) among 4 parameters.

TABLE II – RELATIONSHIP OF ERRα EXPRESSION WITH CLINICOPATHOLOGICAL FINDINGS IN HUMAN PROSTATIC CANCER ($N = 106$)

	ERRα immunoreactivity[1]		*p*-value
	Weak ($n = 62$)	Strong ($n = 44$)	
Age	66.1 ± 5.8	67.4 ± 6.0	0.28
Serum PSA (ng/dl)	13.6 ± 13.0	20.5 ± 25.0	0.07
Gleason score			
2–7	43 (69.4)	20 (30.6)	0.0135
8–10	19 (44.2)	24 (55.8)	
Pathological Stage			
B, C	56 (60.9)	36 (39.1)	0.2
DI	6 (42.9)	8 (57.1)	

[1]Immunoreactivity (IR) score (0–8) was obtained as the sum of the proportion and the intensity of immunoreactivity. Proportion (0, none; 1, <1/100; 2, 1/100 to 1/10; 3, 1/10 to 1/3; 4, 1/3 to 2/3; and 5, >2/3), Intensity (0, none; 1, weak; 2, moderate; and 3, strong).IR score 0–4 and 5–8 were defined as weak and strong immunoreactivity, respectively.

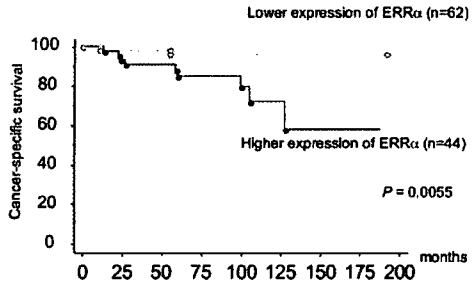

FIGURE 3 – Cancer-specific survival in 106 patients with PC according to the immunoreactivity of ERRα. Cancer-specific survival of patients with higher ERRα expression (IR score ≥ 5) was significantly worse than that of lower expression (IR score < 5) cases ($p = 0.0055$).

Discussion

Androgen deprivation and estrogen therapy have been the standard treatment for PC.[3,25,26] The growth-inhibitory effects of endocrine therapies are associated with the status of steroid receptors, such as the androgen receptor (AR) and estrogen receptor (ER).[25,26] The emergence of techniques to clone the orphan nuclear receptors in the 1980s prompted to investigate physiological functions of the orphan nuclear receptors in the targeted organs.[12,13] Among the orphan nuclear receptors, ERRα, β and γ, the three closely related members of the ERR family, all have functional links with the activities of the ERs. Two findings suggest that ERRα modulates the actions of the ERs. Firstly, ERRα shares a significant homology to ERα at the DNA-binding domain (DBD). Secondly, ERRα recognizes the ERE.[14,21,22,27,28] The ERRα gene is located on the long arm of chromosome 11.[29] Human ERRα was isolated from kidney and heart cDNA libraries by screening with an ERα-DBD cDNA probe.[11] ERRα mRNA was highly expressed in the heart and skeletal muscle and to a lesser degree in the kidney, pancreas, small intestine and colon.[29] Several investigations have implicated ERRα in the development in human breast cancer and colorectal cancer.[19,20,30] Further, ERRα mRNA has recently been detected in PC cell lines and human prostate tissues.[22] The present study is the first to reveal that ERRα expression is significantly higher in higher-GS cancer than in lower-GS cancer. These findings suggest that ERRα is involved in the normal and neoplastic growth of human prostate tissue.

Elevated ERRα expression has been identified as a poor prognostic factor in human breast cancer,[19,20] and has been reported to be correlated with higher histological grade and TNM stage of colorectal cancer.[30] However, there are conflicting data as to the ERRα expression in human prostate tissues. We found increased ERRα expression in PC, compared with that in benign epithelium. The previous study summarized the data and concluded that ERR proteins were detected as nuclear proteins in epithelial cells, whereas their expression became reduced in neoplastic prostate cells.[22] However, close interpretation of the results may suggest that these findings are more prominent in ERRβ expression, whereas ERRα rather expressed variably in PC on both the cell lines and human tissues. A figure of immunohistochemical analysis in the previous study demonstrated heterogeneous stain of ERRα in a low Gleason grade cancer, as the legend indicated.[22] Although the previous study did not identify number of cases examined with immunohistochemistry, we believed that our results obtained from 106 surgically resected prostate samples clearly demonstrate ERRα expression status in human prostate tissues and its potential significance in the cancer development. Of course, further investigations are warranted, and may let us gain better understanding on this interesting matter.

The present study suggests that ERRα participates in the regulation of PC besides ERs (α, β and βcx). How do these receptors correlate with the development of PC? We make two possible hypotheses. One is a functional cross-talk between ERRα and ERs in endocrine cancers in which ER exists. The binding of ERRα to several functional EREs has prompted speculation that ERRα can modify the ER function by either forming ER-ERRα heterodimer, by competing with ER for binding to ERE, or steroid receptor co-activators (SRCs).[12–14] Far-Western analysis[14] and glutathione S-transferase pull-down assays have demonstrated direct interactions between ERα and ERRα.[31] Another hypothesis is that these ERs and ERRα receptors act independently. ERα and ERRα separately modulate pS2 expression in human breast cancer.[20] As we previously assessed the expression of ERs (α/ β/ βcx) in fifty patients with PC and showed their clinical significance,[2] we estimated the correlation of ERRα with ERs (α/ β/ βcx) in overlapping fifty cases. Subsequently, no significant correlations among them were identified (R^2: 0.004 for ERα vs. ERRα, R^2: 0.006 for ERβ vs. ERRα and R^2: 0.241 for ERβcx vs. ERRα). Interestingly, similar findings were reported in breast cancer,[20]and it was suggested that ERRα might modulate the activity of estrogen responsive genes, independently of ERs. Therefore, estrogen-signaling pathway via ERs (α, β and βcx), and ERRα is so complicated that we can not reach a conclusion on the basis of current findings.

Although several investigations proved that ERRα activate a variety of estrogen target genes such as pS2, aromatase and osteopontin (OPN) and play important roles in some target organs,[13] the mechanism of ERRα in PC development remains unclear at this time. For example, ERRα regulates the expression of pS2, which increase breast cancer growth.[15,20] ERRα also activates aromatase in breast, HepG2 and bone cells.[15] Aromatase, which converts androgens to estrogens, stimulates the growth of breast cancer.[32] Recent studies focus on the surveillance about anti-aromatase effects on breast cancer.[32] Aromatase is also well known to have an important role in endocrine metabolism at the prostate. Interestingly aromatase was expressed and active in LNCaP, PC-3 and DU145 cells, whereas benign prostate epithelial cells showed no expression or activity.[33] It is not demystified how over expression of aromatase in PC correlate with PC development similar to that in breast cancer[32] because estrogens are generally considered to have protective effects on PC progressions. The local synthesis of estrogens via aromatase enzyme might contribute to the estrogen-signaling pathway through ERs in PC. In addition, OPN participates in prostate biology. For instance, elevated OPN expression is found in PC both the cell lines and human tissues.[34] Increased expression of OPN is associated with Gleason score and poor cancer-specific survival.[34] These findings suggest that further investigations are needed to verify whether the ERRα-mediated effects on PC correlate with the activation of estrogen responsive genes.

Selective estrogen receptor modulators (SERMs) are synthetic estrogen ligands that can exhibit either estrogenic or anti-estrogenic effects depending on tissue types.[35] SERMs such as tamoxifene (TAM), 4-Hydroxytamoxifen (4-OHT) and raloxifene can induce apoptosis in PC cell lines such as PC-3, DU145 and LNCaP.[36–39] Toremifene treatment significantly reduces the incidence of PC in the transgenic adenocarcinoma of mouse prostate (TRAMP) mice.[40] Toremifene also reduces the incidence of PC in high-grade intraepithelial neoplasia (PIN) patients.[41] It may be that the anti-proliferate effects of SERMs on PC are mediated via ERs due to their positive expression in the prostate. Diethylstilbestrol (DES), an agent widely used for the treatment of advanced PC, represses the molecular activities of ERRα such as reporter gene trans-activation and interaction with co-activator fragments.[42] Thus, the SERMs might inhibit PC by modulating the estrogen-signaling pathway via ERRs besides the ERs. The prognostic value of enhanced ERRα expression as an independent predictor of PC suggests that an ERRα antagonist capable of specifically blocking ERRα activity may prove useful as a therapeutic agent against PC.

TABLE III – UNIVARIATE AND INULTIVARIATE PROPORTIONAL HAZARD ANALYSES OF CANCER-SPECIFIC SURVIVAL ($N = 106$)

Variable	Univariate			Multivariate		
	Hazard ratio	95% index	*p*-value	Hazard ratio	95% index	*p*-value
PSA (>10 vs. ≤10)	0.79	0.23–2.8	0.73	0.47	0.13–1.76	0.26
Gleason score (High vs. Low)[1]	2.63	1.77–108.4	0.0123	11.3	1.33–95.7	0.0264
Pathological stage (DI vs. B, C)	3.77	1.01–12.9	0.0352	1.37	0.36–5.26	0.64
ERRα (Strong vs Weak)[2]	6.84	1.47–31.8	0.0141	5.24	1.11–25.7	0.0367

[1]High Gleason score: 8–10, low: 2–7.–[2]IR score 0–4 and 5–8 were defined as weak and strong immunoreactivity, respectively.

References

1. Huggins C, Hodges CV. Studies on prostatic cancer. I. The effect of castration, of estrogen and androgen injection on serum phosphatases in metastatic carcinoma of the prostate. CA Cancer J Clin 1972;22: 232–40.
2. Fujimura T, Takahashi S, Urano T, Ogawa S, Ouchi Y, Kitamura T, Muramatsu M, Inoue S. Differential expression of estrogen receptor β (ERβ) and its C-terminal truncated splice variant ERβx as prognostic predictors in human prostatic cancer. Biochem Biophys Res Commun 2001;289:692–9.
3. Ho SM. Estrogens and anti-estrogens: key mediators of prostate carcinogenesis and new therapeutic candidates. J Cell Biochem 2004;91: 491–503.
4. Kirschenbaum A, Ren M, Erenburg I, Schachter B, Levine AC. Estrogen receptor messenger RNA expression in human benign prostatic hyperplasia: detection, localization and modulation with a long-acting gonadotropin-releasing hormone agonist. J Androl 1994;15:528–33.
5. Lau KM, LaSpina M, Long J, Ho SM. Expression of estrogen receptor (ER)-α and ER-β in normal and malignant prostatic epithelial cells: regulation by methylation and involvement in growth regulation. Cancer Res 2000;60:3175–82.
6. Ehara H, Koji T, Deguchi T, Yoshii A, Nakano M, Nakane PK, Kawada Y. Expression of estrogen receptor in diseased human prostate assessed by non-radioactive in situ hybridization and immunohistochemistry. Prostate 1995;27:304–13.
7. Pasquali D, Staibano S, Prezioso D, Franco R, Esposito D, Notaro A, De Rosa G, Bellastella A, Sinisi AA. Estrogen receptor β expression in human prostate tissue. Mol Cell Endocrinol 2001;178:47–50.
8. Horvath LG, Henshall SM, Lee CS, Head DR, Quinn DI, Makela S, Delprado W, Golovsky D, Brenner PC, O'Neill G, Kooner R, Stricker PD, et al. Frequent loss of estrogen receptor-β expression in prostate cancer. Cancer Res 2001;61:5331–5.
9. Pasquali D, Rossi V, Esposito D, Abbondanza C, Puca GA, Bellastella A, Sinisi AA. Loss of estrogen receptor β expression in malignant human prostate cells in primary cultures and in prostate cancer tissues. J Clin Endocrinol Metab 2001;86:2051–5.
10. Latil A, Bieche I, Vidaud D, Lidereau R, Berthon P, Cussenot O, Vidaud M. Evaluation of androgen, estrogen (ER α and ER β), and progesterone receptor expression in human prostate cancer by real-time quantitative reverse transcription-polymerase chain reaction assays. Cancer Res 2001;61:1919–26.
11. Giguere V, Yang N, Segui P, Evans RM. Identification of a new class of steroid hormone receptors. Nature 1988;331:91–4.
12. Horard B, Vanacker JM. Estrogen receptor-related receptors: orphan receptors desperately seeking a ligand. J Mol Endocrinol 2003;31:349–57.
13. Giguere V. To ERR in the estrogen pathway. Trends Endocrinol Metab 2002;13:220–5.
14. Yang N, Shigeta H, Shi H, Teng CT. Estrogen-related receptor, hERR1, modulates estrogen receptor-mediated response of human lactoferrin gene promoter. J Biol Chem 1996;271:5795–804.
15. Bonnelye E, Aubin JE. Estrogen receptor-related receptor α: a mediator of estrogen response in bone. J Clin Endocrinol Metab 2005;90: 3115–21.
16. Bonnelye E, Vanacker JM, Spruyt N, Alric S, Fournier B, Desbiens X, Laudet V. Expression of the estrogen-related receptor 1 (ERR-1) orphan receptor during mouse development. Mech Dev 1997;65:71–85.
17. Luo J, Sladek R, Carrier J, Bader JA, Richard D, Giguere V. Reduced fat mass in mice lacking orphan nuclear receptor estrogen-related receptor α. Mol Cell Biol 2003;23:7947–56.
18. Vega RB, Kelly DP. A role for estrogen-related receptor α in the control of mitochondrial fatty acid β-oxidation during brown adipocyte differentiation. J Biol Chem 1997;272:31693–9.
19. Ariazi EA, Clark GM, Mertz JE. Estrogen-related receptor α and estrogen-related receptor γ associate with unfavorable and favorable biomarkers, respectively, in human breast cancer. Cancer Res 2002;62: 6510–18.
20. Suzuki T, Miki Y, Moriya T, Shimada N, Ishida T, Hirakawa H, Ohuchi N, Sasano H. Estrogen-related receptor α in human breast carcinoma as a potent prognostic factor. Cancer Res 2004;64:4670–6.
21. Kraus RJ, Ariazi EA, Farrell ML, Mertz JE. Estrogen-related receptor α1 actively antagonizes estrogen receptor-regulated transcription in MCF-7 mammary cells. J Biol Chem 2002;277:24826–34.
22. Cheung CP, Yu S, Wong KB, Chan LW, Lai FM, Wang X, Suetsugi M, Chen S, Chan FL. Expression and functional study of estrogen receptor-related receptors in human prostatic cells and tissues. J Clin Endocrinol Metab 2005;90:1830–44.
23. Urano T, Takahashi S, Suzuki T, Fujimura T, Fujita M, Kumagai J, Horie-Inoue K, Sasano H, Kitamura T, Ouchi Y, Inoue S. 14-3-3sigma is down-regulated in human prostate cancer. Biochem Biophys Res Commun 2004;319:795–800.